

Application of Solid Phase Micro-Extraction (SPME) - GC-MS
for Identifying Pyrolysis Compounds in Textiles

by

Brock Bradford

A Thesis submitted to the Faculty of Graduate Studies of
The University of Manitoba
in partial fulfilment of the requirements of the degree of

MASTER OF SCIENCE

Department of Chemistry
University of Manitoba
Winnipeg

Copyright© 2016 by Brock Bradford

Acknowledgments

I would like to thank all my family and friends who supported me throughout graduate school (it was a long haul but I made it!). I would especially like to thank Dr. Douglas Goltz from the University of Winnipeg who continually motivated me as a supervisor, mentor and a friend. I am honored to have worked with him on this project. I would also like to thank Dr. Stephen Duffy from Mount Allison University for contributing his knowledge and ideas to the project, Anna Henderson for her contributions with the project (good luck in graduate school!), my fellow grad student Shokoufeh Ahmadi for all of her contributions and advice. Finally, I would also like to thank Joel Smigelski from the University of Winnipeg for his continual instrument support.

Abstract

This thesis project describes research using headspace solid phase micro-extraction with gas chromatography (HS-SPME GC-MS) as an analytical tool for assessing textile fibres. It was found that this method required a temperature of $>500^{\circ}\text{C}$ to pyrolyze the textile sample. A total of 5 minutes was determined to be the optimal time for collecting the volatile analytes.

Numerous analytes were found to be chemical markers for each of the individual textile fibres.

The chemical markers are qualitatively used to describe each textile uniquely, and it was found that by using the chromatographic patterns, the textiles could be identified individually and in mixtures containing two textiles.

Lastly, by accelerating the age of the textile fibres by means of heat, ultra-violet light, and humidity, a comparison was made between the un-aged and aged fibres. It was found that each of the techniques arose different results and in some cases new compounds.

Table of Contents

ACKNOWLEDGMENTS	1
ABSTRACT	2
TABLE OF CONTENTS	3
LIST OF FIGURES	5
LIST OF TABLES	9
SUMMARY	10
CHAPTER 1: INTRODUCTION	13
1.1 Textiles	13
1.1a Textile Samples	13
1.1b Textile Classification	15
1.1c Current Techniques for Analysing Textiles	21
1.1d Solid Phase Micro-extraction Gas Chromatography Mass Spectrometry (SPME GC-MS)	31
1.2 Research Objectives	35
1.3 Experimental	36
1.3a Sample Preparation	36
1.3b Method Protocol.....	36
1.3c Instrumentation	37
CHAPTER 2: FEASIBILITY OF ANALYSING TEXTILES FOR IDENTIFICATION USING SPME GC-MS	40
2.1 Temperature Optimization	40
2.1a Conclusions of Temperature Optimization	53
2.3 Sample Size	56
2.4 Identifying Chemical Markers	62
2.5 Textile Brand Comparison	66
2.6 Fourier Transform Infrared Spectroscopy (FT-IR) Investigations	68

2.6a Experimental	68
2.6b FT-IR Results and Discussion.....	69
2.6c FT-IR brand comparison	71
2.6d FT-IR analysis of accelerated aged wool.....	73
CHAPTER 3: ANALYSIS OF TEXTILE MIXTURES	75
3.1 Textile Mixture Conclusions	84
CHAPTER 4: CHEMICAL MARKERS OF ACCELERATED AGED TEXTILES	87
4.1 Experimental	88
4.2 Heat Accelerated Aging of Textiles	89
4.3 Humidity Accelerated Aging of Textiles	99
4.4 Ultra-Violet (UV) light Accelerated Aging of Textiles.....	106
CONCLUSIONS	113
REFERENCES.....	116
APPENDIX.....	124

List of Figures

Figure 1. Classification of commonly used textile fibres.	12
Figure 2. Backbone structure of wool (forms helically) and silk (forms non-helically) – where for wool R comprises most commonly of H (glycine), C₄H₉ (leucine), C₂H₄COOH (glutamic acid) and CH₂OH (serine). For silk, R comprises most commonly of H (glycine), CH₃ (alanine), and CH₂OH (serine).	14
Figure 3. Chemical structure of cellulose - The backbone of cotton, flax, and rayon fibres. ...	15
Figure 4. Chemical structure of cellulose acetate.	16
Figure 5. Chemical structure of nylon 6, 6.	17
Figure 6. Chemical structure of polyethylene terephthalate (an example of a polyester). ..	18
Figure 7. Ethylene (a) and Propylene (b) armake up the main monomer units in polyolefin fibers.	18
Figure 8. Chemical structure of a polyurethane backbone structure.	19
Figure 9. HS-SPME 100 µm polydimethylsiloxane (PDMS) SPME fibre.	35
Figure 10. Sample chamber containing the platinum coil wrapped around a quartz sample vessel.	36
Figure 11. Effects of pyrolysis temperature on the number of compounds released from olefin fibre (a) Temperature setting 1 (Top of crucible: 190-200°C Bottom of crucible: 120-130°C) (b) Temperature setting 2 (Top of crucible: 260-270°C Bottom of crucible: 190-200°C) (c) Temperature setting 3 (Top of crucible: 290-300°C Bottom of crucible: 230-240°C) (d) Temperature setting 4 (Full pyrolysis >500°C).	39
Figure 12. Chemical structure of volatile compounds collected from olefin (see appendix for mass spectrum). (a) 2-methylbutyl-cyclopentane (b) 1, 1-dimethyl-2-propylcyclohexane	40
Figure 13. Effects of pyrolysis temperature on the number of compounds released from cotton fibre (a) Temperature setting 1 (Top of crucible: 190-200°C Bottom of crucible: 120-130°C) (b) Temperature setting 2 (Top of crucible: 290-300°C Bottom of crucible: 230-240°C) (c) Temperature setting 3 (Top of crucible: 340-350°C Bottom of crucible: 260-267°C) (d) Temperature setting 4 (Full pyrolysis >500°C).	42
Figure 14. Chemical structure of volatile compounds collected from cotton (see appendix for mass spectrum). (a) Dodecanal (b) 5-methyl-2-furfural	43
Figure 15. Effects of pyrolysis temperature on the number of compounds released from wool fibre (a) Temperature setting 1 (Top of crucible: 260-270°C Bottom of crucible: 190-200°C) (b) Temperature setting 2 (Top of crucible: 340-350°C Bottom of crucible: 260-267°C) (c) Temperature setting 3 (Top of crucible: 390-400°C Bottom of crucible: 290-300°C) (d) Temperature setting 4 (Full pyrolysis >500°C).	44
Figure 16. Chemical structure of volatile compounds collected from wool (see appendix for mass spectrum). (a) 4-methyl-2-nitrophenol (b) Benzenepropanenitrile	45

Figure 17. Effects of pyrolysis temperature on the number of compounds released from polyester fibre (a) Temperature setting 1 (Top of crucible: 260-270°C Bottom of crucible: 190-200°C) (b) Temperature setting 2 (Top of crucible: 350-360°C Bottom of crucible: 270-280°C) (c) Temperature setting 3 (Top of crucible: 390-400°C Bottom of crucible: 290-300°C) (d) Temperature setting 4 (Full pyrolysis >500°C)	46
Figure 18. Chemical structure of volatile compounds collected from polyester (see appendix for mass spectrum). (a) 4-methylbenzamide (b) 4-methyl-2,6-dihydroxyquinoline	47
Figure 19. Chemical structure of volatile compounds collected from acrylic (see appendix for mass spectrum). (a) 4-methylbenzotrile (b) O-ethylbenzotrile	48
Figure 20. Effects of pyrolysis temperature on the number of compounds released from acrylic fibre (a) Temperature setting 1 (Top of crucible: 190-200°C Bottom of crucible: 120-130°C) (b) Temperature setting 2 (Top of crucible: 260-270°C Bottom of crucible: 190-200°C) (c) Temperature setting 3 (Top of crucible: 290-300°C Bottom of crucible: 230-240°C) (d) Temperature setting 4 (Full pyrolysis >500°C).....	49
Figure 21. Determination of SPME collection time (a) S/N vs. Collection time (b) Counts/Signal vs. Collection time.....	52
Figure 22. Effects of mass on the compounds released from wool (a) 1.5mg wool (b) 1.0 mg wool (c) 0.25 mg wool (d) 0.02 mg wool.....	54
Figure 23. Effects of mass on the compounds released from cotton (a) 1.5 mg cotton (b) 0.08 mg cotton (c) 0.02 mg cotton	55
Figure 24. Effects of mass on the compounds released from olefin (a) 1.5 mg olefin (b) 0.1 mg olefin (c) 0.02 mg olefin.....	57
Figure 25. Effects of mass on the compounds released from polyester (a) 1.5 mg polyester (b) 0.05 mg polyester (c) 0.02 mg polyester.....	58
Figure 26. Chromatograms of pyrolysed textile fibres (T>500°C) (a) 100% Cotton (b) 100% Acrylic (c) 100% Wool (d) 100% Polyester (e) 100% Silk (f) 100% Olefin.....	61
Figure 27. Brand comparison of the pyrolysis of cotton. Listed from top to bottom - Bernat Handicrafter, Paton Grace, J+P, DMC, Anchor.....	67
Figure 28. The analysis of various textiles using mid-infrared spectroscopy (a) Cotton (b) Acrylic (c) Wool (d) Polyester (e) Olefin	69
Figure 29. FT-IR analysis of 5 cotton brands. (a) Anchor (b) DMC (c) J+P (d) Bernat Handicrafter (e) Paton	72
Figure 30. FT-IR comparative analysis of non-aged and humid aged wool. (a) non-aged wool (b) humid aged wool	73
Figure 31. 100% Wool and 100% cotton mixtures (total mass=1.5 mg, T>500°C). Cotton peaks displayed as 1-3, wool peaks displayed as 5-8 (a) 1:1 mass ratio (b) 1:3 wool:cotton mass ratio (c) 3:1 wool:cotton mass ratio.....	75
Figure 32. 100% Cotton and 100% olefin mixtures (total mass=1.5 mg, T>500°C). Cotton peaks displayed as 2 and 3, olefin peaks displayed as 1, 4-9 (a) 1:1 mass ratio (b) 1:3 olefin:cotton mass ratio (c) 3:1 olefin:cotton mass ratio.....	77

Figure 33. 100% Cotton and 100% acrylic mixtures (total mass=1.5 mg, T>500°C). Cotton peaks displayed as 1-3, acrylic peaks displayed as 4-7 (a) 1:1 mass ratio (b) 1:3 cotton:acrylic mass ratio (c) 3:1 cotton:acrylic mass ratio.....	78
Figure 34. 100% Wool and 100% olefin mixtures (total mass=1.5 mg, T>500°C). Wool peaks displayed as 1-3, and 5, olefin peaks displayed as 3, 4, and 7-9 (a) 1:1 mass ratio (b) 1:3 wool:olefin mass ratio (c) 3:1 wool:olefin mass ratio.....	80
Figure 35. 100% Acrylic and 100% wool mixtures (total mass=1.5 mg, T>500°C). Acrylic peaks displayed as 1-3, and 7, cotton peaks displayed as 4-6 (a) 1:1 mass ratio (b) 1:3 wool:acrylic mass ratio (c) 3:1 wool:acrylic mass ratio.....	81
Figure 36. 100% Acrylic and 100% olefin mixtures (total mass=1.5 mg, T>500°C). Acrylic peaks displayed as 2, 4 and 5, olefin peaks displayed as 1,3 and 6-8 (a) 1:1 mass ratio (b) 3:1 acrylic:olefin mass ratio (c) 1:3 acrylic:olefin mass ratio.....	83
Figure 37. The aging process using UV light from Black-ray B100AP (100W bulb) high intensity UV lamp (365nm longwave UV source).....	88
Figure 38. (a) Acid-catalyzed hydrolysis of cellulose and oxidation of levulinic acid⁸³ (b) levulinic acid conversion to acetic acid⁸³	90
Figure 39. Acid-catalyzed hydrolysis of xylose to furfural as a result of aging⁸³.....	90
Figure 40. Degradation compounds of cellulose (a) Furfural (b) 5-methyl furfural (c) Decane: an example of a linear hydrocarbon (d) Heptanal: an example of a linear aldehyde (e) Acetic acid	91
Figure 41. Heat accelerated aging of 100% cotton (a) Un-aged cotton (b) Heat aged cotton (90 days at 80°C)	91
Figure 42. Heat accelerated aging of 100% wool (a) Un-aged wool (b) Heat aged wool (90 days at 80°C)	93
Figure 43. Heat accelerated aging of 100% polyester (a) Un-aged polyester (b) Heat aged polyester (90 days at 80°C)	94
Figure 44. Heat accelerated aging of 100% olefin (a) Un-aged olefin (b) Heat aged olefin (90 days at 80°C)	95
Figure 45. Heat accelerated aging of 100% acrylic (a) Un-aged acrylic (b) Heat aged acrylic (90 days at 80°C)	97
Figure 46. Humidity accelerated aging of 100% silk (a) Un-aged silk (b) Humidity aged silk (62 days at 80°C).....	98
Figure 47. Humidity accelerated aging of 100% acrylic (a) Un-aged acrylic (b) Humidity aged acrylic (62 days at 80°C)	100
Figure 48. Humidity accelerated aging of 100% wool (a) Un-aged wool (b) Humidity aged wool (62 days at 80°C)	102
Figure 49. Accelerated humidity aged wool over a period of 62 days at 80°C, 80% relative humidity.	102
Figure 50. Humidity accelerated aging of 100% cotton (a) Un-aged cotton (b) Humidity aged cotton (62 days at 80°C).....	103

Figure 51. Derivatives of Furfural (a) Furanmethanol (b) 2(5h)-furanone (c) 5-methyl-2(5h)-furanone.....	104
Figure 52. Ultraviolet accelerated aging of 100% silk (a) Un-aged silk (b) UV aged silk (96 hours).....	105
Figure 53. Ultraviolet accelerated aging of 100% acrylic (a) Un-aged acrylic (b) UV aged acrylic (96 hours)	106
Figure 54. Ultraviolet accelerated aging of 100% wool (a) Un-aged wool (b) UV aged wool (96 hours)	106
Figure 55. Ultraviolet accelerated aging of 100% cotton (a) Un-aged cotton (b) UV aged cotton (96 hours)	107

List of Tables

Table 1. Examples of SPME coatings and their intended analytes of interest^{57, 58}.	32
Table 2. Textile sample origin, purity and manufacturer.	36
Table 3. S/N of textile peaks for each temperature interval (signal n=23, noise n=535).	52
Table 4. Pyrolysis of textiles cotton, acrylic, wool, polyester, silk, and olefin and the corresponding compounds released from performing HS-SPME with GC-MS (see appendix for mass spectrum). (See Fig. 28)	65
Table 5. Un-aged chromatogram comparison with the heat accelerated aged chromatogram for the relative peak areas of olefin compounds.	95

SUMMARY

Analysis of modern textiles can be evaluated using techniques such as infrared or Raman spectroscopy, microscopy or pyrolysis gas chromatography mass spectrometry. However, with each technique lies limitations and challenges (e.g. limit of detection of IR). A novel approach for assessing the volatile compounds evolving from textiles was developed by combining headspace solid phase micro-extraction (HS-SPME) with gas chromatography mass spectrometry (GC-MS). An apparatus was constructed using a glass sample chamber which contained a platinum coil for heating and a quartz sample vessel. The SPME apparatus sits atop a glass sample chamber 3cm above a quartz sample vessel for collection of the volatile compounds evolving from pyrolysis.

In chapter 2, 3 important properties related to analysis (temperature, sample size, collection time) were studied for silk, cotton, wool, polyester, acrylic and olefin as samples. The resulting chromatograms revealed that the optimal temperature was full pyrolysis ($>500^{\circ}\text{C}$) of the textiles. Full pyrolysis lead to improved signal-to-noise ratio (S/N) of the GC peaks, and displayed the largest number of volatile compounds for each textile. The sample size used for the experiment was 1.5mg, however, it was found for cotton, polyester, olefin and wool that they could evolve detectable compounds at levels of $<0.1\text{mg}$. The sample collection time was evaluated for the SPME sample collection at times of 1, 2, 3, 5 and 8 minutes. It was found that at 5 minutes, the 4-methyl-2-nitro-phenol (representative compound of wool) peak displayed the largest S/N and the largest peak counts, making 5 minutes the optimal collection time. Each textile chromatogram provided a unique set of compounds and respective retention times. In order to identify the reoccurring compounds that could be used to represent each textile, a list was compiled of structurally related textile chemical markers.

In order to evaluate the specificity of SPME, 5 different brands of cotton were collected and compared. It was found that the compounds used to identify cotton did not differ. However, Bernat Handicrafter was found to pyrolyse the largest number of additional compounds not detectable within the other cotton brands.

Upon successful analysis of textiles individually evaluating the capability of HS-SPME-GC-MS, the analysis of blended textiles was studied (chapter 3). It was determined that the chemical markers in each textile allowed for successful identification of mixtures containing two different textiles. However, it was difficult to evaluate the composition of each textile based on the relative peak area of the volatile compounds.

Chapter 4 of this thesis involved accelerated aging of textiles for identifying chemical degradation markers. The preservation of textiles is of equal importance, as many historical pieces that have been found in relatively good condition, will continue to degrade over time. Three types of accelerated aging were applied consisting of heat, humidity, and ultra-violet (UV – 365 nm) light. Wool produced new compounds 1-isocyano-2-methyl-benzene, 2-methyl-5-nitro-benzamine, and toluene. Benzaldehyde and benzonitrile displayed increased relative peak area consistently and could as well be used as potential degradation markers. Silk displayed an increased relative peak area for the following compounds were benzaldehyde, cyanobenzene, and benzylnitrile. Acrylic displayed drastic relative peak area increases with accelerated aging for acetic acid and benzonitrile. Polyester consistently experienced increased relative peak area for biphenyl and decreased relative peak areas for phenol and benzoic acid. Cotton displayed unexpectedly mixed results, with and increased relative peak area for 2, 5-furandicarboxaldehyde in the heat and humidity accelerated chromatograms, and increases for known degradation compounds furfural and 5-methyl-2-furfural in the UV accelerated aged chromatogram. All of

these compounds could potentially be regarded as chemical degradation markers. Olefin was the only textile that did not display any significant changes after becoming subject to accelerated aging.

Chapter 1: Introduction

1.1 Textiles

1.1a Textile Samples

Textiles are various forms of woven cloth that differ by their physical and chemical structures. Textile fibres consist of a series of monomer units bonded to create chain polymers, which assemble into complex structures. All textile fibres have been found to share one thing in common; the fundamental molecules that each consists of, are long, and threadlike¹. The molecules that make up the threadlike fibres are what give each textile its unique properties. The ability of polymer molecules to stack and fit together is important as this determines strength of a fibre. Functional groups that are attached to the base structure may not stack well and will therefore, make the thread more vulnerable and weak. Intermolecular forces of attraction (e.g. van der Waals) between closely stacked molecules will form the strongest type of fibre. The size of the polymer unit can also have an effect on the properties of the fibre's appearance and texture, for example smaller monomers like glucose are responsible for the makeup of cellulose (e.g. cotton), whereas larger monomers like polyethylene terephthalate (e.g. a form of polyester) are responsible for synthetic type fibres.

A textile fibre is described as having a length of at least one hundred times the diameter in the form that allows it to be spun into yarn². Fibres can be classified into two main types, manufactured or natural². Natural fibres originate either from an animal or plant base. Natural fibres can further be classified into animal, vegetable, leaf, seed, and bast (phloem base) types². Manufactured fibres refer to any fibre that has been synthetically made or any natural fibre that has been processed chemically (ex. polyester)². Manufactured fibres became widely available at the end of the 19th century with the development of viscose/rayon. This was in response to the

increasing commercial demand for new fabrics³. Rayon is a textile form of cellulose that has been regenerated. Viscose is form of rayon which refers to a semi-synthetic fibre where cellulose has been treated with sodium hydroxide and carbon disulfide to create a spinnable viscose fibre.

Manufactured fibres can be further classified as either regenerated fibres or synthetic fibres. Regenerated fibres refer to a dissolved natural fibre that is restored through a process called extrusion and precipitation (e.g. cellulose is dissolved and restored to become rayon). One example of this is called the Chardonnet process where an ether/alcohol mixture is added to cellulose nitrate (cellulose nitrate is produced by treating mulberry leaves in H_2SO_4 and HNO_3) and then evaporated in open air (dry spinning)⁴. The resulting fibre is then reconverted to cellulose. More commonly used practices are the cuprammonium process and the viscose process⁴. Synthetic fibres are formed by joining synthesized monomer units of a specific compound into a polymer or long filamentous fibre (e.g. acrylic).

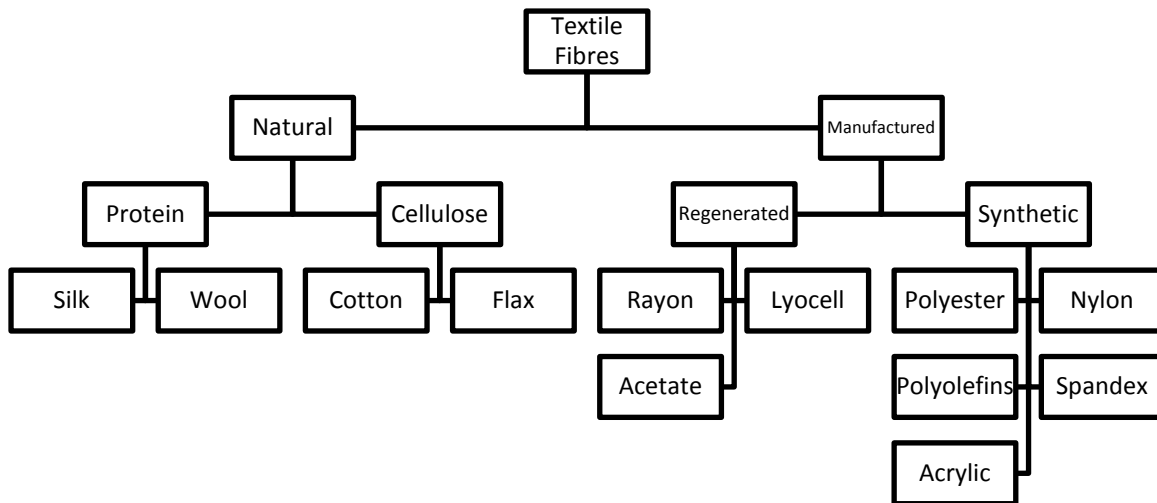


Figure 1. Classification of commonly used textile fibres.

1.1b Textile Classification

Textile fibres may have many classification types which include many natural and manufactured forms. Due to the increasing ability for researchers to modify polymer structures of textile fibres, many new categories of textiles have been created. Figure 1 lists the main categorical breakdown of the common types of fibres that are currently produced; however, there are many subcategories of wool, silk, polyester, nylon among others that can be further classified into differentiating forms.

Natural Protein Fibres

Wool

Wool fibre is made up of monomer units of the protein keratin. This serves as a base molecule in which various functional groups can be attached to keratin giving multiple types of wool. Keratin has many sources of external animal structures such as hairs, nails, claws, horns, feathers and hoofs. Fibrous forms of keratin are most commonly referred to as wool and come typically, from hair. Wool stacks helically and is primarily composed of the amino acids of glycine (10.9 mol %), leucine (7.6 mol %), glutamic acid (15.5 mol %), and serine (9.9 mol %) which makes up the protein keratin⁵.

Wool fibres appeal to manufacturing industries due to their unique tenacity and fibre curvature⁶. These particular properties are desirable and research into wool proteome mapping by gel and non-gel techniques has been used to further understand wool fibres⁶. Understanding how wool proteome is mapped is beneficial for designing synthetic fibres that can mimic the properties of wool without having to spend the time and money to harvest it.

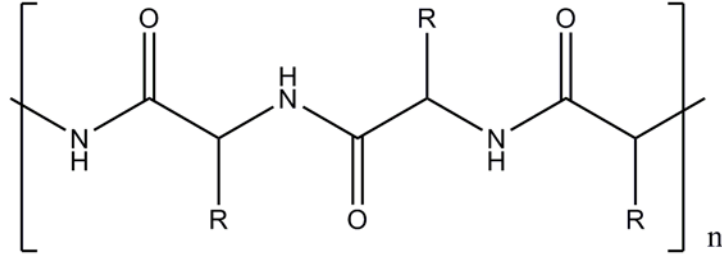


Figure 2. Backbone structure of wool (forms helically) and silk (forms non-helically) – where for wool R comprises most commonly of H (glycine), C₄H₉ (leucine), C₂H₄COOH (glutamic acid) and CH₂OH (serine). For silk, R comprises most commonly of H (glycine), CH₃ (alanine), and CH₂OH (serine).

Silk

Secreted protein fibres come from insects such as the bombyx mori silkworm (silk fibronin) and spiders (dragline silk) which are responsible for the fibre commonly named silk. Silk protein chains will stack on top of each other and primarily contain glycine, alanine and serine. Silk is attractive due to the features it exhibits such as breaking strength, high initial stiffness and is easily processed⁷. Silk fibres however, are found in many important historic textiles and artifacts⁸. Currently, silk is being extensively exploited for new material engineering especially for biomedical applications⁹.

Natural Cellulose Fibres

Cotton

Cotton is the most widely used textile in the world and is harvested from the *Gossypium* plant. Cotton in its natural form consists of roughly 90% cellulose which makes it highly vulnerable to decomposition¹⁰. The stability of interchain hydrogen bonding in cellulose allows cotton to be a versatile textile fiber that can be used for a wide range of clothing applications.

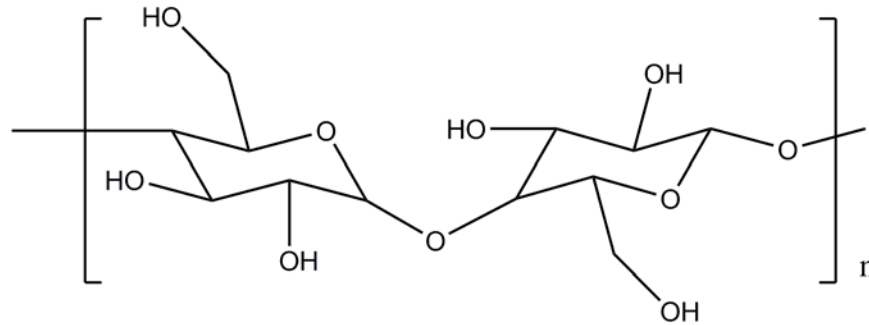


Figure 3. Chemical structure of cellulose - The backbone of cotton, flax, and rayon fibres.

Flax

Flax is another example of a cellulose-based fibre and is often made into linen. Flax contains about 70% cellulose and is derived from the stalk of the *Linum Usitatissimum* plant (linseed). Flax is one of the first natural fibres to be extracted, spun and woven into textiles and has been dated back to 5000 BC¹¹. The large amount of hydroxyl groups in flax and cotton results in a hydrophilic properties for natural fibres when used to reinforce hydrophobic matrices¹¹. Flax fibres are generally very strong and durable and have minimal elasticity.

Manufactured Regenerated Fibres

Rayons

Rayons are forms of cellulose (originating from lignin) that have been regenerated (e.g. lyocell is one form of rayon). The definition of rayon refers to the chemical structure of cellulose where no more than 15% of the hydrogen's have been replaced by hydroxyl substituents. Lignin is often hard to separate into a fibrous form, which is why purifying methods are needed. Nitrocellulose was one of the first methods developed in the mid-eighteenth century that treated cellulose with nitric acid. The resulting nitrocellulose however, was extremely flammable and explosive and this resulted in a useless product as a textile but did prove useful for explosive applications (replacing gun powder). Further research found that

when the nitrocellulose was dissolved into ether, then alcohol, and then evaporated (alcohol and ether), it could be spun into yarn².

Acetate (also known as Triacetate)

A fibre forming substance that is manufactured as cellulose acetate is also commonly described as “acetate”. The acetate refers to cellulose that has at least 92% of the hydroxyl groups acetylated. Acetate is sometimes referred to as triacetate wherein 3 of the hydroxyl groups on the component glucose monomers are acetylated. Cellulose acetate contains bulky acetate groups throughout that make sterically difficult stacking. To add to steric hindrance, the acetate group has replaced many hydroxyl groups which have previously made for a strong stacking attraction between the molecules. The resulting acetate fabric is heat sensitive (vulnerable to melting when ironed), delicate and has such properties as high lustre, low static and low cost to produce. Acetate fibre is most often used to produce clothing with no creases such as dresses.

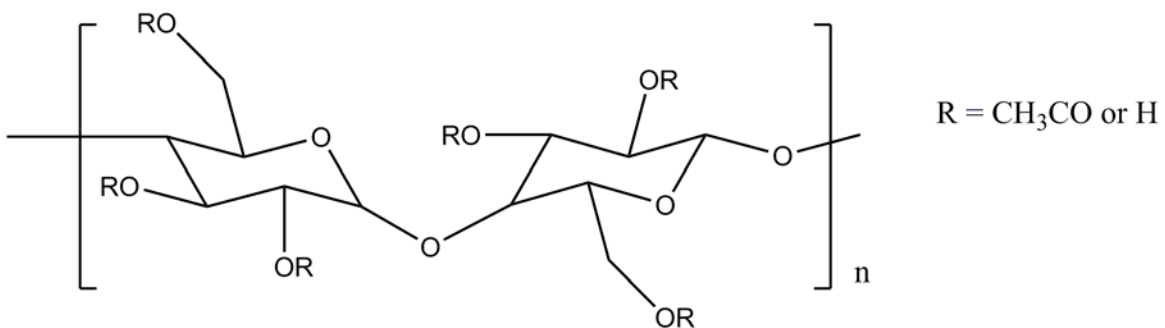


Figure 4. Chemical structure of cellulose acetate.

Manufactured Synthetic Fibres

Polyamide fibres

Polyamides are polymer chains which have repeating amide groups incorporated into their structure. Nylon is one of the most common types of polyamides that are currently used today. One example of how synthetic polyamides are formed is by a condensation reaction in which the linkage of the molecules occurs through the formation of amide groups². The reactant molecules are selected to yield linear molecules of polyamide after reaction has taken place. The linear polyamides are then spun to create nylon fibres.

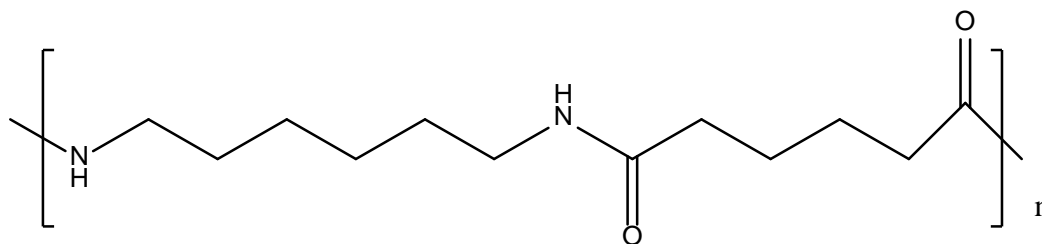


Figure 5. Chemical structure of nylon 6, 6.

Polyester fibres (Polyethylene Terephthalate)

Polyester is a polymer chain containing at least 85% (w/w) of an ester of a substituted aromatic carboxylic acid which includes substituted terephthalate units and para substituted hydroxybenzoate units. Polyester is made by condensing ethylene glycol with terephthalic acid or dimethyl terephthalate². The advantages of polyester are that it is UV resistant, light weight, and versatile for blending with other types of fibres. It is useful for clothing, home furnishings, and outdoor applications.

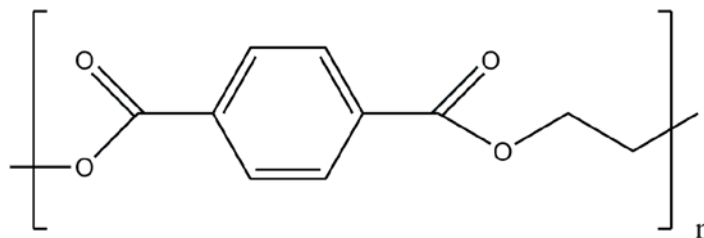


Figure 6. Chemical structure of polyethylene terephthalate (an example of a polyester).

Polyolefin fibres

Polyolefin fibers are made up of a combination (at least 85% total) of the two compounds ethylene and propylene. One of the advantages of polyolefin is that they are very abundant. They are a by-product from the petroleum industry which produces polypropylene as a cheap raw material. The unique characteristics of polyolefin fibre is that it is very light, strong, stain, static, sunlight, and odor-resistant, non-allergenic and it is very fast drying. It is found in carpets and also used for making shrink wrap.

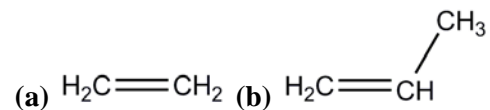


Figure 7. Ethylene(a) and Propylene(b) make up the main monomer units in polyolefin fibers.

Polyurethane fibres

Polyurethane fibres are created by the addition of urethane groups (-NHCOO-) to a polymer. One example is the addition of butane diol with toluene di-isocyanate to form polyurethane². The most common type of polyurethane fabric is spandex. Spandex by definition is a manufactured fibre that is a long chain synthetic polymer comprised of at least 85% of segmented polyurethane². Spandex is well known for the fibre elasticity and ability to stretch multiple times the fibre's length. Spandex is particularly comfortable and can be used for clothing or underwear.

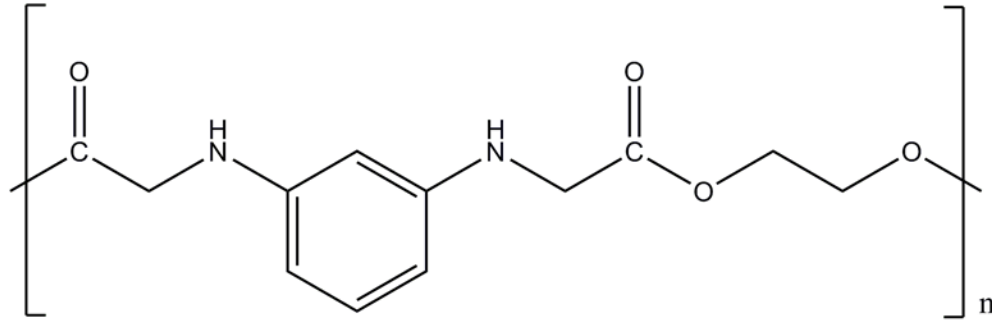


Figure 8. Chemical structure of a polyurethane backbone structure.

1.1c Current Techniques for Analysing Textiles

There are numerous techniques used for studying textiles either quantitatively or qualitatively. Some are used for identifying dyes within the textile (e.g. high performance liquid chromatography) while others are used to study the fibre itself (e.g. pyrolysis mass spectrometry). Other analysis techniques rely on the physical properties of textile fibres such as tensile strength tests. Each technique has its own advantages and disadvantages for studying textile fibres and the drawback of one technique could be the advantage of another and vice versa.

Microscopy

Historically, one of the most common techniques for examining textiles is microscopy. There are various forms of optical microscopy (OM) that can be used including fluorescence microscopy (FM), polarized light microscopy (PLM), stereomicroscope (SM), or scanning electron microscopy (SEM).

In some cases with textile fibres, sample preparation such as specific cutting techniques may be applied or the addition of an adhering compound to help the sample stay on the slide. This can lead to higher quality images specifically for yarns, fibres and fabrics (e.g. denim or

faux fur)¹². For identification of textile fibres using microscopy, the most common preparation techniques are longitudinal and cross-sectional. Longitudinal preparation involves placing a fibre lengthwise with each end dipped in either cellulose acetate or cellulose nitrate to adhere to a glass microscope slide¹². Cross section preparation technique involves immobilizing fibres in supporting material and then cutting the fibres into small sections that are perpendicular to their longitudinal axis (~15 µm)¹².

Routine analysis is most common for blend level determinations, flaw analysis and quality assurance that require fast preparation techniques¹². When dealing with historical textiles, their preservation is of utmost importance. When this is the case, then a more sensitive approach for handling may be applied such as grinding¹².

Scanning electron microscopy (SEM) has been used for fibre analysis for over 20 years¹³. Scanning electron microscopy can provide a very high definition view with minimal sample required (5-10 mm in length)^{13, 15}. Fibre identification, treatment validation, and forensic analyses are a few applications where SEM can be applied. Wilson *et al.* used SEM-EDX (Energy-dispersive X-ray spectroscopy) for the validation of model iron-tannate dyed textiles¹⁴. Energy-dispersive X-ray spectroscopy can be used for elemental analysis of a sample by applying an X-ray beam and measuring the energy from the elemental emission. Scanning electron microscopy EDX was used to scan historical textiles to determine the presence of iron dyes. Once Fe was identified in the textiles, it was found that the Fe-tannate dyes increased surface acidity from tannic acid on the textile and made it more brittle¹⁴. In forensic analysis, Pelton proposed SEM as a method to distinguish the cause of textile fibre fractures.¹³

For ancient samples that are often deteriorated, SEM and OM are used with a variety of other analytical techniques for identification of the fibre. Liu et al applied high performance liquid chromatography with photodiode detection, OM, SEM, and Fourier transform infrared spectroscopy (FT-IR) to identify ancient textiles from Yingpan, Xinjiang¹⁵. SEM was used to determine longitude outline characteristics and the cross section strip shape was described using OM which was used for identifying ancient silk¹⁵. Using multiple techniques makes it possible to identify both modern and ancient fibres. Physical damage and artificial counterfeits often make the textile fibres identification very difficult¹⁶. Damaged textile fibres can produce hindered measurements (e.g. cross sectional distance or surface analysis) which are used for identification. This results in a textile fibre that is difficult to examine as there will no longer be a match with reference measurements.

Vibrational Spectroscopy (Raman and Infrared)

Infrared spectroscopy (IR) is used in forensic science as an identification method for textile fibres¹⁷. Infrared spectroscopy can be applied to a variety of areas for textile analysis such as characterization of age markers, routine industrial applications, and quality control. Infrared spectroscopy relies on the bonding structure of a compound for identification and this can be used to distinguish the cellulosic, proteinaceous and regenerated natural fibres and the many different types of synthetic fibres⁸. Infrared spectroscopy does have its own disadvantages. Infrared spectroscopy for the use of identifying textiles can be a lengthy process as you are piecing together the compound by identifying the individual transmittance peaks obtained in the IR spectrum (the peaks are not specific and refer to functional groups which must be pieced together by the researcher). This type of spectroscopy utilizes both stretching and bending vibrations for analysis. Different bonds may absorb within similar ranges (stretching and

bending), which can produce overlapping peaks making it difficult to identify each bond type within the compound of interest. For example an overlap can occur between a strong, broad O-H where stretching occurs between $3200-3650\text{cm}^{-1}$, while amine stretching N-H (2°) is much weaker and absorbs between $3300-3400\text{cm}^{-1}$. Overlapping peaks can cause IR spectroscopy to be a difficult technique on its own for textile identification, and often may require other methods to verify the identity of fibres. Lowe *et al.* used the combination of ATR-FT-IR with GC-MS to determine lipid decomposition by-products in buried textiles¹⁸. When using these techniques for analysis it was determined that FT-IR was more of a qualitative method for determining the degradation effects of buried textiles, and GC-MS was more quantitative, sensitive and accurate for identifying the lipid decomposition by-products of the buried textile samples¹⁸.

Infrared (IR) spectroscopy has also been utilized as a method for the qualitative decomposition analysis of aged silk fabric¹⁹⁻²². The fibronin that makes up the greater part of silk has been used as a key compound that displays yellowing with age. Koperska *et al.* applied IR spectroscopy to fibronin deterioration and aging to characterize degradation markers of silk¹⁹. Structural changes in wool fibre keratin have been evaluated after being treated with orthosilic acid using FT-IR and Raman spectroscopy²³. Infrared spectroscopy was found to be particularly useful for monitoring disulphide bonds within the keratin structure²³.

Infrared spectroscopy is a method that can be effective for routine analysis such as quality control in textile factories to maximize quality and efficiency. Chung *et al.* used FT-IR to develop a method for the routine analysis of cotton after it has gone through the scouring process. The presence of wax/pectin that remains on the fabric after scouring can be identified using FT-IR²⁴.

Raman spectroscopy is also a vibrational spectroscopy technique that depends on the light scattering caused by bond vibrations of a sample. Raman spectroscopy can be more useful for analysing a polymer chain than infrared spectroscopy because the polymer backbone bonds do not have large dipole moments (IR requires dipole moments) owing to the repetitious identical functional groups²⁵. A common benefit that both IR and Raman spectroscopy share is that they are non-destructive techniques and may require little to no sample preparation when analysing textile fibres. This is particularly useful for the analysis of artifacts and valuable objects. Andreev *et al.* analysed historical textiles using near IR Raman spectroscopy to determine the dyes and natural substances within plants that are used for dyeing textiles (e.g. Xanthone dyes)²⁶. Dyes are often associated with specific textiles and may contain information that is specific to the fibre. Indigo, Turmeric, Pomegranate, and Kamala are a few examples of dyes that have geographical significance for historical textiles²⁷. Dyes used in historical textiles can be isolated to specific geographical regions based on the culture of that region, and availability of the ingredients used to make them. The limited availability of animal sources of dyestuffs and the difficulty of extracting and producing the dyestuffs from these sources explains why they have been so highly valued during certain periods of history²⁹.

Surface enhanced Raman spectroscopy (SERS) is a common approach of Raman which provides surface-sensitivity whereby it may be possible to detect single molecules^{29,30}. The small sample size required has led to successful identification of madder in a 25 μm sample from an ancient Egyptian painted leather fragment²⁹. When using SERS, the signal is enhanced when organic molecules with large are adsorbed on atomically rough metallic substrates²⁹. By utilizing nano particles, the Raman analysis becomes more sensitive and limited sample is required for analysis.

Raman spectroscopy can be used to analyse chemical compounds or biological compounds that reside either on the surface or intertwined in the textile fabric. Ali *et al.* explored a national security application of confocal Raman microscopy for detecting explosives on clothing such as pentaerythritol tetranitrate (PETN), trinitrotoluene (TNT), and ammonium nitrate as well as the explosives precursor's hexamethylenetetraamine (HMTA) and pentaerythritol³¹. Raman spectroscopy can detect these compounds so it is widely becoming utilized by government agencies⁹⁶. Raman spectroscopy also has drug identification applications. Ali *et al.* utilized Raman spectroscopy for the detection of cocaine hydrochloride in clothing that has been contaminated with the illegal substance³².

Raman spectroscopy has also been used for microbiological applications in textiles. Raman was applied to cotton and polyester for the identification of *Escherichia coli* bacteria on the fibre surface³³. Raman can be a powerful tool for identifying the presence of particular compounds of both chemical and microbiological origin. Like IR, when using Raman for a sample containing a combination of compounds (e.g. fibre mixture) it can result in difficulty for the identification of each individual textile due to the lack of sensitivity.

Atomic Spectroscopy

Inductively coupled plasma mass spectrometry (ICP-MS) is a method of analysis associated with aged textiles. ICP-MS is more specifically used to identify metals woven into fibres, sequins, or in chemical compounds used as dyes¹⁵. Gold, Ag, Cu, and their combinations or alloys in ancient times were used as decorative pieces that were woven into textiles³⁴. More recently ICP-MS was used to determine trace metals that are of environmental concern in textiles (e.g. Cr and Cd). Textiles can take up such metals during the production, dying process, storage, and from the surrounding environment. Pranaitytė *et al.* created a method for extracting trace

heavy metals Cd, Cr, Cu, Ni and Pb from textiles using aqueous 0.07 mol/l HCl solution³⁵. Each metal was found to be extractable to some extent, but because each differs in physical and/or chemical binding capacity to the textile, they were not all equal in concentration (mg/kg)³⁵. This method was not particularly useful for Cd with extractable levels below the detectable limit, Cr and Ni ranged from 15-20%, Cu and Pb were 60%³⁵.

Atomic absorption spectroscopy (AAS) is another method described for identifying metal components in textiles by dissolving the fiber prior to analysis³⁴. X-ray fluorescence (XRF) spectroscopy is also a powerful tool for determining elements present in a particular sample. Ide-Ektessabi *et al.* and Wilson *et al.* used XRF for the analysis of historical textiles to determine their elemental composition non-destructively, and found they contained Fe, Ca, Ti, Cu, Pb, Zn, As, Rb, K and Au^{36, 37}.

Separation Methods

Separation methods are techniques analytical chemists use for determining what compounds may be in a sample. A separation of these compounds is performed by many different ways depending on the sample type. For example, volatile samples are well suited for gas chromatography (GC) and liquid samples would be ideal for high-performance liquid chromatography (HPLC). When using separation methods there is a mobile phase and a stationary phase. The mobile phase refers to the mobility of the sample with the carrier gas through the column. The column can be comprised of a solid or liquid inner coating, each of which interacts with the sample. This interaction between the compound and the column inner coating is referred to as the stationary phase. The interaction of the mobile sample travelling through the stationary column will separate the compounds based on their partition coefficient between mobile and stationary phases, which causes the compounds to reach the detector at

different times (aka retention time). Many factors affect the compounds retention times including but not limited to column type, temperature, mobile phase reagent/carrier gas or detector type.

Gas chromatography is a particularly useful tool for textile analysis as it is a useful technique that provides information on the sample composition. One stipulation with this technique is that the sample must be volatilized, creating a time consuming preparation phase. Thus, textile fibres cannot be directly analysed using MS unless it has been pyrolysed for GC.

Pyrolysis gas chromatography (PyGC) is a method that can be used for textile analysis. This approach uses a heater element that attaches to the inlet of the GC to pyrolyse the sample prior to injection. The pyrolyser consists of a platinum wire or quartz tube that heats the sample to temperatures $>600^{\circ}\text{C}$ in order to decompose the sample. The pyrolysed sample is then directly sent into the column where the GC separates the compounds produced. Pyrolysis gas chromatography is used to gather chromatographic information of the pyrolysis compounds in order to determine the composition or structure of the original sample³⁸. Pyrolysis GC is part of a broader class of analysis called thermo-analytical methods. Thermo-analytical methods are especially useful for characterizing insoluble polymers (e.g. cross-linked materials)^{38, 39}. Synthetic polymers and natural fibres have also been analysed using PyGC with success³⁸⁻⁴⁴. Causin *et al.* proposed a method for the analysis of colorless acrylic fibres using PyGC-MS to differentiate fibres with similar morphology⁴³. However, it has been found that major drawbacks lie with the PyGC, low reproducibility and the effects that inorganic fillers (as they cannot be separated) have on pyrolysis. The more complex inorganic fillers are made, the more complex the pyrolysis becomes resulting in a GC chromatogram that can be difficult to decipher^{44,45}. For

acrylic, a method has been developed to determine whether reactive co-monomer and/or amino resin are present in the acrylic copolymers⁴⁶.

Catalysts are often used to aid in the pyrolyzation process by decreasing the reaction temperature or reaction time. By doing so, certain compounds are unable to volatilize and others may even be promoted. For example, Yamada *et al.* applied imidazole catalysts to decrease the reaction temperature and increase the speed at which the reaction occurs for characterizing epoxy resins⁴⁷. Screening out the compounds that are not of interest can make the analysis more reproducible and easier for identification. This process can also contribute to removing overlapping peaks that can be caused from unwanted compounds. Another example of this was the work done by Takekoshi *et al.* who combined NaOH with wool prior to analysis to further promote the production of volatile compounds from the amino acid residues in wool protein⁴². Compared with conventional non-catalyzed PyGC, the alkali-catalyzed PyGC was found to greatly improve the detection limit of wool fibre and make it possible to analyze very minute samples of wool fibre (0.2 mg)⁴².

Pyrolysis GC-MS is a method that can be used for identification, as well as the thermal processes that occur from decomposition. Zhu *et al.* was able to determine that there are three stages of the pyrolysis of cellulose (initial pyrolysis stage, main pyrolysis stage and char pyrolysis stage)⁴¹. This information is particularly useful for identifying cotton using pyrolysis techniques. Most pyrolysis compounds are produced from cotton in the main pyrolysis stage⁴¹. This means that in order to achieve the optimal pyrolysis compounds, a temperature of 300-380°C must be reached for cotton. This technique has also been introduced for qualitative determination of banned aromatic amines released from azo dyes on textiles⁴⁸. Pyrolysis GC can be especially useful in cases where other methods (e.g. microscopy, FT-IR) cannot be

successfully used because samples may have experienced partial pyrolysis prior to analysis (e.g. synthetic fibre at a crime scene of a house fire)⁴². Gas chromatography is more efficient when fragments with low molecular weight are introduced to the GC column. The production of high molecular weight fragments can foul the GC detector causing interference with detecting characteristic additive fragments³⁸. When using a pyrolyser, it is often difficult to predict the fragmentation due to the effects that the temperature may have on different compounds. This can lead to large fragments (>550amu) entering the GC column. Larger fragments often have higher boiling points and do not break down into a gas within the column. This can cause the column to become backed up producing irregular flow and hindering future runs.

High performance liquid chromatography (HPLC) is another analytical tool that can be used for textile analysis. This technique is useful for analyzing samples that cannot be run using a GC-MS because of their chemical form because of large molecular weight or volatility. Dyes are often associated with HPLC and textile analysis and can be detected at the ≤ 1 mg/g fibre or fabric²⁸. In order to analyse the dyes within the fibres, extraction techniques must be used. The vigorous conditions of extraction cause hydrolysis of the glycosides, particularly of the yellow flavonoid dyes, and therefore, reduce the information content of the analysis²⁸.

High performance liquid chromatography is particularly useful for identifying dyes in historical textiles like red cochineal dye, which was used in many historical pieces⁴⁹. It has also been used for the characterization of dyestuff in 16–17th-Century Ottoman Silk Brocades⁵⁰. Surowiec et al used HPLC for the analysis of 17th century textiles recovered from peat bogs to determine if any dyes remained and if so what their origin was⁵¹.

1.1d Solid Phase Micro-extraction Gas Chromatography Mass Spectrometry (SPME GC-MS)

Solid phase micro-extraction (SPME) is a sampling method that was first invented in the early 1990's by Professor Janusz Pawliszyn from the University of Waterloo⁵². Since then SPME has been used in a wide range of applications including the analysis of old books, food chemistry, water waste water, and forensic science. Solid phase micro-extraction itself requires little maintenance and makes for a clean, fast process with no hazardous waste. It is a solventless technique that requires no reagents or additional chemicals. Solid phase micro-extraction is an extraction method that combines sampling, compound isolation and equilibration in one step⁵³. It was developed to facilitate rapid sample preparation and is an alternative to traditional methods for separating target analytes from a complex matrix⁵⁵. Solid phase micro-extraction is a technique that can determine very low concentrations of analyte. The portable SPME-GC can detect semi-volatile concentrations in the parts per billion (ppb) to parts per trillion (ppt) range^{55, 56}.

Solid phase micro-extraction consists of a fused silica fibre that is contained within syringe needle. The fibre can be exposed to the sample containing the analyte of interest by pressing the top of the syringe. The analytes adsorb to the fused silica fibre and once an equilibrium is reached (2-30 minutes)⁵⁷. The fibre is retracted within the apparatus and can be analysed using GC-MS analysis at a later time.

Each fused silica fibre is often coated with a polymer that helps adsorb the analyte of interest. For liquid coatings, there is a linear correlation between the amount of analyte adsorbed and the analyte concentration^{57, 58}:

$$n = \frac{K_{fs}V_f C_0 V_s}{K_{fs}V_f + V_s}$$

n = mass of analyte adsorbed by coating

C_0 = initial concentration of analyte in sample

K_{fs} = partition coefficient for analyte between coating and sample matrix

V_f = volume of coating

V_s = volume of sample

There are many different coatings that can be chosen depending on the target analyte of interest (Table 1). Solid phase micro-extraction consists of a fibre that is coated with either a polar or non-polar compound such as polydimethylsiloxane (PDMS). The coating that is attached to the SPME fibre bonds with the target molecules through van der Waals and hydrogen bonding. This holds the target molecules in place until heat is applied to release them from the coated fibre.

Table 1. Examples of SPME coatings and their intended analytes of interest^{57, 58}.

<u>Coating Type</u>	<u>Coating size</u>	<u>Analytes of interest</u>
<i>Polydimethylsiloxane (PDMS)</i>	100µm/ non bonded	-Volatiles
	30µm/ non bonded	-Nonpolar semivolatiles -Moderately polar to nonpolar semivolatiles
<i>Polydimethylsiloxane/Divinylbenzene (PDMS/DVB)</i>	7µm/ bonded	-Polar volatiles
	65µm / partially crosslinked	-General purpose (for HPLC only)
<i>Polydimethylsiloxane/Carboxen (PDMS/Carboxen)</i>	60µm / partially crosslinked	-Trace level volatiles
<i>Carbowax/Divinylbenzene (CW/DVB)</i>	75µm / partially crosslinked	-Polar analytes
<i>Carbowax/Templated Resin (CW/TPR)</i>	65µm / partially crosslinked	-Surfactants (for HPLC only)
<i>Polyacrylate</i>	50µm / partially crosslinked	-Polar semivolatiles
	85µm / partially crosslinked	

Two collection methods have been introduced for SPME. For the first method, the fibre can be directly immersed in a sample for collection (DI-SPME/In vivo SPME). This method is most often associated with liquid samples. In the case of analysing volatile compounds, the second method is more suitable whereby the SPME fibre is placed above the sample in the headspace region (HS-SPME).

Solid phase micro-extraction provides a clean, non-hazardous, and inexpensive means of analysis. When SPME is coupled with GC-MS it is a powerful tool that can be used for analysing textiles. Currently, HS-SPME has been used for identifying degradation compounds. Headspace SPME GC-MS has been found as a viable technique for quantitative and qualitative analysis of volatile degradation products in paper⁵⁹⁻⁶². Headspace SPME has been applied to textile clothing samples in a successful attempt to identifying volatile organic carbon compounds evolving from the clothing⁶³. Solid phase micro-extraction is a versatile technique that can be used in other areas of textile research. For example, Lisovac *et al.* analysed sheep wool for volatile organic carbon compounds using HS-SPME to determine the odour differences⁶⁴. Essentially any liquid or gaseous sample with a target analyte applicable to the SPME coating can be analysed, including water and wastewater, pharmaceuticals, pesticides, or food products. Hu *et al.* used HS-SPME to analyse organophosphate pesticides found in cotton⁶⁵ and Wang *et al.* used in vivo SPME to determine various contaminants in wastewater effluent and their bioaccumulation effects on exposed fish⁵⁴.

GC-MS is highly sensitive technique that requires a very small sample (<0.5mL). With HS-SPME the pyrolysis occurs in a sealed vessel or container separate from the GC itself. Py-GC-MS has a pyrolyser attached to the top of the injection port, so the sample is directly sent into port once pyrolysed. For SPME, the potential problems with fouling the GC detector are

avoided, and only volatile compounds are collected. After each collection using the SPME apparatus, the injection port temperature that causes the compounds to dissociate from the fibre acts as a cleaning process. The SPME apparatus can immediately be used for another collection with essentially no maintenance. Once the SPME apparatus has been placed into the injection port, the GC-MS analysis works the same way as previously described with Py-GC-MS. With HS-SPME GC-MS, there is less chance of producing non-target analyte peaks as the coating will adsorb only the designated analyte types. This will produce a cleaner chromatogram in comparison to direct pyrolysis, making it easier to identify target analytes. Another advantage of this technique is that the collection and analysis are separate. Therefore, the collection can occur in a different location than the analysis.

1.2 Research Objectives

The first objective of this research is to develop methodology for identifying textile fibres from volatile compounds evolved from textile objects by applying HS-SPME. The compounds examined are in the form of a gaseous mixture, and are identified by the GC-MS. Properties associated with the method were evaluated by effects of each had on the resulting chromatographic pattern. These properties refer to the temperature, the sample size, and collection time. Determining the effects each has on the chromatogram can be seen by identifying the compounds associated with each textile and monitoring any changes with the volatile compounds within the chromatogram.

The second objective was to evaluate the capability of HS-SPME GC-MS for studying blended textile samples. By varying the composition quantities for each of the individual textiles within a blend, it will represent the ability for the method to assess the effects on the properties of individual textiles in higher or lower concentration. Three combinations of composition quantities were used: 50%/50%, 25%/75%, 75%/25%.

The third and final objective was to use HS-SPME GC-MS to identify changes in the volatile compounds that evolve in aged samples. The application of SPME GC-MS to aged textiles can possibly be used to identify chemical markers of degradation. This could be useful for determining the age of the textile, and provide information on ways to preserve textiles in the future. The accelerated aging processes used will include humidity, ultraviolet light (UV), and heat. This will be applied to mimic the conditions a naturally aged textile will undergo within a given time period. The textiles used for these experiments were polyester, cotton, wool, acrylic, silk, and olefin.

1.3 Experimental

1.3a Sample Preparation

For un-aged samples, each textile was separately placed in a desiccator for a period of 24 hours prior to analysis. Textile samples were weighed using a 5 decimal point balance (Mettler Toledo XP 105). Once the samples were weighed, they were analysed within the same day (in most cases within a period of 2 hours). Table 1 provides a list of the textile samples used.

Table 2. Textile sample origin, purity and manufacturer.

Textile	Manufacturer	Origin
100% Polyester	Red Heart	Turkey
100% Acrylic	Red Heart	Turkey
100% Cotton	Bernat Handicrafter	Canada
100% Wool	Johnstons of Elgin	Scotland
100% Silk	Unknown	Canada
100% Olefin	Unknown	Canada

1.3b Method Protocol

Before any textiles were analysed, a sample blank was collected in order to ensure there are no contaminants contributing to the textile collection. The cleaning process involves immersing the glass sample tube in a 50 % (w/v) HCl solution for a minimum of 1 hour. The glass sample tube is removed and scrubbed with a brush using copious amounts of distilled water to rinse and left to dry. The quartz cup cleaning process involves using a brush to scrub the cuvette and also applying tweezers to scrape down any residue that is left. Extreme heat 600-700°C was applied to the cup to drive off any leftover material that cannot be removed using tweezers. Cleaning occurs every time the apparatus will be used for collection. Once cleaned,

the sample blank can be collected. The sample blank involves running the full method aside from the sample preparation, as there is no sample. Upon collection, SPME can be placed in the GC-MS inlet for chromatographic analysis. When no compounds evolve within the chromatogram of the sample blank, the textile samples can be analysed.

1.3c Instrumentation

Headspace Solid Phase Micro-Extraction (HS-SPME)

The volatile compounds collected from each sample were achieved using a 100 μm polydimethylsiloxane (PDMS) SPME fibre from Supelco (57300-U) (Fig. 10). The SPME fibre was conditioned prior to use at a temperature of 250°C for 30 minutes as instructed by the Supelco user manual. During the collection stage, the exposed SPME fibre collects analytes inside a glass tube sampling apparatus which contains a platinum coil where the quartz sample cup sits (see Fig.11). The platinum coil is connected to a Variac autotransformer (Staco Energy Products Output 0-120/140 V), which controls the output of current. The output of current will increase or decrease the amount of heat created from the resistance of the platinum coil. The quartz cup with the sample inside heats up and the volatile gases will evolve. The SPME fibre extends to 3 cm above the quartz sample cup for collection.



Figure 9. HS-SPME 100 μm polydimethylsiloxane (PDMS) SPME fibre.

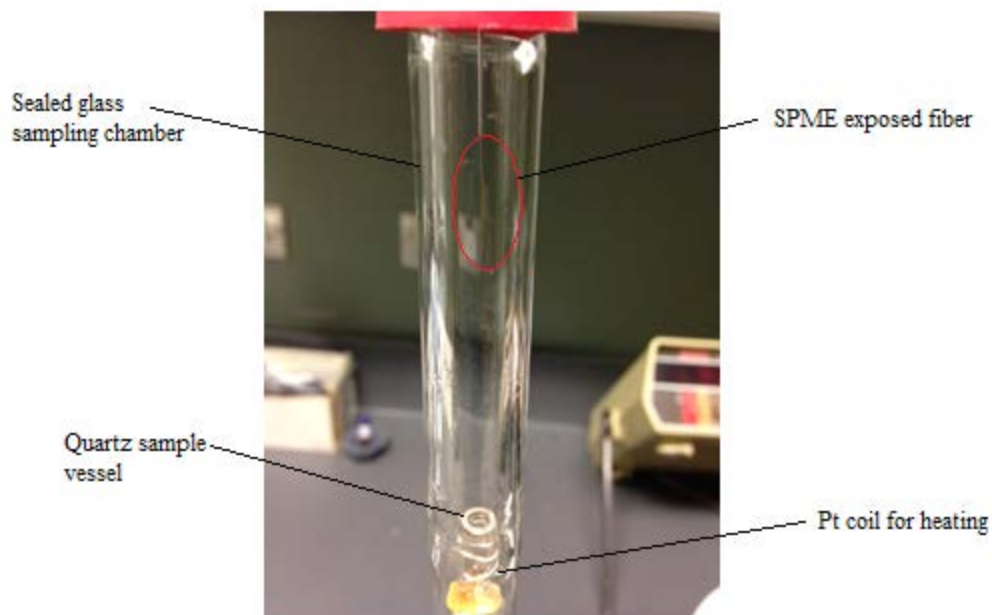


Figure 10. Sample chamber containing the platinum coil wrapped around a quartz sample vessel.

Gas Chromatography Mass Spectrometry (GC-MS)

The instrument used was the Agilent Technologies 7890A GC-MS System. The SPME fibre was manually inserted into the injection port for each run. The column used was an HP-5MS (30m x 250 μ m x 0.25 μ m) column with a stationary phase of 5% phenyl-methylpolysiloxane using He as the carrier gas. The ion source was 230 $^{\circ}$ C for all scans and was performed on electron ionization mode. The MS scan range was set from 50 to 550 m/z. The oven program for determining the optimal temperature for SPME collection experiment was performed starting at 70 $^{\circ}$ C for 2 minutes, then increasing 7 $^{\circ}$ C/min up to 200 $^{\circ}$ C and held for 1 minute. The oven program for all other analysis began at 40 $^{\circ}$ C and increased 5 $^{\circ}$ C/minute up to 270 $^{\circ}$ C and held at that temperature for 5 minutes. This program method was referred to as 'ZED2INLET250.M'. The total time for the temperature program was 61 minutes. The column used was kept at a flow rate of 1.2mL/min at a pressure of 9.1psi with a total flow of 39.723cm/s. The hold time was 1.2 minutes at a constant flow and the post run was performed at a rate of

2mL/min. The inlet had a heater with a temperature of 250°C, pressure of 9.1 psi, and a total flow of 24.2 mL/min, with the septum purge flow at 3mL/min. NIST 2008 9th edition (Wiley Registry®) was used as an additional level of conformation for the identity of compounds.

Chapter 2: Feasibility of Analysing Textiles for Identification using SPME GC-MS

Chapter 2 explores the properties of using pyrolysis sampling and HS-SPME GC-MS for detecting unique chromatographic patterns. The properties that are associated with the method such as temperature, sample size, collection time, chemical markers, and textile source comparison will be assessed.

2.1 Temperature Optimization

The temperature was investigated to determine the effects if any it has on the peak counts and shape and if there was any relationship between this and the volatility of compounds. At different temperatures it is not known if there will be competition among volatile compounds for adsorption sites on the SPME coating. Additionally, factors such as temperature and pH of the surrounding environment can affect the PDMS coated fibre's ability to extract compounds⁶⁷. Therefore, it is possible that different pyrolysis temperatures could produce different volatile compounds.

In these experiments the temperature intervals were increased from 120°C to full pyrolysis (>500°C). The heat from the platinum coil that is applied to the quartz sample vessel differs slightly from the top to the bottom. This is due to the apparatus having an insulated sealant to hold the coil in place (causing a slightly lower temperature at the bottom of the quartz vessel) and to prevent the heat from being distributed in unwanted places. The temperature was measured using an IR thermometer with K-type thermocouple (Omega OS730K) in order to accommodate to the small size of the sampling apparatus. "Full pyrolysis" for this experiment is described as the temperature of (>500°C).

The signal to noise ratio(S/N) will be used to calculate the peak changes if any. The signal to noise ratio is an accurate method for calculating changes in chromatographic peaks that may not be visible. The S/N also accounts for elevated signals, which can occur from time to time depending on the instrument. The S/N is calculated⁶⁶ by determining the average counts of a signal or peak (μ) and dividing that by the standard deviation of the noise (σ). The noise can vary from run to run so it was calculated separately for each chromatogram analysed.

$$\frac{S}{N} \text{ ratio} = \frac{\mu}{\sigma}$$

Olefin

Starting with olefin, temperature settings from 120°C were applied to determine the effects of temperature on the volatile compounds that are released from the textile. Four temperature intervals were used for olefin and the results are displayed in Figure 13:

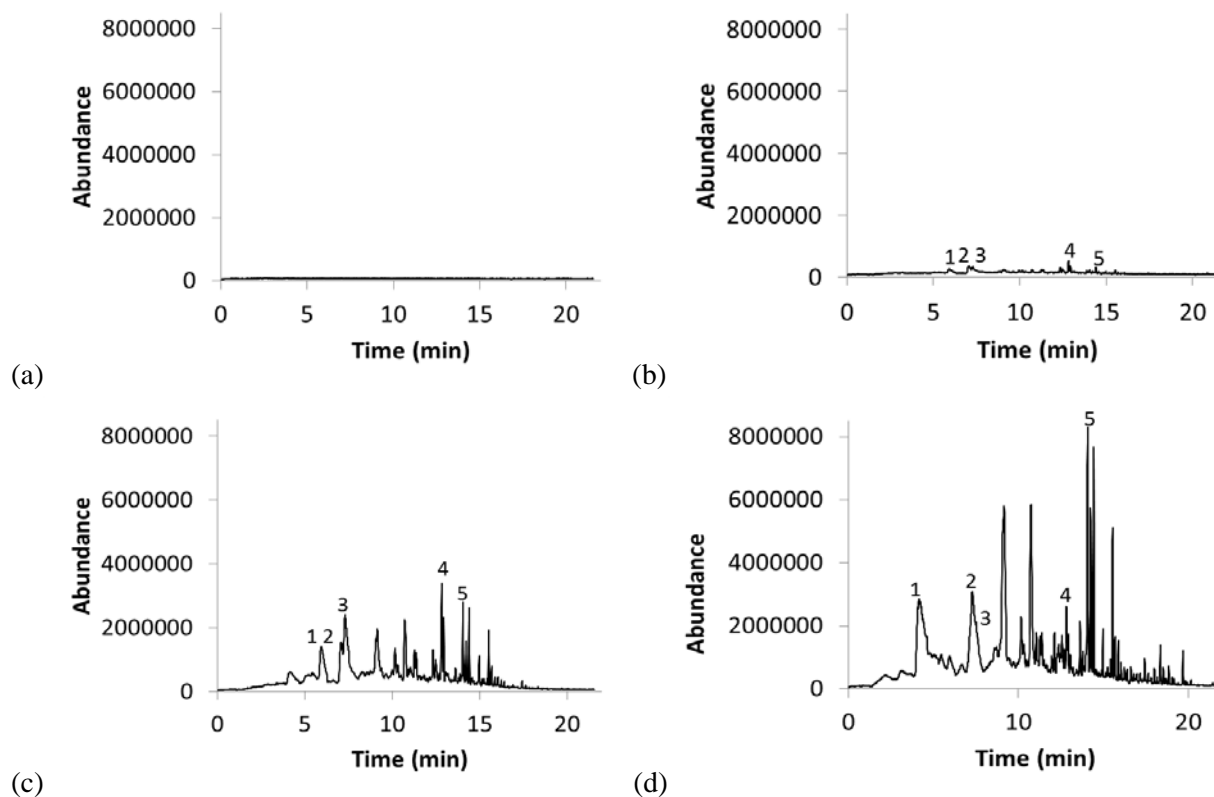


Figure 11. Effects of pyrolysis temperature on the number of compounds released from olefin fibre (a) Temperature setting 1 (Top of crucible: 190-200°C Bottom of crucible: 120-130°C) (b) Temperature setting 2 (Top of crucible: 260-270°C Bottom of crucible: 190-200°C) (c) Temperature setting 3 (Top of crucible: 290-300°C Bottom of crucible: 230-240°C) (d) Temperature setting 4 (Full pyrolysis >500°C)

Olefin displayed the largest number of compounds at the highest temperature (>500°C full pyrolysis). At 120°C, there were no visible peaks that can be detected from the baseline in the chromatogram. At 190°C, the first sign of compounds with a total of 5 peaks. From 230°C to >500°C a very distinguishable set of chromatographic patterns containing multiple compounds can be seen. Peaks 1-5 are displayed consistently through Fig. 11(b), 11(c) and 11(d) (190°C to >500°C).

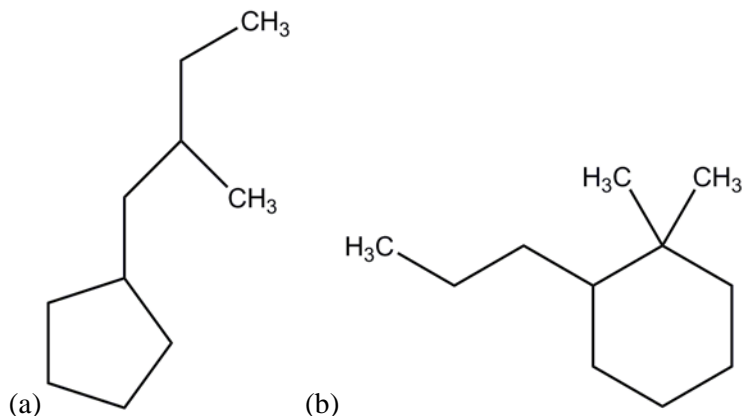


Figure 12. Chemical structure of volatile compounds collected from olefin (see appendix for mass spectrum). (a) 2-methylbutyl-cyclopentane (b) 1, 1-dimethyl-2-propylcyclohexane

The compounds correlating to the labelled peaks in Fig. 11 are 2-methylbutyl-cyclopentane (1), 7-methyl-1-undecene (2), 1, 2-diethyl-1-methylcyclohexane (3), 3, 3, 5-trimethylcyclohexanol (4), and 1, 1-dimethyl-2-propylcyclohexane (5).

The compounds displayed generally consist of simple alkyl chains with minimal branching which can be attributed to the simple structure of olefin. These compounds are related to the temperature at which they are being released (e.g. 3, 3, 5-trimethylcyclohexanol has a boiling point of 198°C⁶⁸). The base compounds that describe peaks (1), (2), (3) and (5) are undecene (~192°C), cyclohexane (~80°C) and cyclopentane (~50°C) which fall within the temperatures analysed. It is surprising that there was a not higher count in the first chromatogram for the compounds that were lower than 100°C. The compound 1, 1-dimethyl-2-propylcyclohexane increased in counts significantly each temperature interval from 67203 counts at 120°C to 7669862 counts at >500°C. The increase in peak counts has also occurred with 3, 3, 5-trimethylcyclohexanol with increasing temperature (120°C to 230°C) from 73409 counts to 3375488 counts. However, for 3, 3, 5-trimethylcyclohexanol at a temperature of >500°C, the counts decreased by 37% for a value of 2070196 counts. The reason for the decrease in counts at a higher temperature for 3, 3, 5-trimethylcyclohexanol could be due to increased fragmentation

at higher temperatures causing the compound to break down and give higher counts to smaller compounds. Ultimately, peak compound counts reaches a maximum, and as 3, 3, 5-trimethylcyclohexanol has proven, the increase in temperature is does not directly correlate to increased counts.

The S/N was 24.75 for 7-methyl-1-undecene in Fig. 11(b), and for 11(c) and 11(d) the S/N increased to 201.5 and 193.5 respectively. Olefin completely melted and began effervescing during the heating stage of analysis. The first temperature setting which was also the lowest, only partially melted the sample during heating. This can relate to the compounds and their respective counts, the lowest temperature experienced the least abundant compounds while the full pyrolysis experienced the most. At higher temperatures ($>500^{\circ}\text{C}$) olefin appears to fragment into numerous compounds in comparison to lower temperatures where less compounds are detected.

Cotton

Cotton has three stages of pyrolysis: initial, main, and char decomposition⁴¹. To maximize the volatile compounds being released from the cotton, the temperature intervals were set according to the stages of pyrolysis. The initial pyrolysis stage of cotton occurs between $0-300^{\circ}\text{C}$, main stage $300-400^{\circ}\text{C}$ and char decomposition $>400^{\circ}\text{C}$ ⁴¹. The results for cotton are displayed in the following Fig. 13:

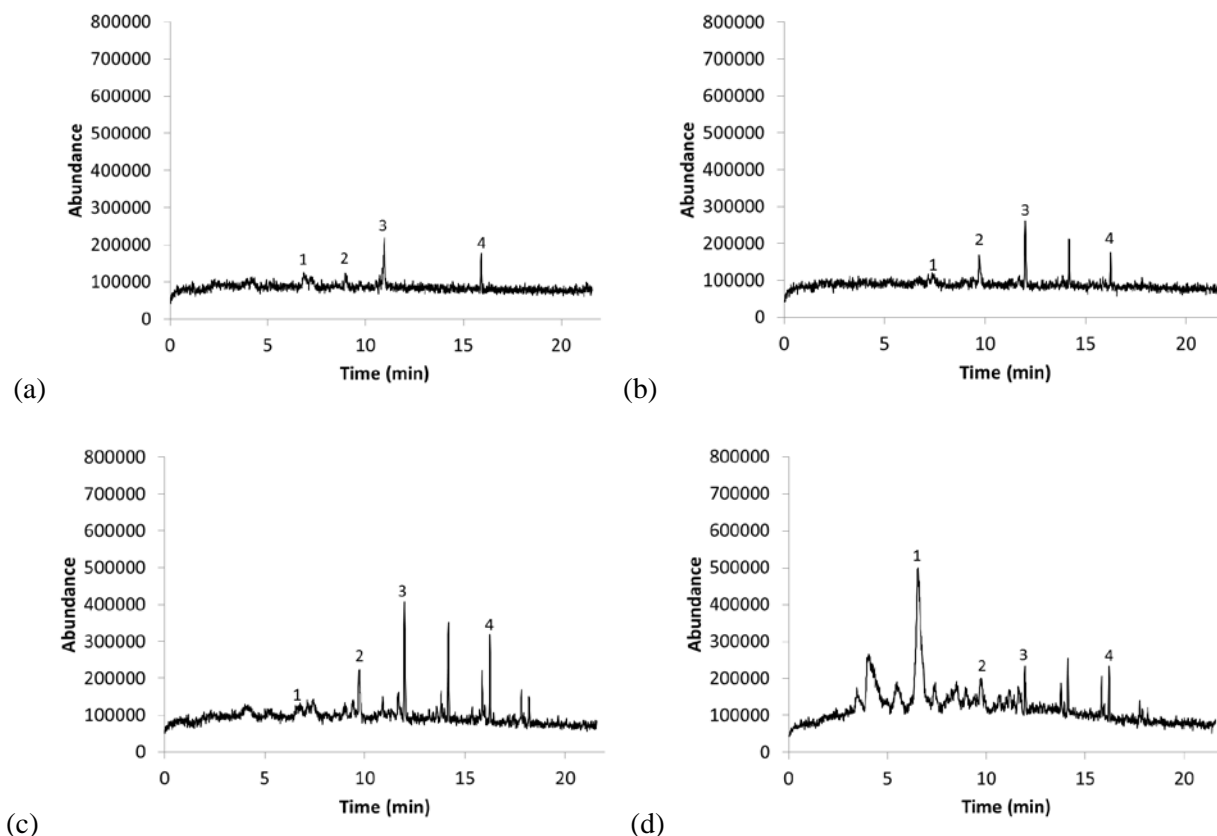


Figure 13. Effects of pyrolysis temperature on the number of compounds released from cotton fibre
 (a) Temperature setting 1 (Top of crucible: 190-200°C Bottom of crucible: 120-130°C) (b) Temperature setting 2 (Top of crucible: 290-300°C Bottom of crucible: 230-240°C) (c) Temperature setting 3 (Top of crucible: 340-350°C Bottom of crucible: 260-267°C) (d) Temperature setting 4 (Full pyrolysis >500°C)

The peak patterns in the cotton chromatograms were different from the olefin chromatograms. Figure 13(a) displayed peaks 1-4 which are marked throughout the cotton chromatograms as they appear. A total of 12 peaks were displayed in Fig. 13(d) the full pyrolysis of cotton (4 original and 8 additional peaks). The compounds responsible for each of the following peaks are 5-methyl-2-furfural (1), 1-methylcyclooctene (2), cyclooctane (3), and dodecanal (4). The compound 5-methyl-2-furfural (1) increases substantially during full pyrolysis which could be attributed to the burning stages of cotton and the higher boiling point (~188°C).

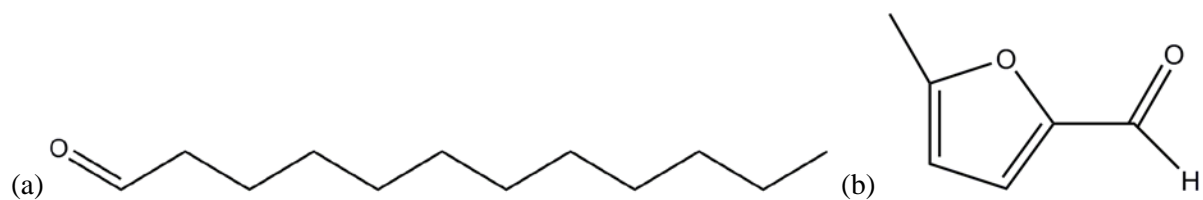


Figure 14. Chemical structure of volatile compounds collected from cotton (see appendix for mass spectrum). (a) Dodecanal (b) 5-methyl-2-furfural

It appears that 5-methyl-2-furfural favors higher temperatures for combustion. The counts increased from 101976 to 496037 from 340 to >500°C. From 190 to >500°C, cyclooctane varies in counts from 217430 to 213651 respectively, with a maximum of 407049 counts at 340°C. Methylcyclooctene and dodecanal doubled in counts from 190 to >500°C as 98129 counts to 194457 counts and 88753 counts to 190814 counts respectively.

The S/N was the largest during full pyrolysis occurring at 36.54 min for peak (1). The optimal temperature was deemed to be full pyrolysis. This was based on the number of peaks that were displayed during full pyrolysis and the S/N. It was observed during the full pyrolysis heating stage, cotton sample completely burned.

Wool

The chromatographic patterns for wool did not differ greatly with different temperatures. At 190°C there were 4 peaks displayed which increased to a total of 7 peaks at >500°C. The compounds responsible for peaks 1-4 are as follows benzaldehyde (1), 2-nitro-phenol (2), benzenepropanenitrile (3), and 4-methyl-2-nitrophenol (4).

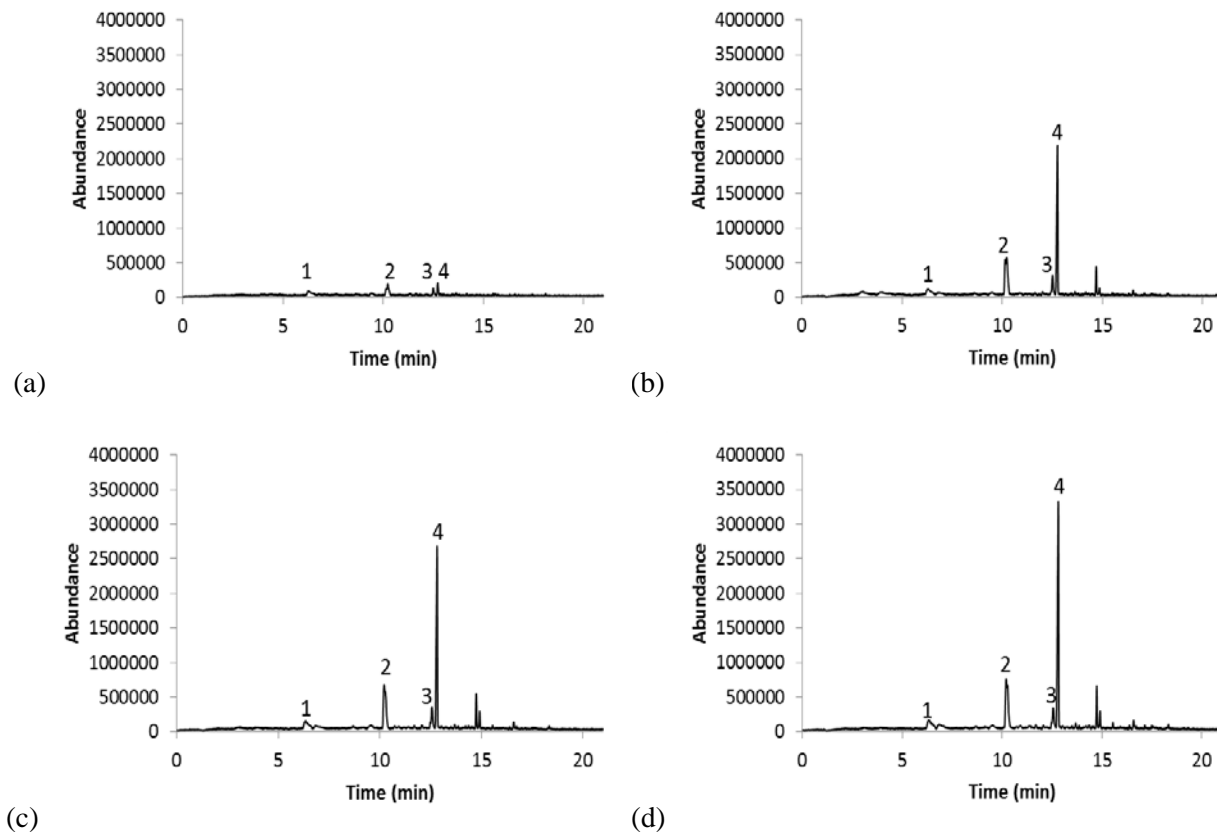


Figure 15. Effects of pyrolysis temperature on the number of compounds released from wool fibre (a) Temperature setting 1 (Top of crucible: 260-270°C Bottom of crucible: 190-200°C) (b) Temperature setting 2 (Top of crucible: 340-350°C Bottom of crucible: 260-267°C) (c) Temperature setting 3 (Top of crucible: 390-400°C Bottom of crucible: 290-300°C) (d) Temperature setting 4 (Full pyrolysis >500°C)

Each compound (1-4) increased as the temperature increased for wool. Benzaldehyde doubled from 190->500°C with an increase of 82251 counts to 167615 counts, while compounds 2-nitro-phenol, benzenepropanenitrile, and 4-methyl-2-nitrophenol increased nearly fivefold.

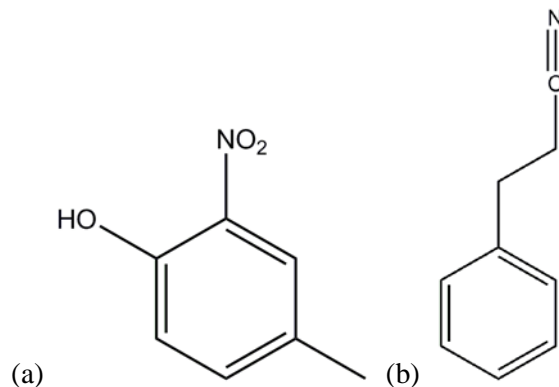


Figure 16. Chemical structure of volatile compounds collected from wool (see appendix for mass spectrum). (a) 4-methyl-2-nitrophenol (b) Benzenepropanenitrile

The compounds that are displayed for peaks 1-4 contain a number of functional groups (e.g. nitrile, nitro, aldehyde, and phenol) which correlates to the amino acid composition of wool. The S/N increased for 2-nitro-phenol from 13.53 in Fig. 15(a) to 43.62 in Fig. 15(d). The wool sample itself did not change much visibly while it was being heated. In every trial regardless of the applied temperature, the wool sample appeared charred once heated.

Polyester

Polyester did not display any distinguishable peaks from 190-200°C. However, between 270 and 280°C a total of 7 peaks were discovered and from 290 to 300°C a total of 9 peaks. When temperatures reached >500°C, the number of peaks doubled to 18 total peaks.

Polyester is made up of ester functional groups and it was found that the volatile compounds released are structurally related. The compounds in the chromatographic pattern are as follows phenol(1), acetophenone(2), 1-phenyl-1,2-propanedione(3), benzoic acid(4), 4-methylbenzamide(5), 1-(4-ethylphenyl)-ethanone(6), 3-phenyl-2-propenal(7), biphenyl(8), 4-methyl-2,6-dihydroxyquinoline(9). Each higher temperature interval increased the counts for each compound. The compounds were undetectable before 270°C which correlates with the

boiling point of compounds released such as benzoic acid (249°C) and biphenyl (255°C), among others. The largest increase in counts occurs between the temperature range of 290 to >500°C, where in some cases the counts increased fivefold (1-phenyl-1,2-propanedione 1127449 counts to 5202391 counts) and six fold (benzoic acid 102254 counts to 665005 counts).

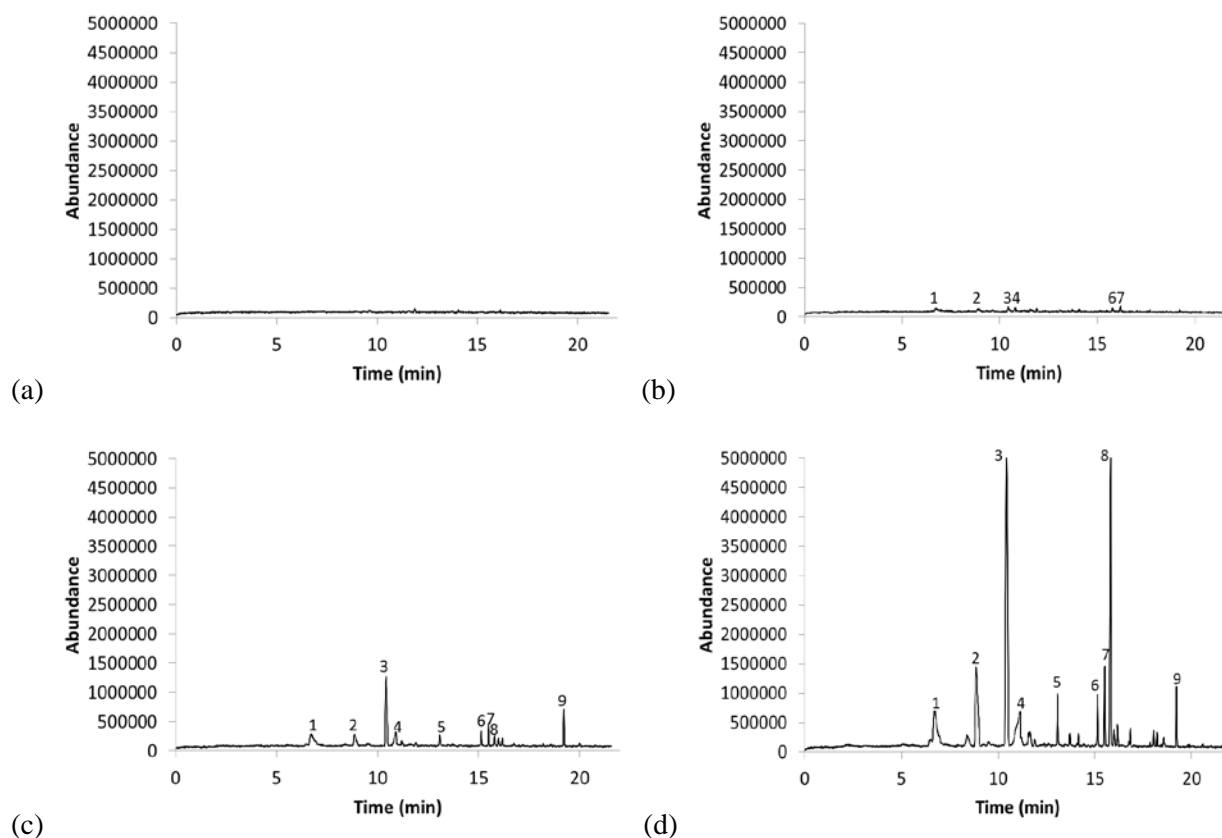


Figure 17. Effects of pyrolysis temperature on the number of compounds released from polyester fibre (a) Temperature setting 1 (Top of crucible: 260-270°C Bottom of crucible: 190-200°C) (b) Temperature setting 2 (Top of crucible: 350-360°C Bottom of crucible: 270-280°C) (c) Temperature setting 3 (Top of crucible: 390-400°C Bottom of crucible: 290-300°C) (d) Temperature setting 4 (Full pyrolysis >500°C)

The compounds detected consist of a variety of aldehydes, carboxylic acids, ketones, alcohols and phenyl groups. These functional groups can be attributed to the recombination of the polyester structure. However, 4-methylbenzamide and 4-methyl-2,6-dihydroxyquinoline

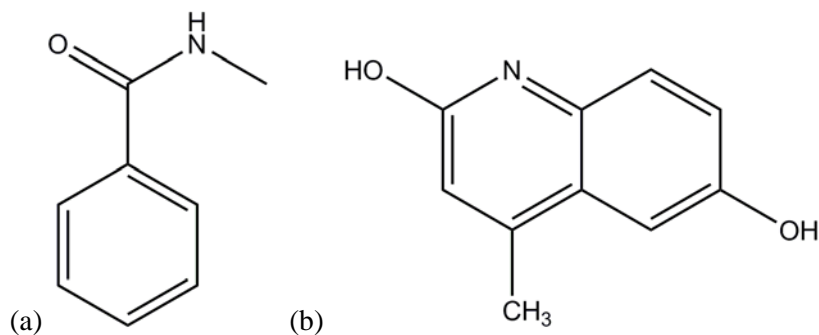


Figure 18. Chemical structure of volatile compounds collected from polyester (see appendix for mass spectrum). (a) 4-methylbenzamide (b) 4-methyl-2,6-dihydroxyquinoline

are nitrogen containing compounds and it is possible their occurrence is due to an impurity. Full pyrolysis had the largest counts for each peak as well as the highest S/N of 37.28 for peak (9) compared to 26.70 in Fig. 17(c).

Acrylic

In comparison to the other textile chromatograms, acrylic was the most difficult for compound identification (while using the same GC heating program). At a temperature between 190 to 200°C, a total of 4 peaks were displayed increasing to 7 peaks when the temperature increased to 230 to 240°C and 11 peaks when further increased to >500°C. The compounds responsible for peaks 1-4 are as follows 4-methylbenzamide (1), O-ethylbenzamide (2), 3, 4-dimethylbenzamide (3), 2-dodecanol (4). All 4 compounds increased in counts from the lowest temperature interval to full pyrolysis. 4-methylbenzamide

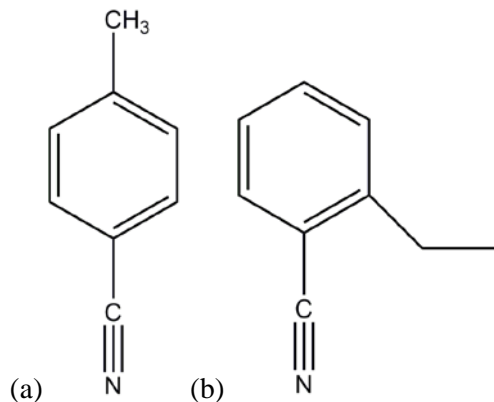


Figure 19. Chemical structure of volatile compounds collected from acrylic (see appendix for mass spectrum). (a) 4-methylbenzonitrile (b) O-ethylbenzonitrile

displayed the largest increase from 73884 counts at 120-130°C to 483272 counts at a temperature of >500°C. The remaining compounds O-ethylbenzonitrile, 3,4-1,3-benzenedicarbonitrile, 2-dodecanol increased from 76961 to 187431 counts, 65572 to 155133 counts, and 59127 to 138566 counts respectively for the temperature range of 120 to 130°C and >500°C.

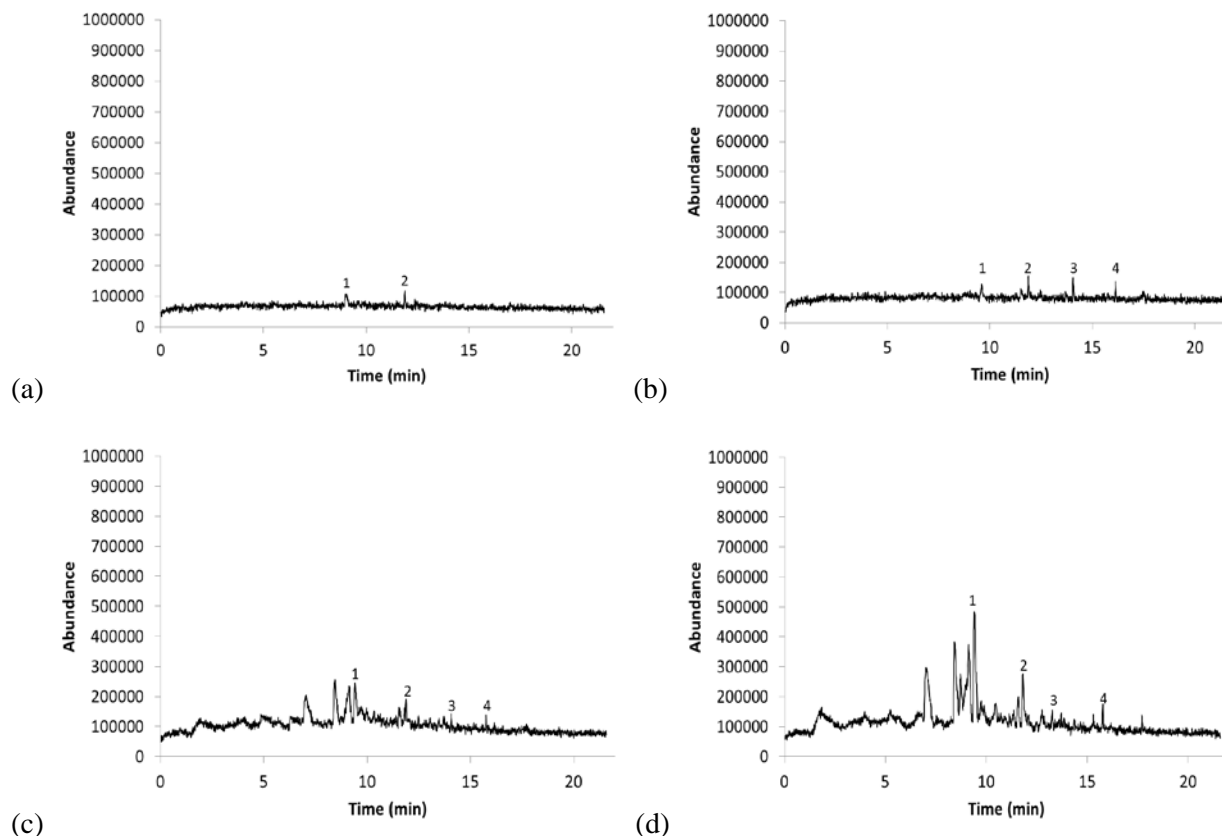


Figure 20. Effects of pyrolysis temperature on the number of compounds released from acrylic fibre (a) Temperature setting 1 (Top of crucible: 190-200°C Bottom of crucible: 120-130°C) (b) Temperature setting 2 (Top of crucible: 260-270°C Bottom of crucible: 190-200°C) (c) Temperature setting 3 (Top of crucible: 290-300°C Bottom of crucible: 230-240°C) (d) Temperature setting 4 (Full pyrolysis >500°C)

Acrylonitrile contains a triple bonded nitrile group which is likely to produce compounds structurally related to, or containing a nitrile functional group. The compound 2-dodecanol is an unexpected peak found in the chromatogram because unlike the acrylic structure, 2-dodecanol contains no nitrile based functional groups. However, it can be concluded that the source of 2-dodecanol is possibly due to its usage as a softening agent for textiles during the manufacturing process⁶⁹. Figure 20(d) had the largest peak counts and the largest S/N of 35.53 for 4-methylbenzotrile.

2.1a Conclusions of Temperature Optimization

Each textile displayed the largest counts and S/N for their respective peaks during full pyrolysis with the exception of olefin. The S/N is only one approach that can be used to describe the change of each compound and their respective peak, but it is not the only factor involved when determining the optimal temperature. The optimal temperature can also be chosen based on the peaks that are reproducible at that temperature and the presence of compounds that are of interest. Compounds that are deemed important should be related to the chemical structure of the textile in such a way that it can be deciphered from the original textile structure. Based on the S/N of each of the textile temperature intervals and the compounds that were structurally related (numbered peaks) that displayed reproducibility, the optimal temperature is the full pyrolysis temperature (>500°C). A unique representation of peaks is displayed with different retention times for each textile chromatographic pattern.

For these experiments, the oven temperature program of the GC started at 70°C (hold for 2 min) with an increase of 7°C/min up to 200°C (hold 1 min). Some of the peaks in the chromatograms were broad (e.g. cotton peak 1). Therefore, for the rest of this project the initial oven temperature used was 40°C (hold 2 min) with an increase of 5°C/min up to 270°C (hold 5 min).

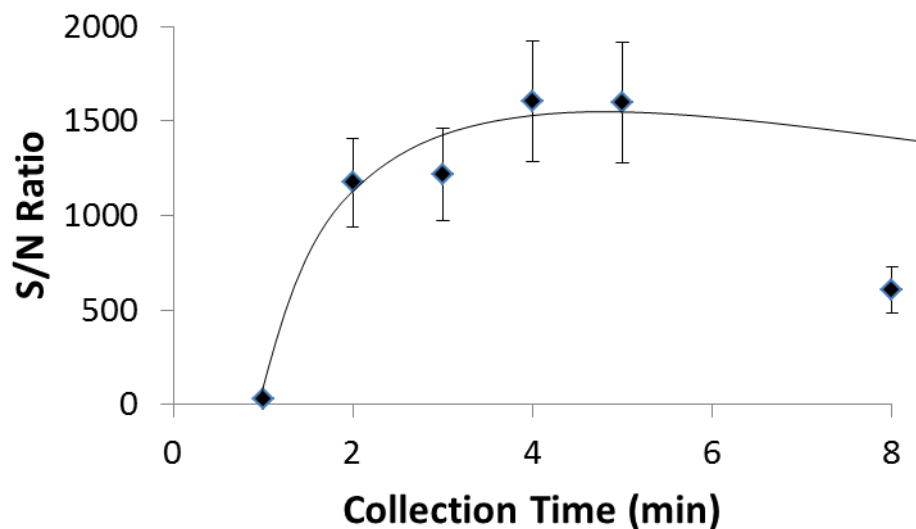
Table 3. S/N of textile peaks for each temperature interval (signal n=23, noise n=535).

Textile	Temperature Interval	Peak #	S/N ratio
<i>Olefin</i>	190-200°C	2	12.98
	260-270°C		24.75
	290-300°C		201.5
	>500°C		193.5
<i>Cotton</i>	190-200°C	1	13.56
	290-300°C		14.01
	340-350°C		16.48
	>500°C		36.54
<i>Wool</i>	260-270°C	2	13.53
	340-350°C		33.77
	390-400°C		35.34
	>500°C		43.62
<i>Polyester</i>	260-270°C	9	13.69
	340-350°C		13.67
	390-400°C		26.70
	>500°C		37.28
<i>Acrylic</i>	190-200°C	1	1.07
	260-270°C		14.31
	290-300°C		31.47
	>500°C		35.53

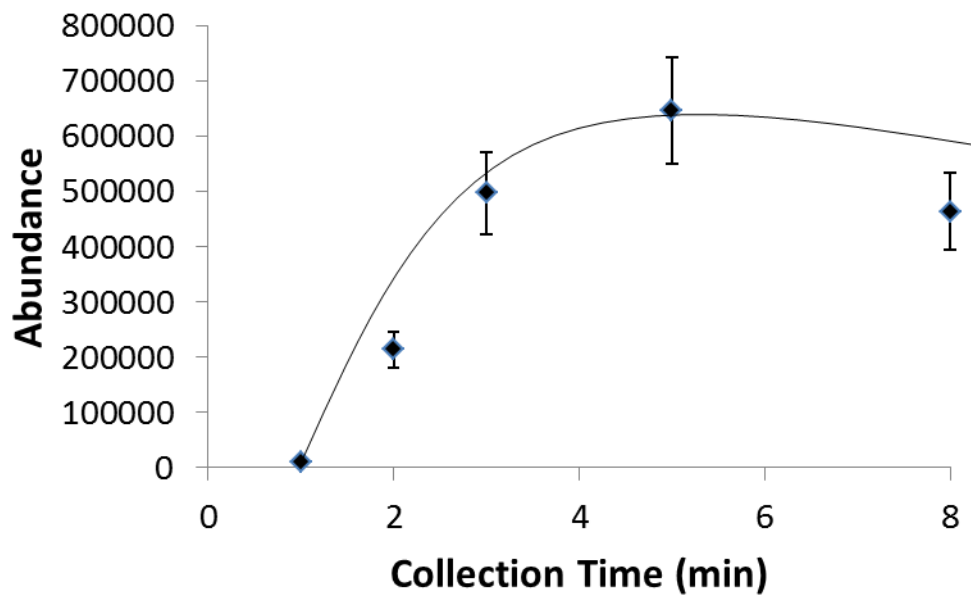
2.2 Determination of SPME Collection Time

The analysis of textiles using SPME requires a defined collection time in order to achieve the optimal compound selection. The collection time is defined as the amount of time it takes to achieve relative equilibrium with the analytes. As there are multiple compounds within each chromatogram, any of the textile chromatograms can be used for determining the optimal collection time. However, 4-methyl-2-nitro-phenol from wool was chosen to represent of the group. Time intervals of 1, 2, 3, 4, 5 and 8 minutes were collected using 1.5 mg of wool that has

been heated to $>500^{\circ}\text{C}$. The heating time was consistently set to two minutes, and the collection time was started after the heating stage.



(a)



(b)

Figure 21. Determination of SPME collection time (a) S/N vs. Collection time (b) Counts/Signal vs. Collection time

The S/N in Fig. 21(a) represents that at 4(S/N=1603) and 5(S/N=1599) minutes of collection, 4-methyl-2-nitro-phenol has achieved the greatest signal in regards to the noise

produced in that chromatogram. A maximum or leveling out affect appears to have occurred for the adsorption on the SPME of this compound. Furthermore, at 8 minutes the S/N decreases. This suggests that if SPME is exposed for too long, compounds may desorb or become displaced by less volatile compounds. In Fig. 21(b) the largest counts occurs at 5 minutes. At 8 minutes in Fig. 21(b), the counts decrease much like the S/N in Fig. 21(a). In both cases of the data presented in Fig. 21, the 5 minute collection time is the optimal collection time. Other literature has suggested collection times of 100s when analysing for polycyclic aromatic hydrocarbons (PAHs) evolving from pyrolysis of biomass⁹⁵.

2.3 Sample Size

Sample size is important when dealing with valuable textiles. The sample size required to produce a chromatographic pattern that best represents the textile of analysis is important for identification. Too little sample can produce a chromatographic pattern that may not be detectable. The goal of this part of the experiment is to assess the relationship and effects between sample size and the textile's correlating peaks. This method is destructive, so ideally the least amount of sample that is required would be ideal. Sample sizes ranging from 1.5-0.02mg (3-0.2 cm in length respectively) for wool, cotton, olefin and polyester are displayed in the following figures below.

Wool

Wool was the first textile sample collected at the following sample sizes of 1.5, 1, 0.25, and 0.02 mg with a temperature (T) >500°C:

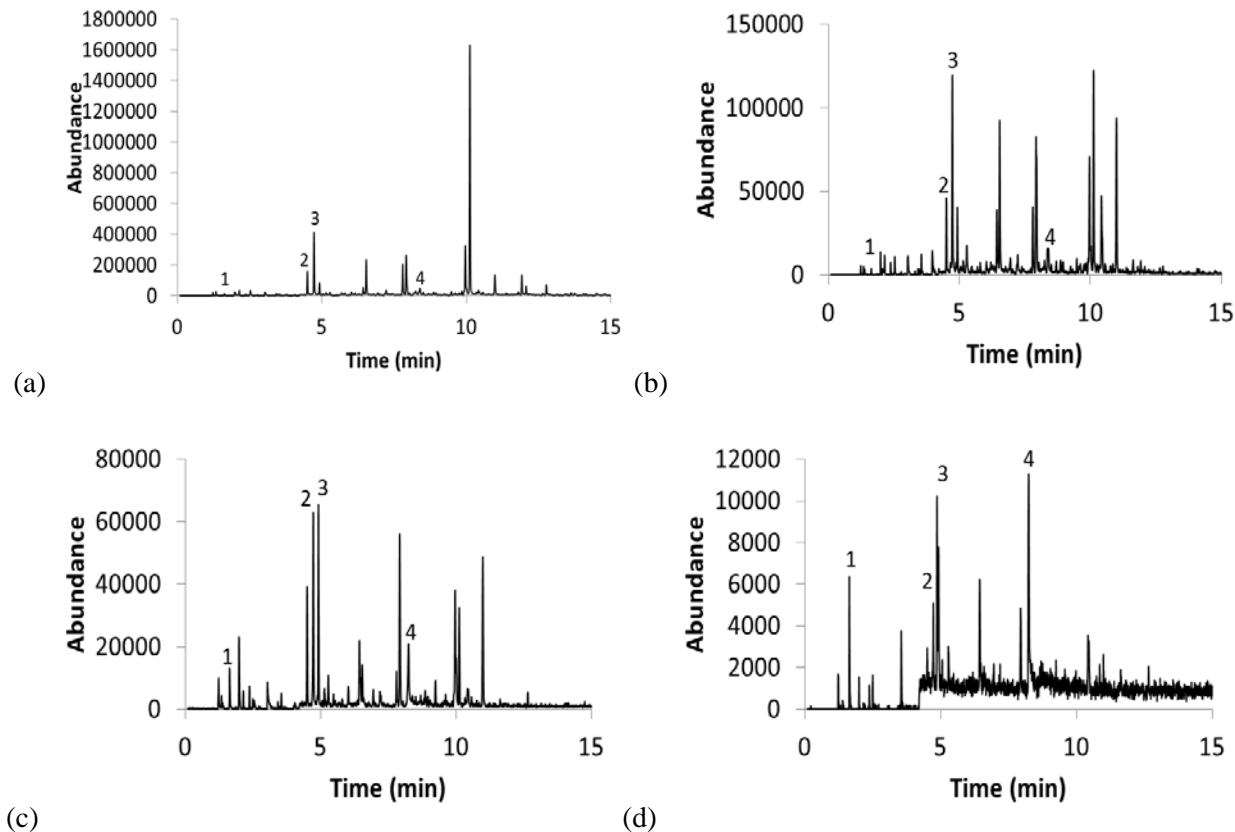


Figure 22. Effects of mass on the compounds released from wool (a) 1.5mg wool (b) 1.0 mg wool (c) 0.25 mg wool (d) 0.02 mg wool

The resulting analysis for wool displayed peaks in the lowest sample size of 0.02 mg. The compounds responsible for each peak are as follows benzene (1), phenol (2), benzonitrile (3), and benzoic acid (4). Each of the compounds had an increasing relative peak area as the sample size decreased. The quantity of peaks decreased from 1.5mg to 0.02 mg of sample which can result in an increased relative peak area for the remaining peaks. The S/N decreased from 543.0 (1.5mg) to 155.08 (0.02 mg) which is important to note. For a small mass of 0.02 mg the S/N is still relatively large, suggesting that these compounds can be detected at even smaller sample masses. As a result, the four compounds found in 0.02 mg of sample, could be used as chemical markers for identifying wool. However, there are more compounds that can be used as

compound markers at larger sample sizes such as 1.5 mg which will be described in the next section.

Cotton

The sample sizes for each chromatogram displayed a different number of peaks. The chromatogram containing a sample size of 0.02 mg (Fig.23c) displayed the fewest number of peaks and counts for each peak, while the 1.5 mg chromatogram (Fig.23a) displayed the largest number of peaks and as well as, the largest peak counts. The compounds responsible for each peak are as follows, 2(H)-furan-3-one (1), 2-furanmethanol (2), phenol (3), and dodecanal (4).

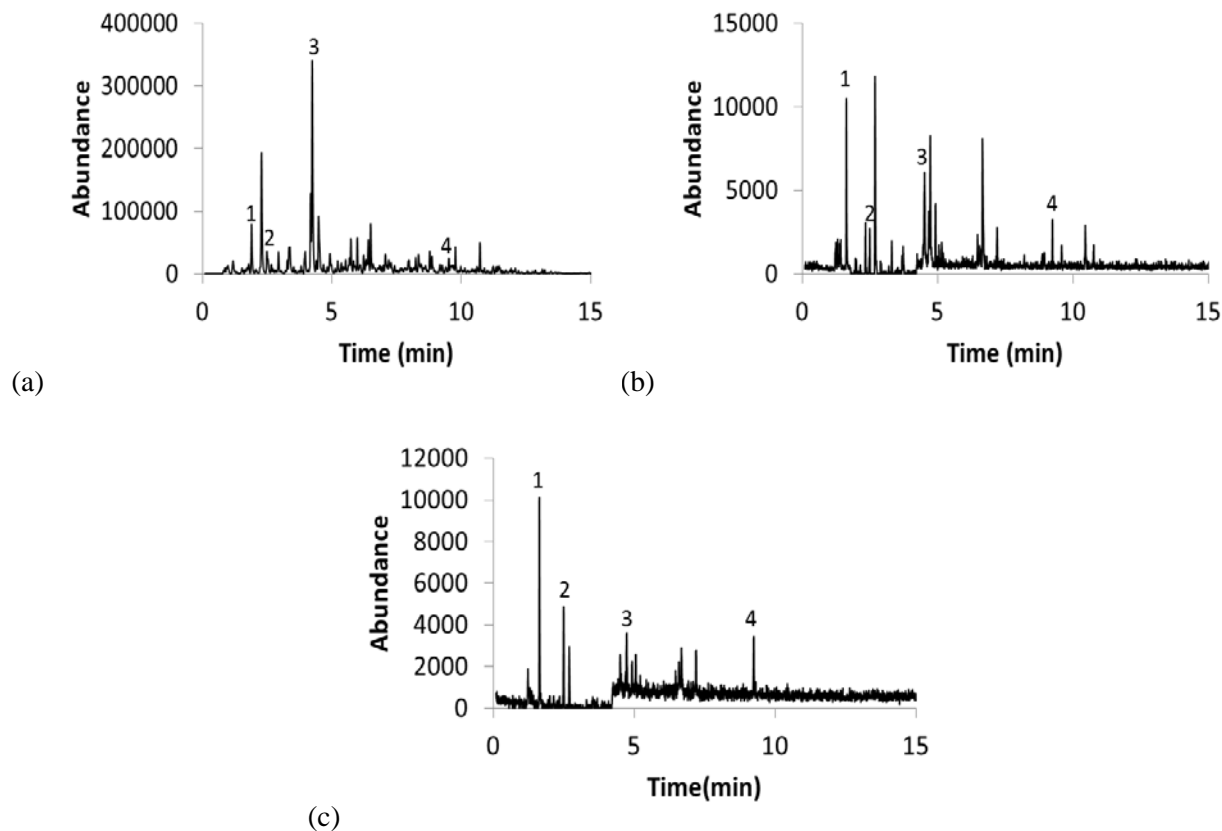


Figure 23. Effects of mass on the compounds released from cotton (a) 1.5 mg cotton (b) 0.08 mg cotton (c) 0.02 mg cotton

2(H)-furan-3-one (1) displayed a relative peak area of 5.06% (1.5 mg) which increased nearly threefold to 15.54% for 0.02 mg. 2-Furanmethanol (2) displayed a relative peak area of

3.40%, 2.61%, and 7.70% for 1.5, 0.08, 0.02 mg respectively. The dodecanal relative peak area decreased with increasing sample for 1.5, 0.08, and 0.02 mg respectively. The relative peak area for phenol (3) did not change drastically between each sample size for each chromatogram. The relative peak area for phenol (3) is 8.07%, 7.68%, and 5.66% for 1.5, 0.08, and 0.02 mg. The S/N decreased from 220.7 (1.5 mg) to 12.42 (0.02 mg), which signifies that cotton may not be detectable at masses of <0.02 mg.

Olefin

Of all of the textiles, olefin provided the largest number of peaks at the lowest sample mass of 0.02mg. The S/N of 309.2 was the largest for 0.1mg, and decreased to 71.59 for 0.02 mg. It was expected that the largest sample size of 1.5mg would have the greatest S/N; however this was not the case.

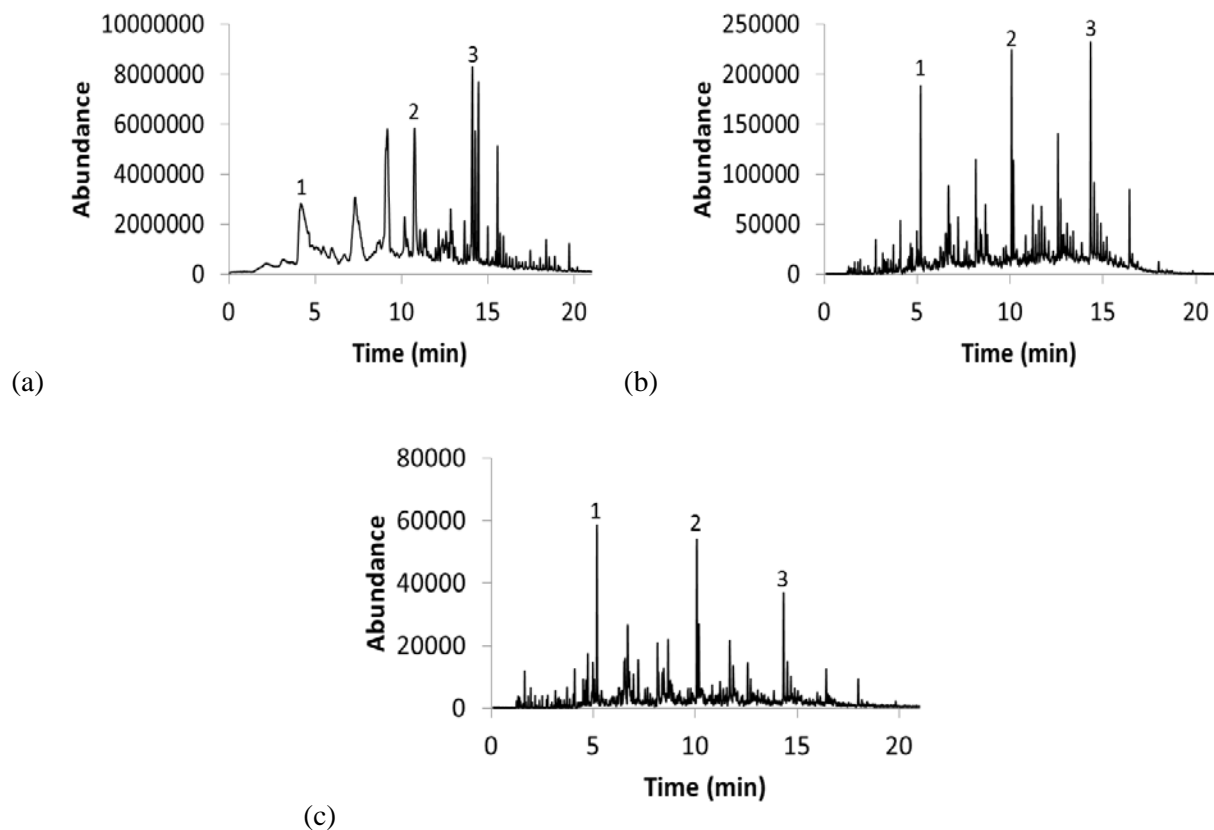


Figure 24. Effects of mass on the compounds released from olefin (a) 1.5 mg olefin (b) 0.1 mg olefin (c) 0.02 mg olefin

The three peaks that were chosen as the most distinguishable at the 0.02 mg sample size consisting of cyclohexyl formate(1), 1,1-dimethyl-2-cyclopropane(2), (+)-3,3-dimethylnopinone(3). Each compound was consistently identified throughout the multiple sample sizes with relative peak areas for 0.02mg of 6.04%, 7.17% and 8.38% for cyclohexyl formate(1), 1,1-dimethyl-2-cyclopropane(2), and (+)-3,3-dimethylnopinone(3) respectively. The large relative peak areas for the three compounds identified for olefin along with a relatively large S/N at 0.02 mg, makes olefin a good candidate for detection at <0.02 mg.

Polyester

Polyester had the cleanest chromatograms for each sample size by having the most distinguishable peaks in comparison to the background signal noise. At a sample mass of 0.02 mg the S/N was 354.5.

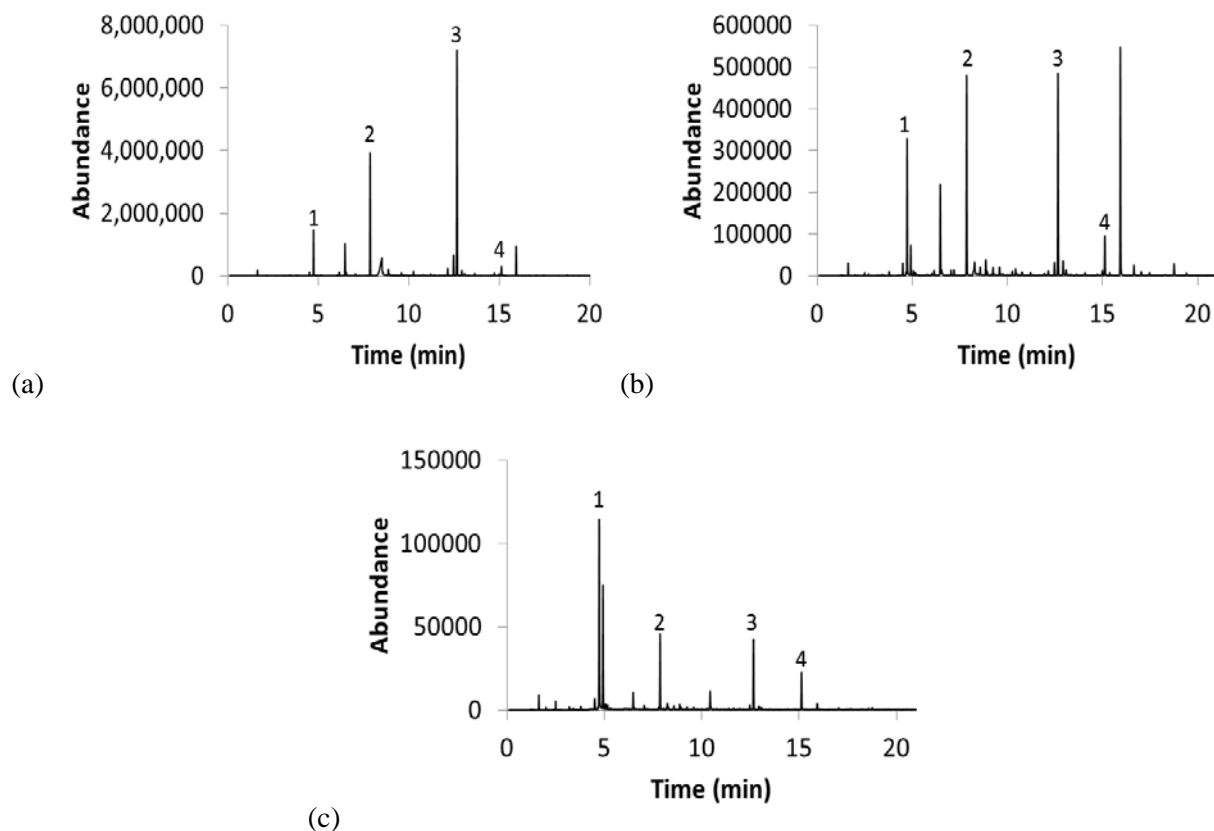


Figure 25. Effects of mass on the compounds released from polyester (a) 1.5 mg polyester (b) 0.05 mg polyester (c) 0.02 mg polyester

The compounds responsible for each peak are phenol (1), ethylbenzene (2), biphenyl (3), and dibenzofuran (4). The relative peak area for phenol (1) increased with decreasing sample size from 7.43%, 11.64%, and 31.46% for 1.5, 0.05, 0.02 mg respectively. Ethylbenzene(2) displayed opposite results from phenol (1) as it decreased with decreasing sample size from 20.62%, 17.43%, and 13.07% for 1.5, 0.05 and 0.02 mg respectively. Biphenyl (3) displayed similar results to ethylbenzene (2) with relative peak areas of 42.31%, 19.07%, and 12.69% for

1.5, 0.05, and 0.02 mg respectively. Dibenzofuran (4) displayed similar results to phenol (1) with relative peak areas of 2.00%, 4.08%, and 7.15% for 1.5, 0.05, and 0.02 mg respectively.

In summary, each textile displayed detectable compounds when 0.02 mg of sample was used. Individually, the smallest sample size allowed was based on recognition of the chromatogram and the ability of the software to represent the mass spectrum for each peak. Polyester, cotton, wool, and olefin all provided a distinguishable chromatographic pattern at 0.02 mg of sample size. This was the minimum sample size that was tested for these four textiles, but based on the chromatographic patterns, the S/N and the counts of each peak, it could be possible to correctly identify the textiles using a sample size of <0.02 mg. The relative peak area for each peak in the textile chromatograms differed based on the compound. For some compounds the relative peak area increased with increasing sample size (e.g. ethylbenzene in polyester), while some compounds decreased with increasing sample size (e.g. 2-furanmethanol in cotton). It was observed that a greater number of peaks found when 1.5 mg of sample was used in comparison to the sample sizes of 1- 0.02 mg. The more compounds that are used for identification, the easier the identification will become (especially when the sample contains blends). Therefore, it would be ideal to use a sample size of 1.5 mg if possible for identifying textiles.

2.4 Identifying Chemical Markers

Chemical markers refer to specific compounds that are identifiable consistently within each textile fibre. The purpose of identifying compound markers is to represent each unique textile chromatographic pattern with more information that proves that they indeed differ. For each textile, finding peaks in the respective chromatographic pattern that are compounds structurally related to that textile, is what determines the differences between unknown textiles

and ability to be identified. Each textile is structurally different and based off of that structural difference the chromatographic pattern should also display structural differences. In the previous section, it was determined that the temperature of $>500^{\circ}\text{C}$ (full pyrolysis) of each compound would be used for the remainder of the experiments. Figure 26 shows each textile and their chromatographic pattern with the following labelled peaks:

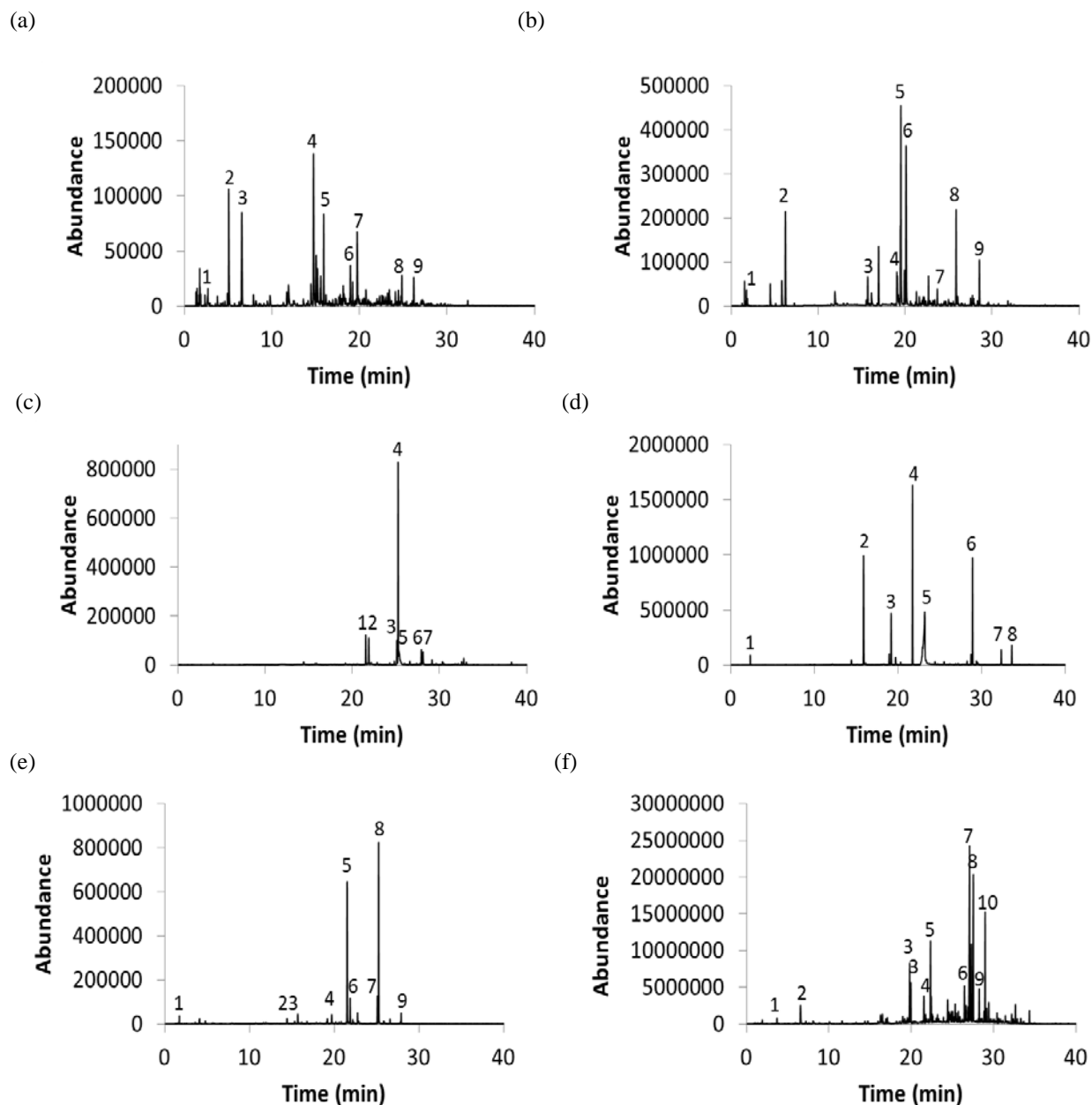


Figure 26. Chromatograms of pyrolysed textile fibres (T>500°C) (a) 100% Cotton (b) 100% Acrylic (c) 100% Wool (d) 100% Polyester (e) 100% Silk (f) 100% Olefin

The chromatograms are useful for distinguishing different textiles but do not indicate structure. In some cases peaks that have the same retention time, may have different compounds associated with them. To confirm that they are real, a mass spectrum was acquired for each peak. The fragmentation was occasionally analysed to confirm the expected structure that was detected. The peaks in each chromatographic pattern are also compared to software used for identification. The following Table 4 displays each compound representing the numbered peaks in each chromatographic pattern.

Table 4. Pyrolysis of textiles cotton, acrylic, wool, polyester, silk, and olefin and the corresponding compounds released from performing HS-SPME with GC-MS (see appendix for mass spectrum). (See Fig. 28)

Cotton			Polyester		
Peak	(time)	Compound	Peak	(time)	Compound
1	2.69	Propanoic Acid	1	2.35	Benzene
2	5.05	2(H)-furan-3-one	2	15.91	Phenol
3	6.55	Furfural	3	19.21	1-Phenyl ethanone
4	14.75	5-Methyl Furfural	4	21.77	Ethylbenzene
5	15.91	Phenol	5	23.08	Benzoic acid
6	18.96	2-Methyl-phenol	6	28.95	Biphenyl
7	19.74	Orcinol	7	32.38	Dibenzofuran
8	24.85	2 (3H) - Benzofuranone	8	33.64	3-Methyliden-2,3,4,5-Tetrahydro-1-Benzoxazepin-one
9	26.20	1-Indanone			
Acrylic			Silk		
1	1.86	2-Methyl-2-Propenenitrile	1	1.74	Nitroethane
2	6.22	Hexamethyl-Cyclotrisiloxane	2	14.44	Benzaldehyde
3	15.70	Benzonitrile	3	15.70	Cyanobenzene
4	19.01	Succinoinitrile	4	19.71	2-Methyl-5-Methylthiophene
5	19.51	Hexenedinitrile	5	21.54	2-Nitro-phenol
6	20.11	Hexenedinitrile	6	21.89	Benzyl nitrile
7	23.71	3,5-Dimethyl-Benzonitrile	7	25.10	Hydrocinnamonitrile
8	25.87	1,2-Benzendicarbonitrile	8	25.25	4-Methyl-2-Nitro-phenol
9	28.55	5-Methyl Isophthalonitrile	9	27.91	(+)-Myrtine
Wool			Olefin		
1	21.56	2-Nitro-Phenol	1	4.14	Methyl-Benzene
2	21.90	Benzyl nitrile	2	6.99	2,4-Dimethylheptane
3	25.12	Hydrocinnamonitrile	3	19.85, 20.01	4-Methyl-2-Undecene
4	25.26	4-Methyl-2-Nitro-Phenol	4	21.58	1,1,4,4-Tetramethyl-cyclohexane
5	25.35	4-Methyl-2-Nitro-Phenol	5	22.36	4,8-Dimethyl-1,7-Nonadiene
6	27.93	N, N-Dimethyl-4-Nitroaniline	6	26.48	1,2,3,5-Tetramethyl-cyclohexane
7	28.12	4-Nitro-Benzoic acid	7	27.04, 27.278	Propagyl octyl ether
			8	27.51	4-Isopropyl-1,3-Cyclohexanedione
			9	28.26	1,1,3,5-Tetramethyl-cyclohexane
			10	28.97	Pentylcyclohexane

2.5 Textile Brand Comparison

In addition to previous experiments, part of assessing the properties associated with this method was to test the reproducibility of HS-SPME GC-MS. By comparing multiple brands of the same textile (cotton), this experiment will determine whether this method can consistently identify the textile regardless of brand type. Five cotton brands were chosen from different manufacturers to assess the reproducibility of the volatile compounds evolved among different sources. The brands of cotton used for this experiment are as follows: Bernat Handicrafter, Paton Grace, J+P cotton, DMC and Anchor.

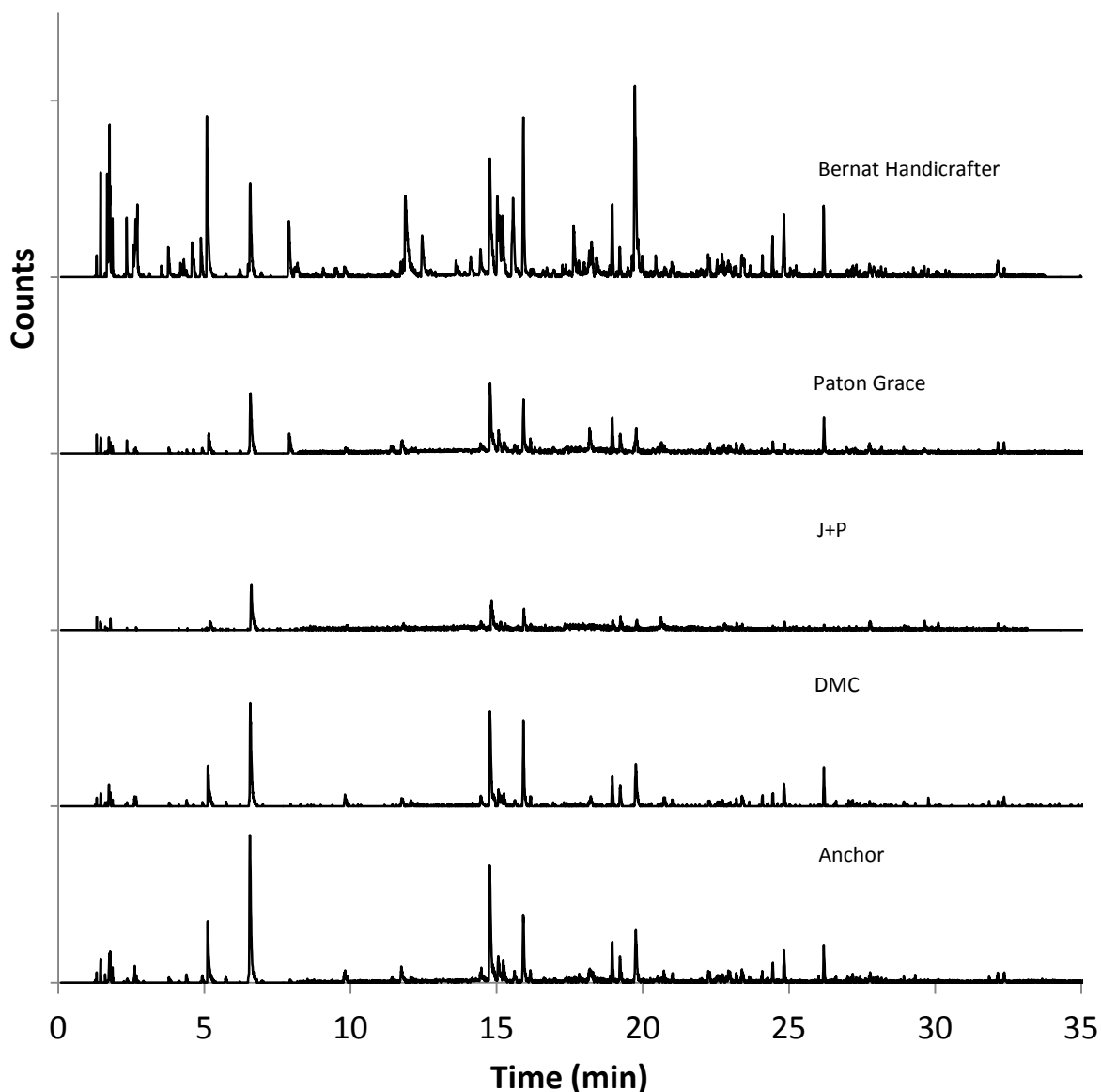


Figure 27. Brand comparison of the pyrolysis of cotton. Listed from top to bottom - Bernat Handicrafter, Paton Grace, J+P, DMC, Anchor

When comparing the different brands of cotton, the compounds that evolved from pyrolysed cotton were consistent but varied in counts. Bernat Handicrafter displays the most abundant peaks, while J+P cotton is the opposite with very low abundant peaks. All the brands share the same chemical markers and the respective retention times (as previously determined in section 2.3). One example is furfural (6.553 min), which is visible in each chromatogram but

does not consistently share counts between brands (Bernat Handicrafter 10614 counts, J+P cotton 5186 counts). The results suggest that HS-SPME GC-MS can decipher textile brands based on their chromatograms. Although the chromatograms include the same volatile compounds used for identification, these compounds can vary in counts based on the textile brand.

2.6 Fourier Transform Infrared Spectroscopy (FT-IR) Investigations

Fourier Transform IR spectroscopy has been widely studied across a range of analytical applications and has been applied to textiles. However, Fourier transform infrared spectroscopy is often used as a supplementary method for qualitative purposes when identifying textiles^{18-22, 78}. The applications of FT-IR with textiles can be shown industrially for fast characterization of the cotton fabric scouring process by examination of C–H stretching region at 2800–3000 cm^{-1} ²⁴. It can be used to determine structural changes in wool²³ as well as identify natural fibres (especially for silk)¹⁵. Six silk degradation estimators have also been found using FT-IR with validation methods¹⁹.

2.6a Experimental

Each textile sample was dried in a desiccator prior to analysis for a minimum of 24 hours. The samples (5mg) were cut into very small fragments using a razor blade and ground with potassium bromide (100mg) to create a pellet for analysis. The pellet was pressed using a Welch 1400 DuoSeal vacuum pump. The analysis was performed with the Varian 1000 FT-IR instrument from 400-4000nm for 32 scans per sample.

2.6b FT-IR Results and Discussion

The following textiles cotton, acrylic, wool, polyester and olefin were the samples used for FT-IR analysis and are displayed in the following Figure 28:

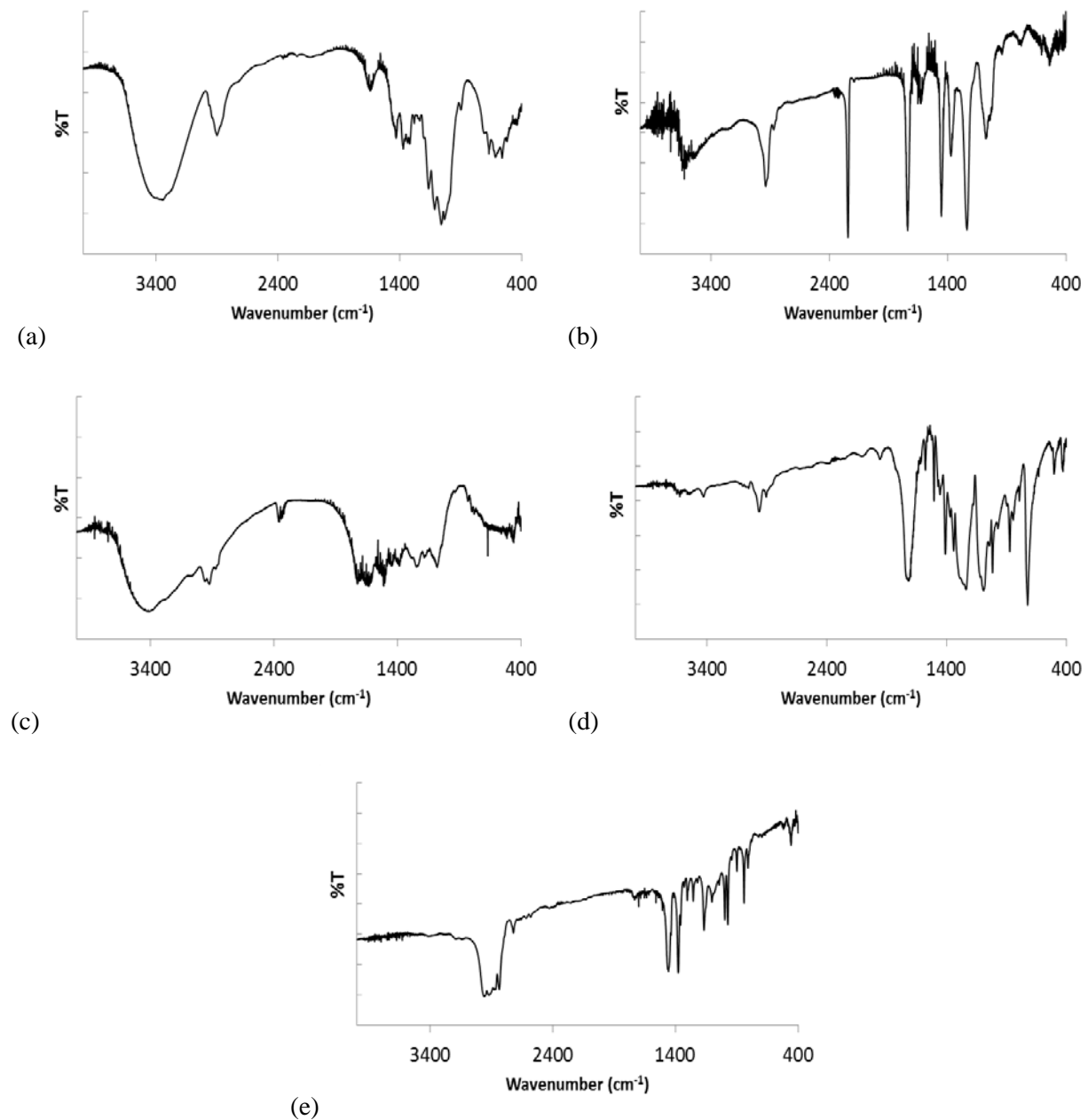


Figure 28. The analysis of various textiles using mid-infrared spectroscopy (a) Cotton (b) Acrylic (c) Wool (d) Polyester (e) Olefin

Cotton consists primarily of cellulose which contains numerous O-H bonds. A large transmittance in the 3400 cm^{-1} range is due to the O-H stretch in cellulose. Visually the spectrums all appear to be unique and differ with their wavelength transmittance as expected. Cotton contains many C-O stretching bonds which are absorbed in the 1100cm^{-1} range. Due to the varying conformations of the C-O bonding within the structure of cellulose, the positive stretching bands can range from $900\text{-}1200\text{ cm}^{-1}$ ⁷⁰. There is a very sharp absorbance occurring at 2240 cm^{-1} which is consistent with nitrile stretching for acrylic⁷¹. Wool primarily consists of an amino acid structure that can have various bonds contained within it. Displayed in Figure 28(c) there is a small O-H peak at 3400 cm^{-1} as wool experiences a positive band at 3418 cm^{-1} ⁷². A small peak for wool also occurred within the C-N region $\sim 1200\text{cm}^{-1}$ and N-H region of 1600cm^{-1} . The transmittances are fairly weak for some textiles like acrylic and wool and can be unclear due to reflection. It is difficult to identify specific peaks which can be a contributing factor of the limitations when using this method for identifying textiles. The polyester spectrum has a large peak spanning from 1600cm^{-1} to 1700cm^{-1} which is the region of absorption for stretching C=O and stretching C=C bonds. This coincides with the ester functionality (C-O) bands that can be found at 1718 and 1252 cm^{-1} with a doublet at 1126 and 1099 cm^{-1} ⁷³. Polyester also experiences aromatic positive bands at 3054 , 1615 , 1578 , 1505 , 1021 , and 725 cm^{-1} ⁷³. Olefin is made up of simple alkane chains which are most prominent at 3300cm^{-1} and 700 cm^{-1} . However the methylene group in particular can vary from $720\text{-}820\text{ cm}^{-1}$, depending on the number of continuous methylene groups⁷⁴. The methyl group positive bands can be displayed between $930\text{-}980\text{ cm}^{-1}$ and that is dependent on the number of continuous propylene groups⁷⁴. There are smaller peaks in the 1400cm^{-1} region which are also due to the C-H bond vibrations within olefins chemical structure. As IR demonstrates, it is possible to acquire different spectra for each

textile compound. However, it is difficult to clearly identify which textile is present merely from the spectra produced by IR. Infrared spectroscopy lacks the specificity for identifying textiles directly, and must rely on the vibration and stretching of functional groups to help piece together the textile compound structure.

2.6c FT-IR brand comparison

Unlike HS-SPME GC-MS, when different brands of the same textile were compared using FT-IR, it was not possible to identify them from one another based on the spectrums as shown in Fig. 31.

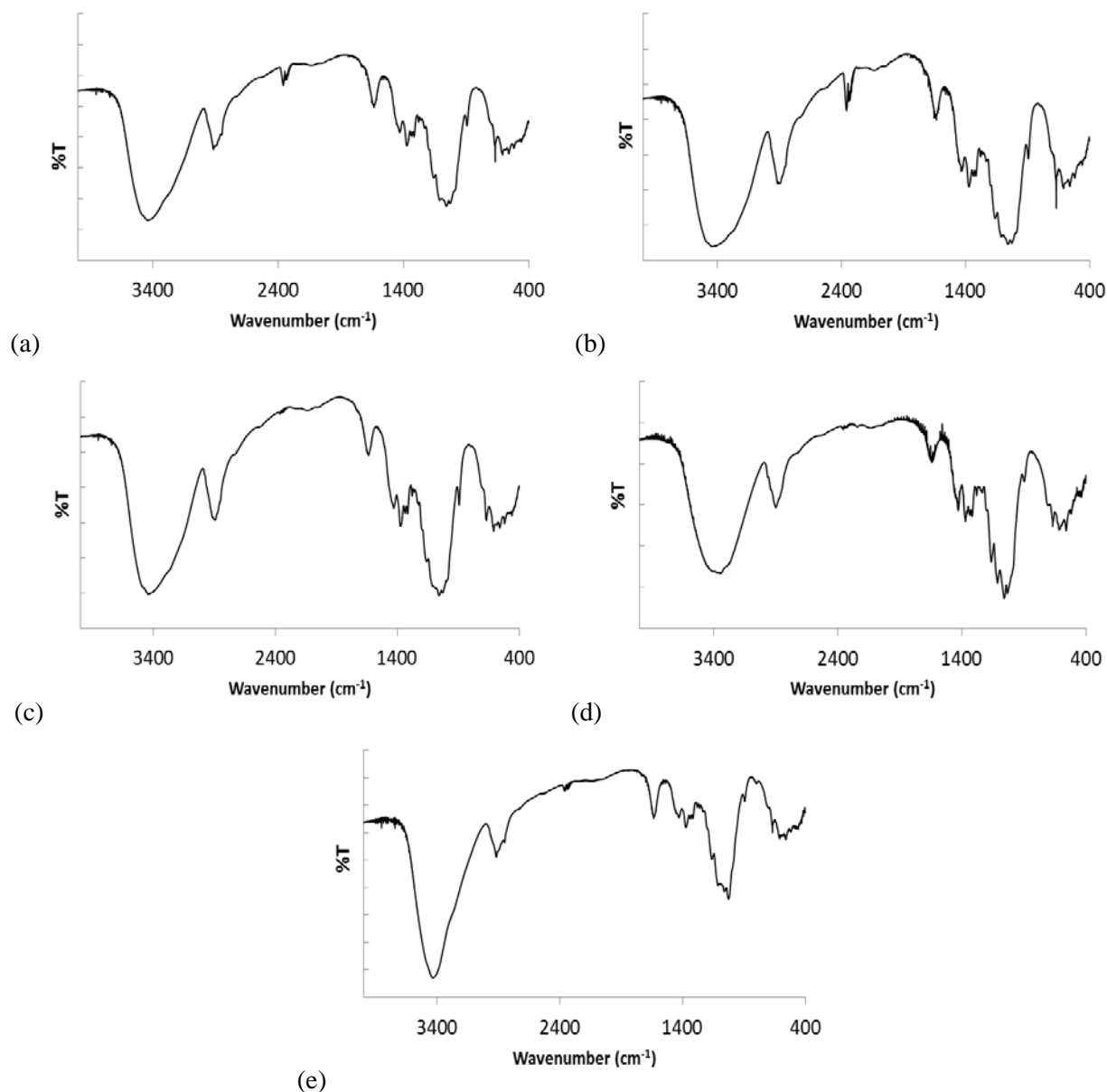


Figure 29. FT-IR analysis of 5 cotton brands. (a) Anchor (b) DMC (c) J+P (d) Bernat Handicrafter (e) Paton

The structure of cotton from brand to brand typically will not change. Since FT-IR relies on the structure for identification and analysis of the stretching/bending bonds, it will become very difficult to decipher sources or brands of the same textile. In each of the 5 brands of cotton, the 3400 cm⁻¹ O-H stretch is clearly displayed as well as the C-O stretching in the 900-1200cm⁻¹ range as previously described. However, there is one noticeable difference between Anchor and

DMC cotton that is either undetectable or very weak in the other brands of cotton. Most prominently displayed in DMC cotton is a short broad peak occurring from 2300-2400 cm^{-1} . This peak is most likely caused by the stretching of $\text{O}=\text{C}=\text{O}$. This is an unlikely bond for cotton to have as it did not appear in other cotton spectrums within the literature. The contamination can most likely be attributed to carbon dioxide stretching occurring either within the background, as a dye or coloring agent.

2.6d FT-IR analysis of accelerated aged wool

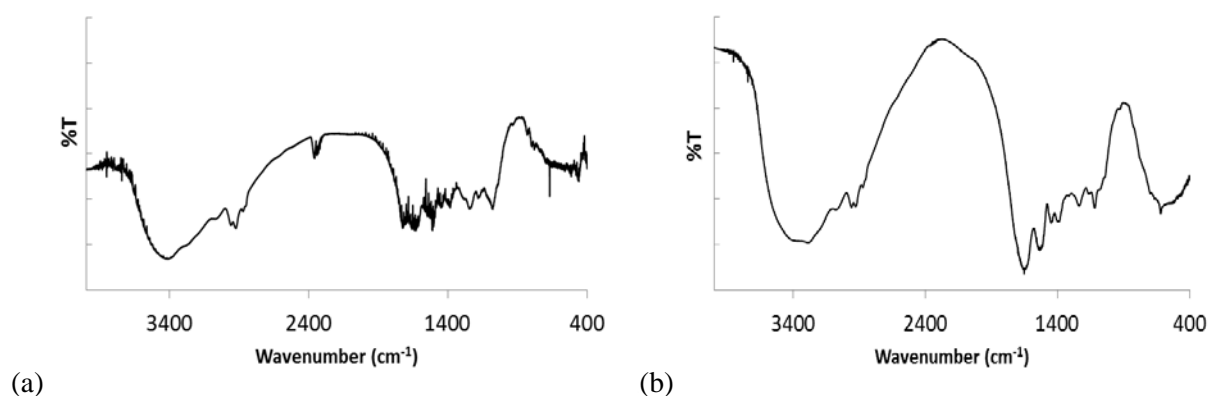


Figure 30. FT-IR comparative analysis of non-aged and humid aged wool. (a) non-aged wool (b) humid aged wool

The comparative analysis for wool between non-aged and aged produced similar results. The aged textile was relatively more efficient to analyze due to the frail and brittle nature of the textile after the aging process. This produced a sample that could easily be pelletized with KBr (The difference can be seen between the two spectrums transmittance). As previously noted, there is a peak within the 2300-2400 cm^{-1} that can be described as an impurity. The transmittance within the aged spectrum was much cleaner than the non-aged spectrum. In both spectrums the O-H stretch can be found in the 3400 cm^{-1} ; peaks contributing to the identification of wool can also be found in the C-N region $\sim 1200\text{cm}^{-1}$ and N-H region of 1600 cm^{-1} . This

experiment confirms the qualitative and sensitivity limitations that FT-IR can achieve. Structural changes in wool and degradation markers in silk fibronin have been found in other research with the use of other analytical methods in addition to IR^{19, 23}. Although useful for identification of textiles, FT-IR was not found to be able to distinguish aged and un-aged textiles, as well as source identification.

Chapter 3: Analysis of Textile Mixtures

When analysing textile blends, there could be two, three or even four types of textiles woven into a piece of clothing or material. This is why it is important to test the feasibility of SPME GC-MS to identify textiles in a mixture/blended sample. Identifying potential interferences or new compound combinations for textile blends is important for testing the feasibility of this method. This also provides a way to potentially push SPME GC-MS to the limits of its capabilities for identification of textiles.

This phase of this study was to determine the effects of mixed textile samples with different mass ratios. The mass ratios of 1:1, 1:3 and 3:1 were prepared with a total mass of 1.5 mg and pyrolysed at a temperature of $>500^{\circ}\text{C}$. The purpose of changing the mass ratios is to determine if one particular textile within the mixture has an influence on the compounds produced.

Wool/Cotton mixture

The 1:1 mass ratios as expected, displayed chemical markers from both cotton and wool that contribute to their identification individually. The cotton related compounds 2(5H)-furan-3-one (1), 5-methyl furfural (2), and phenol (3) was all identifiable within the mixture chromatograms. The compounds in correlation with wool were identifiable as 2-nitro-phenol (5), hydrocinnamitrile (6), and 4-methyl-2-nitro-phenol (7). An additional peak with a retention time of 19.71 minutes was identified as 4-methyl-phenol (4), which was not identified in the individual textile chromatographic patterns.

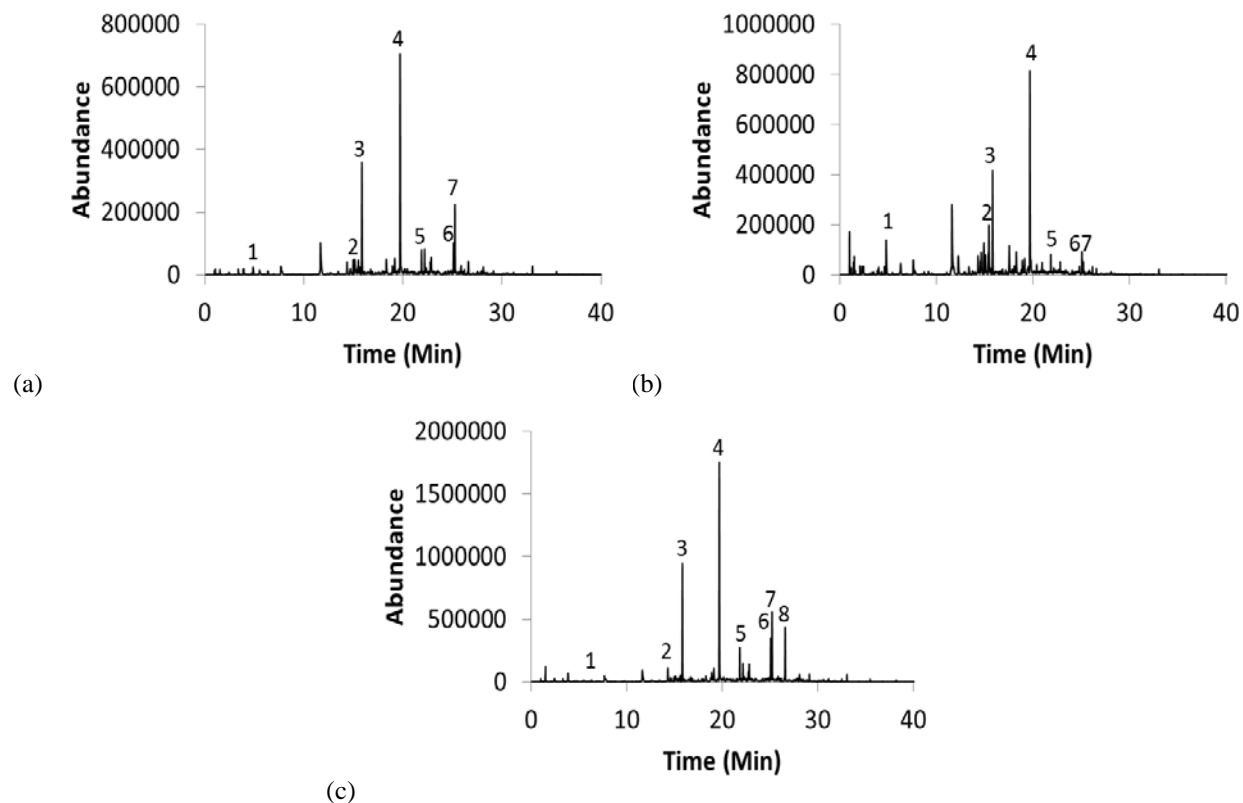


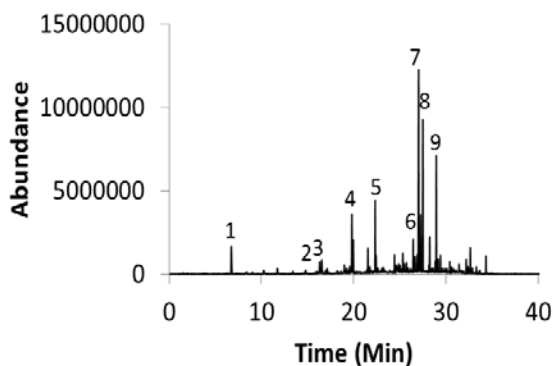
Figure 31. 100% Wool and 100% cotton mixtures (total mass=1.5 mg, T>500°C). Cotton peaks displayed as 1-3, wool peaks displayed as 5-8 (a) 1:1 mass ratio (b) 1:3 wool:cotton mass ratio (c) 3:1 wool:cotton mass ratio

As the mass ratio changed, the counts of the peaks also changed for both the wool and cotton compounds. As expected, the cotton related compounds 2(5H)-furan-3-one (1), 5-methyl furfural (2), were all more prevalent and increased in counts in Fig. 31(b) because of the increased mass ratio of cotton. Phenol (3) was the only compound that did not seem to be affected by the mass ratio and the peak remained relatively consistent in counts throughout each trial. Similarly with wool, hydrocinnamitrile (6), 4-methyl-2-nitro-phenol (7) was affected by the mass ratio change while 2-nitro-phenol (5) remained consistent. The compounds associated with wool increased in counts, and an additionally indole (8) was observed with a retention time of 26.61 minutes. Due to the N present in this compound, the appearance of it is likely attributable to the amino acids in wool. The mass ratio correlates with the peak counts for each

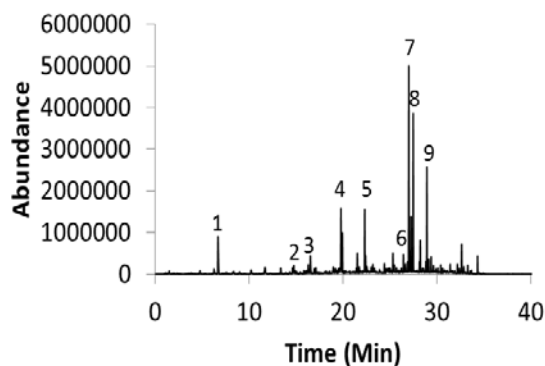
chromatogram. When wool is greater in mass, it displays greater counts peaks and vice versa for cotton. The additional compound 4-methyl-phenol (4) did not fluctuate throughout the mass ratio changes much like phenol (3). It is likely that both wool and cotton could be attributing to this compound and thus giving it consistency throughout each chromatogram. As a result, two new compounds 4-methyl-phenol and indole were formed and the identification of wool and cotton individually using their respective chemical markers was successful.

Cotton/Olefin mixture

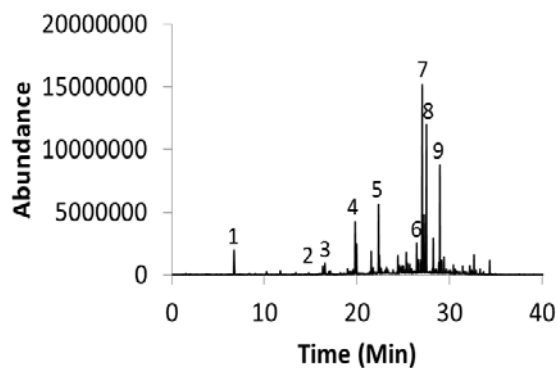
The mixtures of cotton and olefin predominantly showed the expected chemical markers. The peaks associated with cotton had very low relative peak areas and only included 5-methylfurfural (2) and phenol (3). In the 1:1 mass ratio 5-methylfurfural (2) was found to have a 3.19% relative peak area and phenol (3) had a 4.26% relative peak area. These areas decreased to 0.47% for 5-methylfurfural (2) and 1.13% for phenol (3) when the mass ratio was adjusted in favour of olefin. When the textile masses were changed to a 3:1 cotton:olefin ratio, the relative peak areas increased to 8.04% for 5-methylfurfural (2) and 8.36% for phenol (3). Therefore, although the olefin chemical markers were by and large the most predominant peaks in the chromatograms, cotton could still be identified as being present.



(a)



(b)



(c)

Figure 32. 100% Cotton and 100% olefin mixtures (total mass=1.5 mg, T>500°C). Cotton peaks displayed as 2 and 3, olefin peaks displayed as 1, 4-9 (a) 1:1 mass ratio (b) 1:3 olefin:cotton mass ratio (c) 3:1 olefin:cotton mass ratio

The compounds diagnostic for olefin, 2,4-dimethylheptene (1), 4-methyl-2-undecene (4), 1,2,3,5-Tetramethylcyclohexane(5), 4,8-dimethyl-1,7-nonadiene (6), 4-isopropyl-1,3-cyclohexanedione (7,8) and Pentylcyclohexane (9) were recorded in each mixed chromatogram. Despite varying the mass ratios for olefin, the relative peak areas changed only slightly for the designated chemical markers. Therefore, when analysing a mixture of olefin and cotton it may be easier to quantify cotton using the relative peak areas as they vary with the amount of cotton in the mixture. With olefin it may be more difficult as the peak areas do not change as much in each mass ratio.

Cotton/Acrylic mixture

Chemical markers were observed from both cotton and acrylic in the mixture chromatograms. When cotton was pyrolyzed with wool the counts of phenol increased but in the presence of acrylic, phenol (3) is decreased. The compounds 5-methyl furfural (2) and 2(5H)-furan-3-one (1) are present in the acrylic cotton mixture. The compounds 5-methyl furfural (2)

and 2(5H)-furan-3-one (1) had relative peak areas as high as 21.34% and 22.18% respectively, whereas the relative area of the phenol (3) peak was no greater than 7.02%.

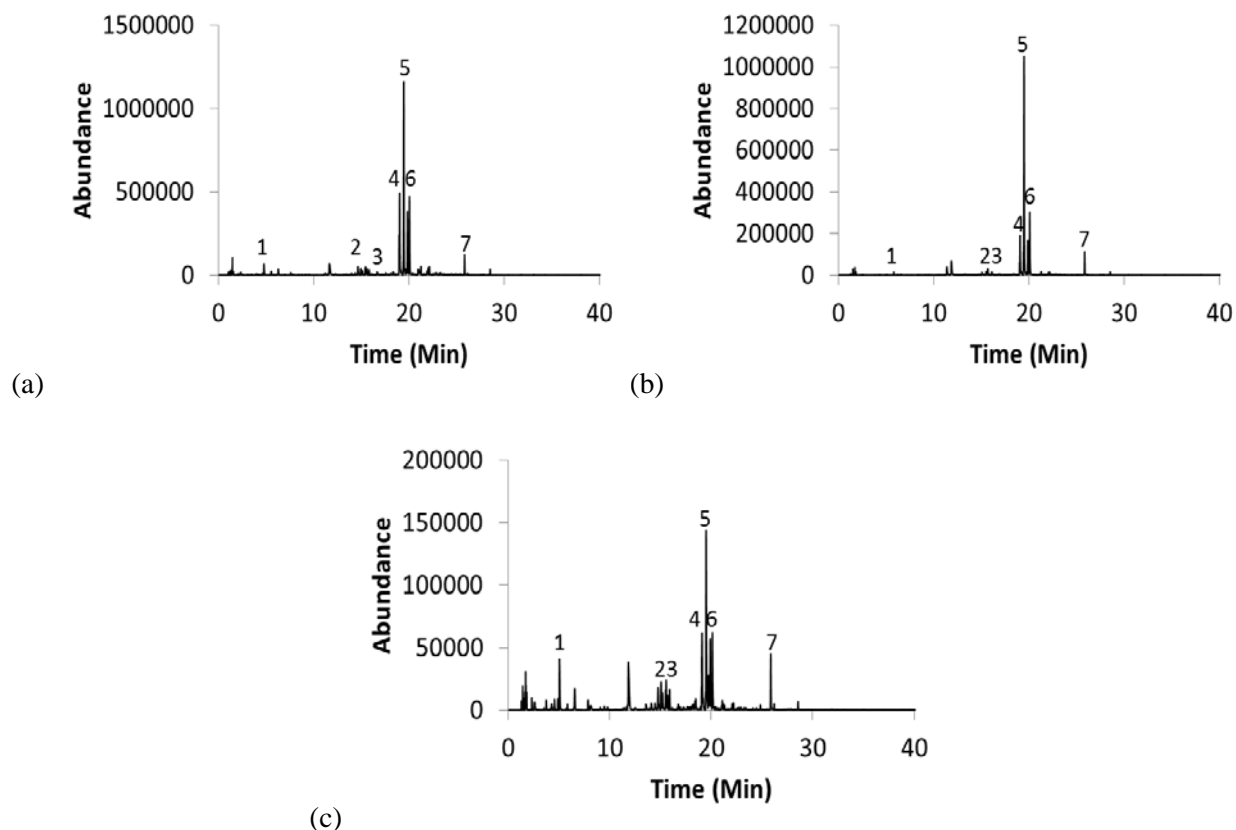


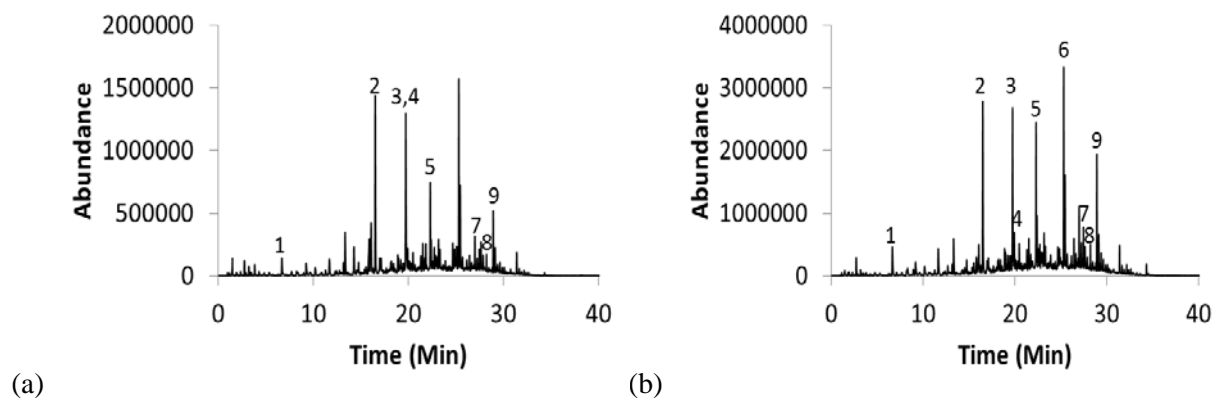
Figure 33. 100% Cotton and 100% acrylic mixtures (total mass=1.5 mg, T>500°C). Cotton peaks displayed as 1-3, acrylic peaks displayed as 4-7 (a) 1:1 mass ratio (b) 1:3 cotton:acrylic mass ratio (c) 3:1 cotton:acrylic mass ratio

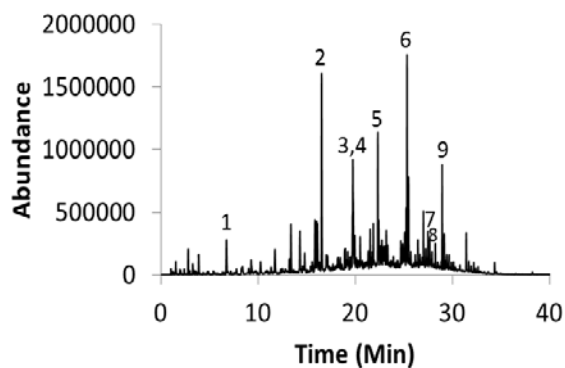
In each ratio (Fig.33), the most abundant peak was hexenedinitrile (5) which is due to acrylic. The peaks that can be associated with acrylic to indicate an increase in textile ratios are hexenedinitrile (6) and 1, 2-benzenedicarbonitrile (7). Succinonitrile (4), although present, does not demonstrate an accurate change in mass ratios as it consistently decreases in each chromatogram regardless of the percentage composition of the textiles. The compounds hexenedinitrile (6) and 1, 2-benzenedicarbonitrile (7) increased in area from 40.89% to 57.78% and 9.95% to 34.22% respectively as the acrylic ratio increased. Compounds 5-methyl furfural

(2) and 2(5H)-furan-3-one (1) were analysed as chemical markers representing cotton in Fig. 33. 2(5H)-furan-3-one (1) was consistently observed to fluctuate with the change in cotton ratio respectively (e.g. when the cotton percentage increased, the peak counts did as well). When the ratio was 1:1, 2(5H)-furan-3-one (1) was found to be around 20% in relative peak area. When the ratio is in favour of acrylic, 2(5H)-furan-3-one (1) decreased to around 10%, but when the textile masses were changed to a 3:1 cotton:acrylic ratio, the relative peak area increased to 44%. 5-methylfufural (2) is observed to decrease in relative area from 22% to 2.15% when the ratio is in favour of acrylic. However, 5-methylfufural (2) is observed to be around 18% when the ratio is in favour of cotton.

Olefin/Wool mixture

The pyrolysis of the wool and olefin blend was found to contain very abundant peaks for their respective chemical markers. Decanoic acid (1) was an unexpected peak that appeared in this mixture because it had not been present in the individual chromatograms of olefin and wool previously (Fig. 26).





(c)

Figure 34. 100% Wool and 100% olefin mixtures (total mass=1.5 mg, T>500°C). Wool peaks displayed as 1-3, and 5, olefin peaks displayed as 3, 4, and 7-9 (a) 1:1 mass ratio (b) 1:3 wool:olefin mass ratio (c) 3:1 wool:olefin mass ratio

There were chemical markers present for both wool and olefin present in each of the three compositions. For wool, 4-methyl-2-nitro-phenol (5) and 2-methyl-phenol (2) displayed relatively large counts in each of the three compositions. The results for olefin analysis in the mixture displayed an increase for 4-methyl-2-undecene (3, 4) when the ratio was increased to a 3:1 olefin:wool ratio (Fig. 34b). When the mass counts of wool increased, the three peaks corresponding to this textile did not increase in relative peak area. 2-methyl-phenol (2) decreases with increasing wool composition which suggests that this compound evolves due not only to the presence of another compound, but also possibly due to the amount of the other compound present. The counts of the olefin peaks (aside from 4-methyl-2-undecene) were not seen to drastically decrease. Under these pyrolysis conditions, olefin will evolve similar counts of compound even if the total amount of olefin is decreased. Wool does not display significant changes in counts with the exception of 2-methyl-phenol which leads to the conclusion that with the composition of olefin and wool it is possible to identify each textile within the blend.

Acrylic/Wool mixture

The pyrolysis of wool and acrylic resulted in the identification of each textile within the three chromatograms in Fig. 35. The following compounds were identified for acrylic succinonitrile (1), hexenedinitrile (2) (3), and 1, 2-benzenedicarbonitrile (7).

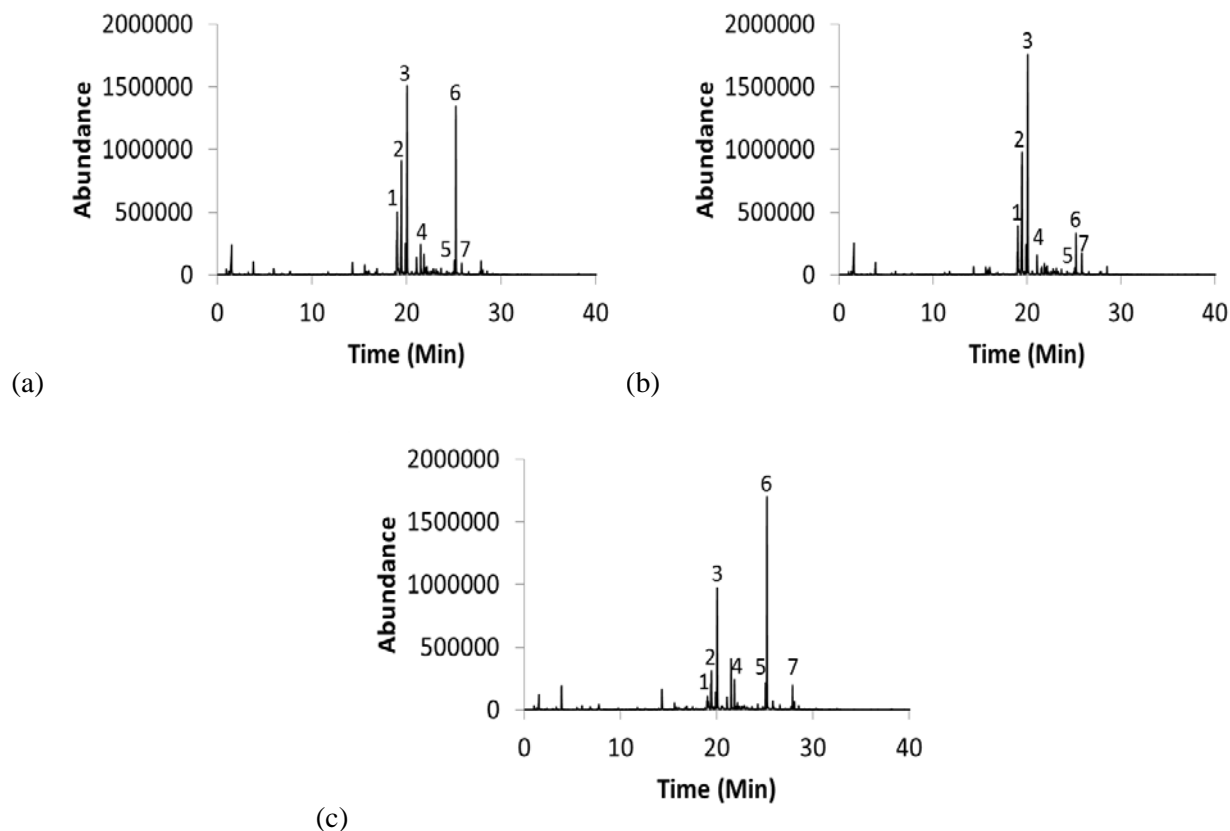


Figure 35. 100% Acrylic and 100% wool mixtures (total mass=1.5 mg, $T > 500^{\circ}\text{C}$). Acrylic peaks displayed as 1-3, and 7, cotton peaks displayed as 4-6 (a) 1:1 mass ratio (b) 1:3 wool:acrylic mass ratio (c) 3:1 wool:acrylic mass ratio

For wool, the following compounds were identified benzylnitrile (4), hydrocinnamitrile (5), and 4-methyl-2-nitro-phenol (6). When the mass ratio was changed in favor of acrylic (Fig. 35(b)), all the chemical markers for wool decreased in relative peak area, while only 1, 2-benzendicarbonitrile (7) was shown to slightly increase. When the ratio was changed in favor of wool, benzylnitrile (4), hydrocinnamitrile (5), and 4-methyl-2-nitro-

phenol (6) all increased in relative peak area. The relative peak area for succinonitrile (1) and hexenedinitrile (2)(3) decreased, while 1,2-benzenedicarbonitrile (7) was relatively unchanged.

Olefin/Acrylic mixture

The olefin and acrylic mixture displayed results as expected for most compounds. The peaks corresponding to 4-isopropyl-1, 3-cyclohexanedione (6, 7), and pentylcyclohexane (8) decreased in relative peak area when the mass of olefin was decreased. These compounds were not observed to increase in relative peak area in the 1:1 mass ratio or with increased olefin mass.

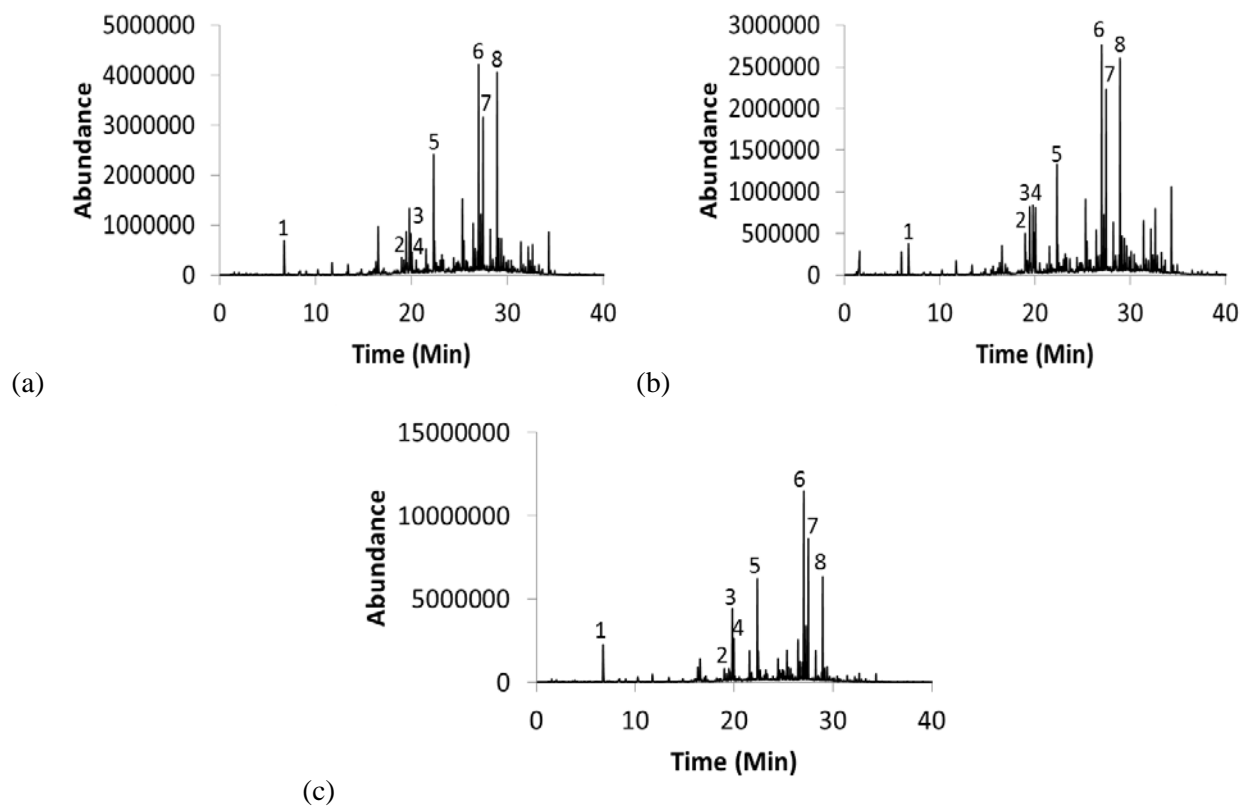


Figure 36. 100% Acrylic and 100% olefin mixtures (total mass=1.5 mg, T>500°C). Acrylic peaks displayed as 2, 4 and 5, olefin peaks displayed as 1,3 and 6-8 (a) 1:1 mass ratio (b) 3:1 acrylic:olefin mass ratio (c) 1:3 acrylic:olefin mass ratio

Other compounds 2, 4-dimethylheptene (1), 4-methyl-2-undecene (3), and 4, 8-dimethyl-1, 7-nonadiene (4) did not change significantly with changing the ratio. An increase in the mass of acrylic gave an increase in the relative peak area of 2-methylene-pentanedinitrile (2). However, the relative peak area of 2-methylene-pentanedinitrile (2) was not seen to decrease significantly when the ratio was changed from 1:1 to 1:3 in favour of olefin. The peaks corresponding to succinonitrile and 1, 2-benzenedicarbonitrile (not labeled, between peak 6 and 7) are not seen to increase or decrease in relative peak area significantly. This suggests that the amount of olefin that may volatilize will not increase after a certain point because the acrylic peaks are not seen to decrease relative to an increase in olefin. Therefore, there is maximum amount of olefin that may be measured. This also suggests that quantitative analysis would be a challenge for olefin.

3.1 Textile Mixture Conclusions

This section of the experiment demonstrated that two textiles in a mixture with different composition percentages can be identified. However, olefin was more time consuming as it was difficult to identify chemical markers due to the number of volatile compounds it evolves.

It was determined that the counts and relative peak area could not be directly associated with the increased composition of each textile for every given chemical marker. Phenol was present in multiple chromatograms each involving wool or cotton and the composition had no consistent effect on the counts or relative peak area and would not be considered as an identifying compound for mixture analysis of textiles. For cotton, 5-methyl furfural was the one compound that consistently correlated with the increase/decrease of the percent composition. The wool compounds that displayed the most consistent correlation with increasing/decreasing percent composition were hydrocinnamonitrile and 4-methyl-2-nitrophenol. For acrylic, the

compounds hexenedinitrile and 1, 2-benzenedicarbonitrile was correlated with the increase/decrease of the relative peak area and the percent composition of cotton. However, when acrylic was mixed with wool, 1, 2-benzenedicarbonitrile displayed an increased correlation with acrylic percent composition but had decreased correlation with the relative peak area. During the acrylic/wool mixture analysis it was also found that succinonitrile and hexenedinitrile had a decreased correlation with the relative peak area and the percent composition of acrylic but did not show an increased correlation. The olefin compounds that were detected displayed little to no significant relative peak area change when the percent composition was increased/decreased. This was unexpected as olefin produced some of the most abundant peaks. When olefin was combined with wool, 4-methyl-2-undecene displayed a correlated increase/decrease with the corresponding percent composition of olefin. Decanoic acid was a new compound found within the wool/olefin mixture that was not displayed in either the wool or olefin chromatograms. The introduction of decanoic acid that appeared in the wool/olefin mixture presents the possibility of other textiles (not included in this experiment) to pyrolyse differently causing new compounds to evolve. Textiles that were blended with olefin were difficult to distinguish individually especially with cotton and acrylic. This limits the quantitative abilities of using the SPME GC-MS method on textiles. It is also possible that the textiles combined with olefin contribute to aiding pyrolysis.

Chapter 4: Chemical Markers of Accelerated Aged Textiles

Researchers find it difficult to analyse aged textiles as they are often in a poor state of conservation due to the environment of exposure over time⁷⁶. Over time textiles will degrade and in some cases start to become discolored. Silk for example, loses its appealing properties like strength and lustre. It can also become brittle and yellow which makes it difficult to handle, exhibit, and use¹⁹. Silk fibres are found in many important historic textiles and artifacts⁸. The compounds responsible for this can be a combination of external and internal factors. For example, the environment that the textile is exposed to (e.g. chemicals in the surrounding atmosphere), can contribute to ‘weathering’. Weathering is described as wearing away or changing the appearance, and/or texture due to long exposure to the air. This over time can cause degradation to occur, and polymer chains to become weak and fragile and break down into smaller polymer chains (Ex. Cotton). The rehabilitation process for historic textiles can be greater understood if knowledge on what has degraded them in the first place is known. The compounds responsible for degradation can lead to information on how to treat the textiles so they no longer degrade or at least slow the process down.

For this experiment, textiles are aged at an accelerated rate using controlled conditions²⁰. Aging textiles manually can be done at an accelerated rate using humidity, heat and ultraviolet light (UV). The purpose of this is to mimic the effects of the degradation process and identify the compounds responsible. A comparison will be made using different sources of controlled conditions and time exposure to them. For example, Zhang *et al.* applied dry thermal ageing, high humidity thermal ageing, and light ageing to silk to measure the amino acid content before and after accelerated aging²⁰.

4.1 Experimental

Heat Aging

Heat aged samples were contained in sealed glass vials and placed in a Precision Economy oven at a temperature of 80°C for a period of 90 days. After 90 days, the samples were left at room temperature in the same sealed container to cool down. Once the vial was room temperature (22°C) the sample was transferred to a 20mL scintillation vial and placed in the desiccator for a minimum of 24 hours. Once put in the desiccator the heat aged sample was prepared the same as previous un-aged samples.

Humidity Aging

Humidity aged samples were placed in scintillation vials and 3 drops of de-ionized water was added to mimic 80% humidity. The sample containing vials were placed in the oven at 80°C for time periods of 5, 15, 40 and 62 days. In order to decrease pressure within the containers, once every week the pressure was released by loosening the top slightly so the air could escape. The top was then screwed back tightly to prevent water vapor from escaping. This had to be done in order to prevent the vial caps from cracking under pressure, and causing water loss from the vial. Upon the completion of the aging process, the vial was then removed from the oven and left to equilibrate temperature with the room. When the vial cooled to room temperature (22°C) it was then transferred to a 20mL scintillation vial and placed in a desiccator for a minimum of 24 hours.

Ultraviolet light Aging

Ultraviolet light (UV) aged samples were placed on a watch glass and centered under the UV light (at room temperature - 22°C). Ultraviolet light was emitted using a Black-ray B100AP (100W bulb) high intensity UV lamp (365nm long wave UV source) (Fig. 37). The samples were exposed for 24, 48, 72, and 96 hour intervals. Once the time interval had elapsed, the sample was placed in a 20mL scintillation vial and put in the desiccator for a minimum of 24 hours. Once in the desiccator, the UV aged sample was prepared the same as previous non-aged samples.



Figure 37. The aging process using UV light from Black-ray B100AP (100W bulb) high intensity UV lamp (365nm long wave UV source).

4.2 Heat Accelerated Aging of Textiles

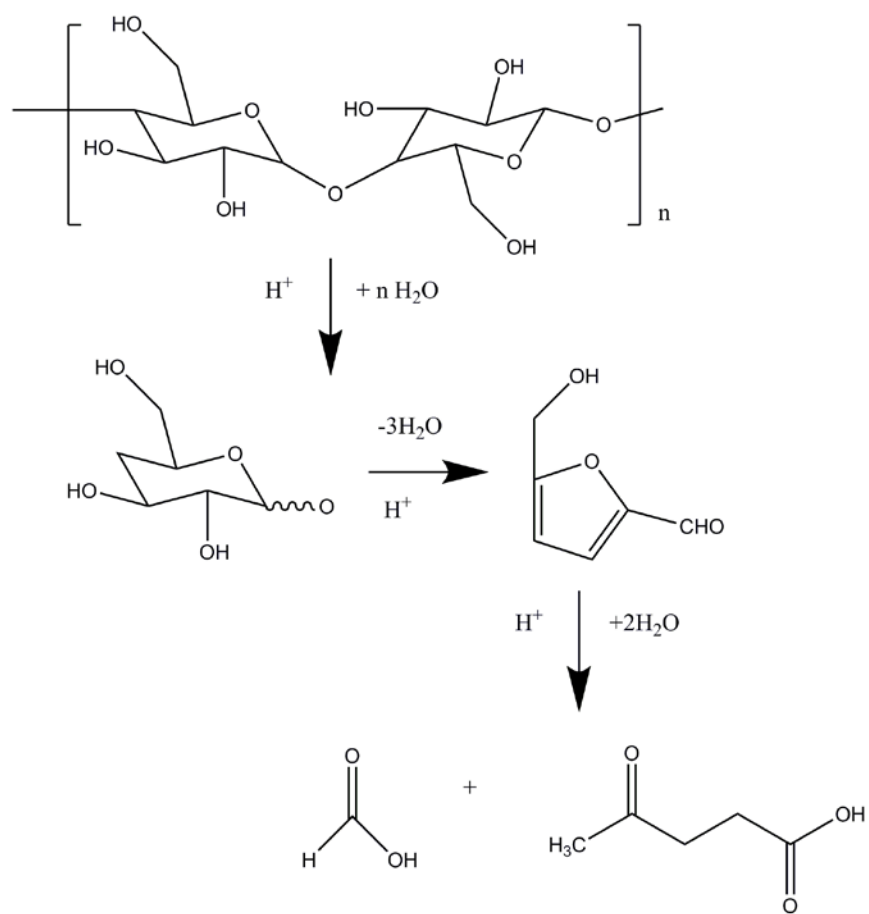
The compounds that differ within the heat accelerated aged textiles can be used for further investigation into preservation methods or treatment of degraded textiles. The analysis will compare non-aged textiles with heat accelerated aged textiles for any difference in the

compounds that are evolved and any changes within the compounds that have already been identified in previous chapters. Cotton, wool, polyester, olefin and acrylic were the textiles of interest for this experiment.

Cotton

Cellulose, the main component of cotton has been studied for degradation compounds previously. Gaspar *et al.* also used SPME for determining degradation compounds found in cotton/linen rag and wood pulp produced paper that was naturally aged⁷⁷. The commonly known degradation compounds discovered for cellulose (Figure 40) are furfural, 5-methyl furfural, linear aldehydes, linear hydrocarbons and acetic acid which are products of acid catalysed hydrolysis^{60, 62, 77-82}.

(a)



(b)

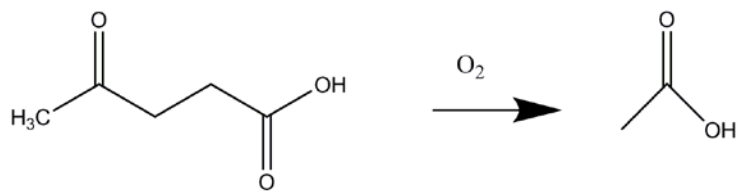


Figure 38. (a) Acid-catalyzed hydrolysis of cellulose and oxidation of levulinic acid⁸³ (b) levulinic acid conversion to acetic acid⁸³

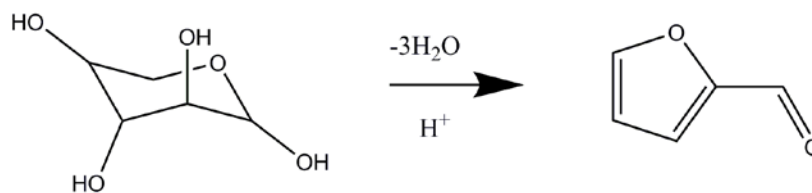


Figure 39. Acid-catalyzed hydrolysis of xylose to furfural as a result of aging⁸³.

Additional compounds such as vanillin and guaiacol have been associated with degradation components of lignin and not directly related to cotton degradation⁶². Lipid oxidation from fatty acids on paper is another form of degradation which leads to the creation of hydroperoxides⁶⁰.

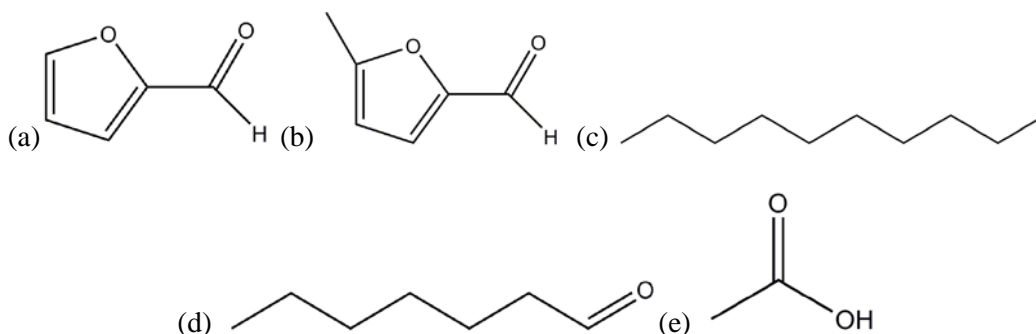


Figure 40. Degradation compounds of cellulose (a) Furfural (b) 5-methyl furfural (c) Decane: an example of a linear hydrocarbon (d) Heptanal: an example of a linear aldehyde (e) Acetic acid

It was expected that there would be an increase in counts and relative peak area in the heat accelerated aged chromatogram for the degradation compounds of cellulose. However, this was not the case, furfural (4) displayed a decreased relative peak area after heat accelerated aging had occurred from 13.92% to 4.82%. 5-methyl furfural (8) also displayed a decrease in relative peak area from 15.28% to 6.57% between non-aged and aged trials.

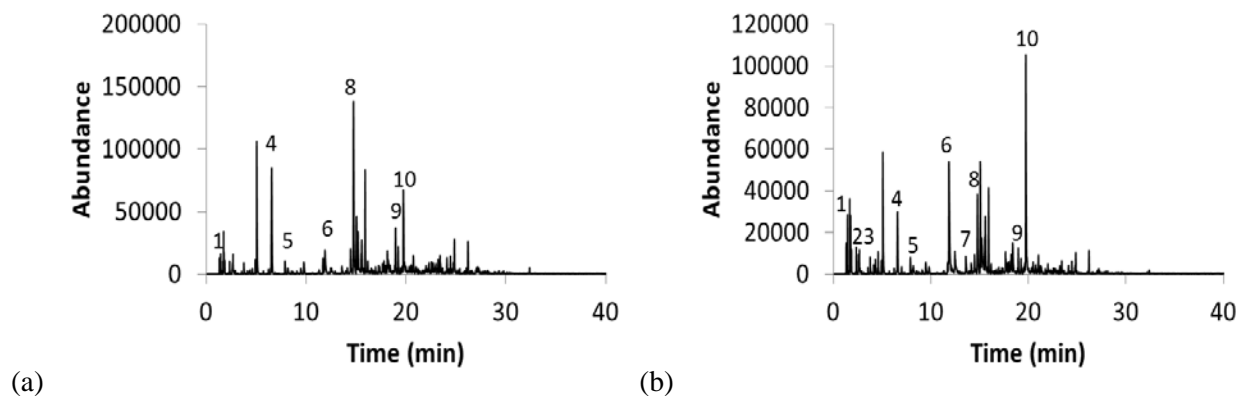


Figure 41. Heat accelerated aging of 100% cotton (a) Un-aged cotton (b) Heat aged cotton (90 days at 80°C)

Acetic acid (1) did not increase significantly in the heat accelerated aged chromatogram having a relative peak area of 1.44% compared to 0.97% in the non-heat accelerated aging chromatogram. The compound 2(5H)-furanone (6) had a distinguishable relative peak area increase from the un-aged to the heat accelerated aged chromatograms from 2.11% to 10.23%. The most distinguishable peak that occurred in the heat accelerated aging was 2, 5-furandicarboxaldehyde (10) which had a relative peak area of 12.90%. Compounds that were undetectable within the un-aged chromatogram but appeared in the heat accelerated aged chromatogram are propanoic acid (2) (3) and 5-methyl-2(3H)-furanone (7). Other compounds had relatively no change in relative peak area in the heat accelerated aged chromatogram than the un-aged chromatogram such as 2-furanmethanol (5) (2.23% to 1.25%), and cyclohexane (9) (2.15% to 0.55%).

Wool

Aged wool is often associated with yellowing, which becomes more visible over time. The appearance of wool after the 90 days of heating was a very light yellow color compared to the original white color it had previous.

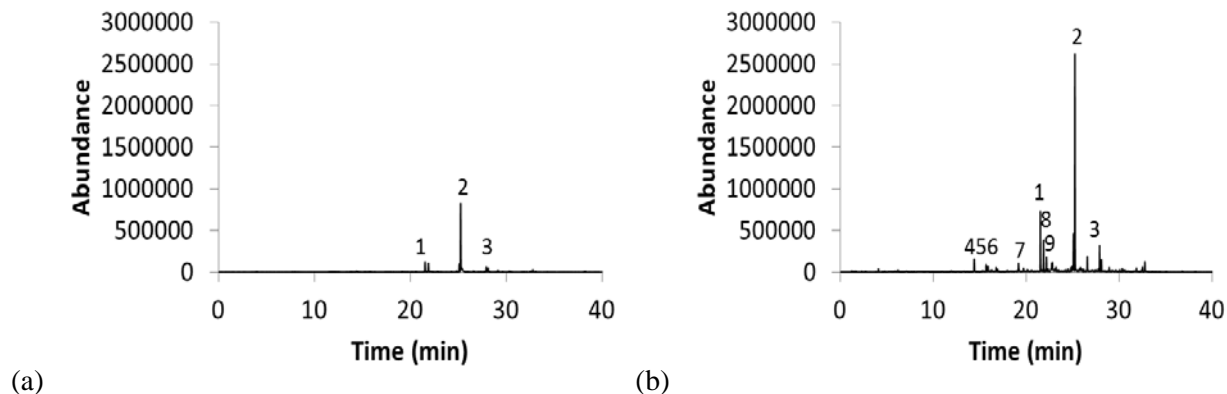


Figure 42. Heat accelerated aging of 100% wool (a) Un-aged wool (b) Heat aged wool (90 days at 80°C)

There were multiple new compounds that arose within the heat accelerated aged chromatogram which included benzaldehyde (4), benzonitrile (5), phenol (6), 3-pyridinecarbonitrile (7), 1H-pyrrole-3-carbonitrile (8), and quinoline (9). It may be possible that multiple compounds are responsible for the yellowing of wool or they could be a result of heat accelerated aging without causing a yellowing effect. The compound 2-nitrophenol (1) displayed an increased relative peak area in the heat accelerated aged chromatogram from 10.05% to 13.01%. The large peak consisting of 4-methyl-2-nitrophenol (2) displayed a decreased relative peak area as well as 3-nitro-benzoic acid (3) from the non-aged chromatogram to the heat accelerated aged chromatogram from 57.88% to 44.00% and 5.10% to 2.66% respectively.

Woolen textiles are often found to be the most fragile, as they cannot be preserved as well as other historical and archaeological artifacts⁷⁶. Irradiation of wool produces hydroperoxide, which may lead to phenoxy radicals from phenol or hydroxylating other aromatic compounds⁸⁴. α -ketocarboxylic acids may be formed by tyrosine(ex. dopa, dityrosine) and related species from tryptophan(ex. hydroxytryptophan, cacrbolines and they are responsible for

yellowing in wool⁸⁴⁻⁸⁶. Peroxynitrite may also contribute to photoyellowing of wool and is caused by the reaction of nitric oxide with superoxide⁸⁵.

Polyester

There are no known reported degradation compounds for polyester as a textile and very little research on heat accelerated aging of polyester. Therefore, it is not known whether there will be little if any difference between aged and un-aged chromatograms. The results are displayed in the following Fig. 43:

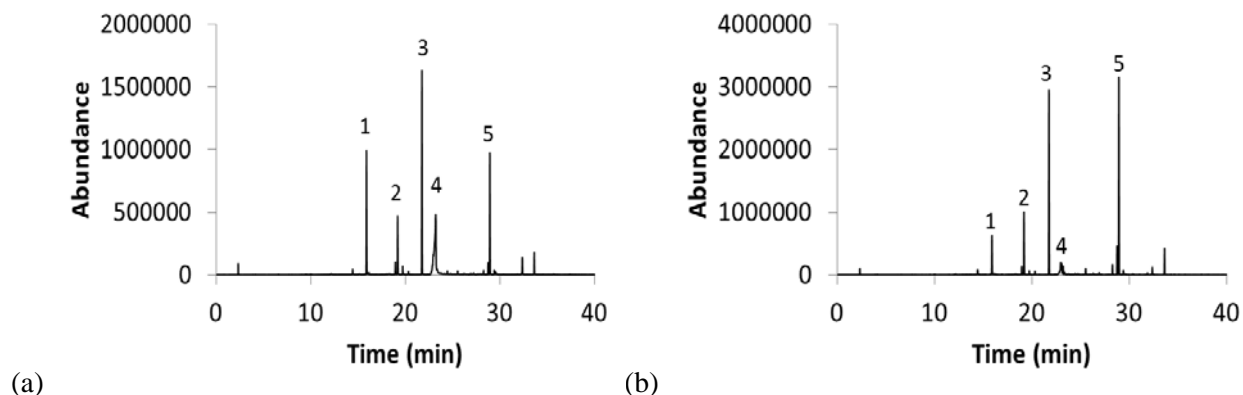


Figure 43. Heat accelerated aging of 100% polyester (a) Un-aged polyester (b) Heat aged polyester (90 days at 80°C)

Polyester did not display different compounds or peaks between the non-aged chromatogram and the heat accelerated aged chromatogram. There was however, a difference between the two chromatograms with the existing compounds and their relative peak areas. Phenol (1) and benzoic acid (4) displayed a large decrease from the non-aged chromatogram to the heat accelerated aged chromatogram with relative peak areas of 21.31% to 7.29% and 7.62% to 2.72% respectively. Compounds that displayed an increased relative peak area include 1-phenyl ethanone (2), and biphenyl (5) which increased from 9.66% to 11.51% and 18.56% to

32.48% respectively. 1,2 propandione (3) remained relatively unchanged in relative peak area for the un-aged chromatogram to the heat accelerated aged chromatogram having relative peak areas of 29.49% and 29.79% for each. Due to the similar chemical structure of benzoic acid and phenol, it is possible that they are the result of the breakdown of biphenyl. If this is indeed the case, the heat accelerated aged chromatogram would be a clear indication that the biphenyl does not break down as easily after experiencing a heated environment. It has been found for polyester foams that formation of alcohol and acid raw products can be detected during natural and artificial aging⁸⁷. However, this was not found to be consistent for heat accelerated aging of polyester fibres.

Olefin

Olefin was the only textile that displayed relatively no changes in relative peak area (<2.15%) for any of the compounds between the un-aged chromatogram and the heat accelerated aged chromatogram. This was expected as similar results occurred when olefin was blended with other textiles. The compounds did not change and their respective peaks counts did not significantly change.

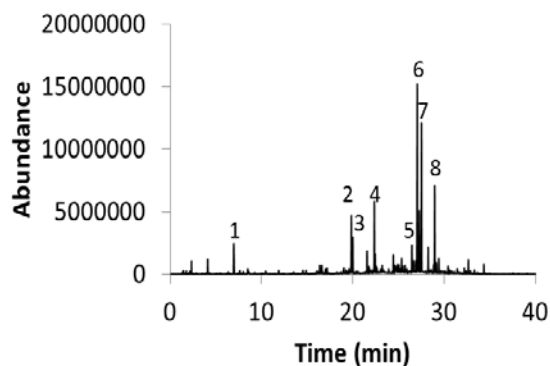
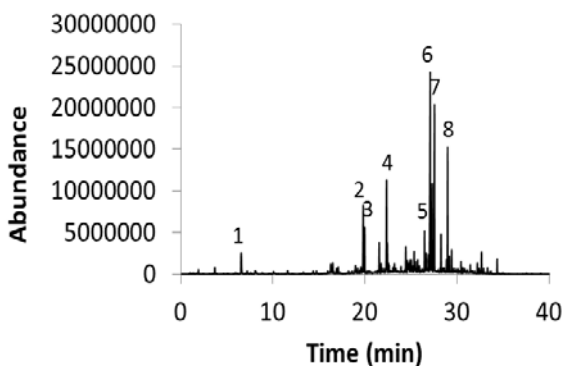


Figure 44. Heat accelerated aging of 100% olefin (a) Un-aged olefin (b) Heat aged olefin (90 days at 80°C)

There were also no new compounds that arose due to the heat accelerated aging process that were detectable. The relative peak areas can be found within the following Table 5:

Table 5. Un-aged chromatogram comparison with the heat accelerated aged chromatogram for the relative peak areas of olefin compounds.

Peak	Compound	Un-aged(%)	Heat aged(%)
1	2,4-dimethyl-1-heptene	3.30	3.76
2	4-methyl-2-undecane	5.12	5.57
3	4-methyl-2-undecane	3.10	3.35
4	4,8-dimethyl-1,7nonadiene	5.98	6.45
5	1,2,3,5-tetramethylcyclohexane	2.60	2.54
6	propargyl octyl ether	21.65	19.52
7	4-isopropyl-1,3-cyclohexandione	15.86	14.54
8	Pentacyclohexane	9.38	8.15

Acrylic

Acrylic displayed many peaks that increased between the un-aged chromatogram and the heat accelerated aged chromatogram. The following compounds succinonitrile (3) and hexenedinitrile (4) all displayed increased relative peak areas of 2.84% to 6.25% and 18.42% to 35.65% respectively (un-aged chromatogram to heat accelerated aged chromatogram).

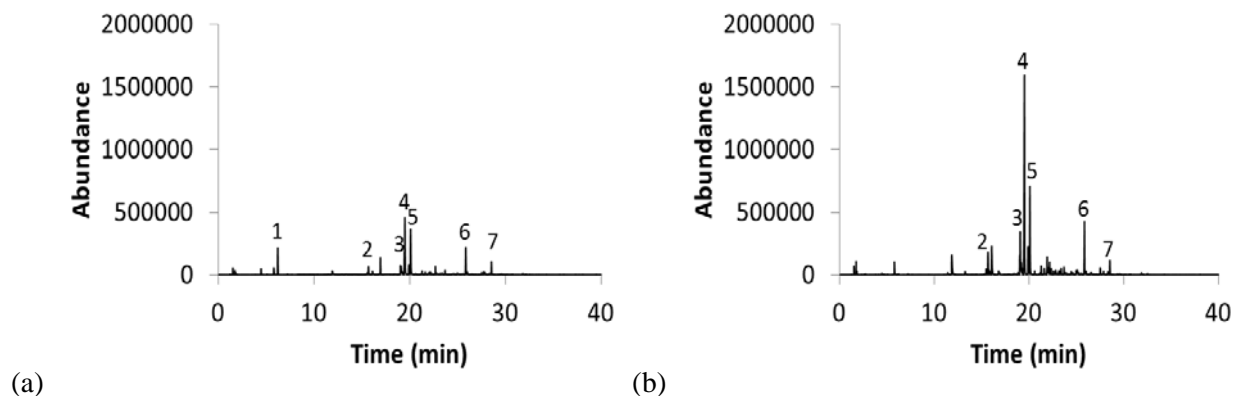


Figure 45. Heat accelerated aging of 100% acrylic (a) Un-aged acrylic (b) Heat aged acrylic (90 days at 80°C)

The following compounds hexenedinitrile (5) and 5-methylisophthalonitrile (7) displayed decreased relative peak areas of 16.69% to 14.16%, and 3.51% to 1.78% respectively (un-aged chromatogram to heat accelerated aged chromatogram). Hexamethyl-cyclotrisiloxane (1) (8.75% relative peak area) was the only compound that was detected in the un-aged chromatogram and not found in the aged chromatogram. It is uncertain what would directly affect this compound to become undetectable within the aged chromatogram but it is known that with some fabrics, poly-dimethylsiloxane (PDMS) polymers have been used as a finishing agent⁸⁸. Hexamethyl-cyclotrisiloxane could be a compound used for acrylic as a finishing agent that once undergoes accelerated aging, may become inert or non-volatile.

There is currently limited literature on acrylic fibre degradation compounds. However, there have been studies regarding polyacrylamide and polyacrylonitrile. Polyacrylonitrile is a liquid compound that is used in making acrylic fibres. Polyacrylamide is similar in structure to acrylic but contains an additional amide substituent. The degradation compounds acetonitrile, acrylonitrile, propionitrile, methacrylonitrile and isobutyronitrile were found for both polyacrylamide and polyacrylonitrile⁸⁹. Although these compounds were not found within the acrylic fibre aged chromatograms, there were similarly, nitrile based compounds that emerged.

4.3 Humidity Accelerated Aging of Textiles

It is known that textile exposure to a humidified environment can cause structural changes within the fibre by processes such as hydrolysis⁸³. Hydrolysis causes the breakdown of a compound using water causing bonds to be cleaved and replaced. Accelerated aging can be implemented by imitating a humidified environment for the textile to reside. This experiment will mimic 80% relative humidity at 80°C as an environment because the effects of accelerated ageing are more pronounced in higher relative humidity conditions⁷⁶. Temperature of the surrounding environment can be a factor when using humidity as an accelerated aging process. The temperature range from 20°C-150°C has been used for heating^{19, 64}. The textiles investigated in this part of the experiment were silk, acrylic, wool and cotton.

Silk

The appearance of silk after it was humidified was rather yellowed in color and had distinguishable frailness as compared to the un-aged silk. Visually, it appeared that the accelerated humidified aging has caused a decrease in overall counts of the volatile compounds that have been released.

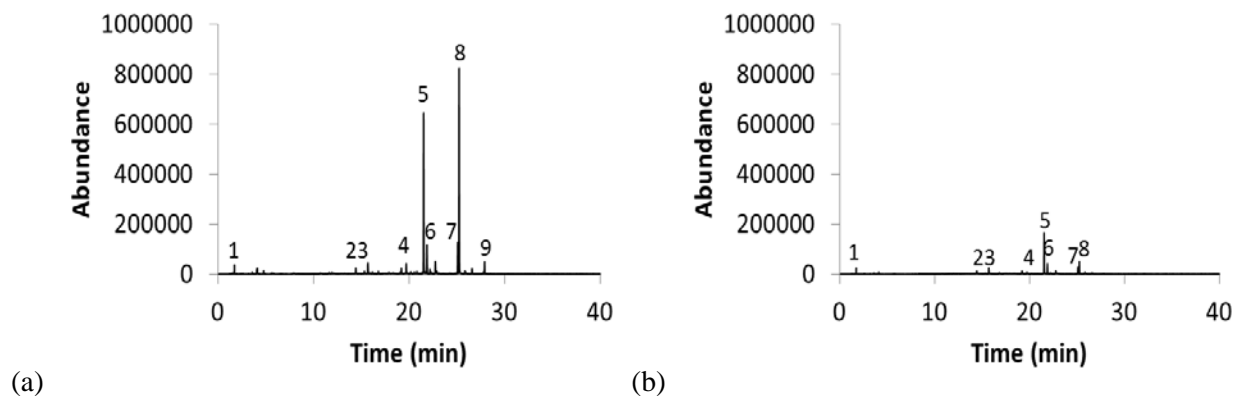


Figure 46. Humidity accelerated aging of 100% silk (a) Un-aged silk (b) Humidity aged silk (62 days at 80°C)

It was found that XRD analyses of silk fibronin shows the growing tendency of random coil concentration, a decreasing trend in amorphous α -helix and crystalline β -sheet counts in fibroin samples exposed to very harsh aging conditions including in O₂, volatile organic carbons (VOCs) and humidity at 150°C for 14 days¹⁹. With the increased β -sheet counts it is expected that the compounds that favour this conformation would be in higher concentration as compared the α -helix confirmation. Despite the decrease in peak counts from non-aged to humidity aged, multiple peaks displayed an increase in relative peak area. Nitroethane(1), benzaldehyde (2), cyanobenzene (3), and benzylnitrile (6) all displayed increases in relative peak area of >80%. The following compounds did not display much change in relative peak area in comparison to the other peaks (<25%) and they consisted of 2-methyl-5-methylthiophene (4), 2-nitro-phenol (5), and hydrocinnamonnitrile (7). The compound 4-methyl-2-nitro-phenol (8) displayed a large decrease in relative peak area from 35.97% to 11.10%. The compound (+)-myrtine (9) was undetectable within the accelerated aged chromatogram. Large fluctuations for relative peak areas of the compounds evolving from silk could be related to the increased conformation of the β -sheet within the fibronin. These compounds that have increased may favor this conformation

and the outliers (+-)-myrtine (9) and 4-methyl-2-nitro-phenol (8) may favor the α -helix for evolving during the heating process. This would make the compounds for silk with the exception of 2-methyl-5-methylthiophene (4), 2-nitro-phenol (5), hydrocinnamitrile (7), and (+-)-myrtine (9), good candidates for degradation markers.

Silk is primarily made up of amino acids forming proteins sericin and fibroin. Sericin gum is often removed during current production practices but for historical textiles, it was either partially removed or not at all²⁰. Sericin protects the silk from damage but can show signs of photoyellowing with age²¹. Photochemical studies on silk and wool mainly focus on reactions producing cysteic acid and aromatic amino acids like tyrosine and tryptophan. Because wool and silk are similar in composition, it is possible that they may share some of the same degradation compound derivatives from tyrosine and tryptophan.

Acrylic

The results for the accelerated humidity aged acrylic physically displayed a yellowing of the fibre. The chromatographic spectrum for the accelerated humidity aged acrylic did not display any new compounds that were detectable but did demonstrate a change with the existing compounds and their presence.

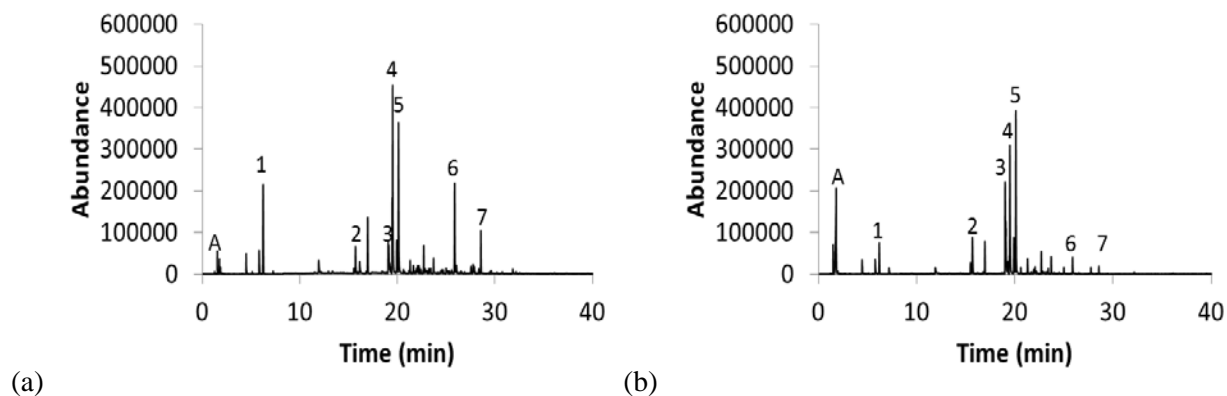


Figure 47. Humidity accelerated aging of 100% acrylic (a) Un-aged acrylic (b) Humidity aged acrylic (62 days at 80°C)

Acetic acid (A) increased drastically in relative peak area from 1.03% to 13.84% for un-aged to accelerated humidity aged respectively. The structure of acrylic does not directly provide information for a degradation pathway, but in the presence of water and air it may have caused acetic acid to be increasingly produced over time. Acetic acid (which has been known to be caused by hydrolysis) could also be used as a candidate for identifying aged acrylic. The compounds that displayed a decrease in relative peak area from un-aged to accelerated humidity aged chromatograms are hexamethyl-cyclotrisiloxane (1), hexenedinitrile (4), 1, 2-benzenedicarbonitrile (6), and 5-methylisophthalonitrile (7) which decreased from 8.75% to 4.18%, 18.42% to 13.73%, 8.44% to 1.93%, and 3.51% to 0.78% respectively. The compounds 1, 2-benzenedicarbonitrile (6) and 5-methylisophthalonitrile (7) were nearly undetectable in the accelerated humidity aged chromatogram and these compounds could be used for decreasing degradation chemical markers. The compound that displayed an increased relative peak area from un-aged to accelerated humidity aged chromatograms was succinonitrile (3), which increased from 2.84% to 8.80%. Succinonitrile (3) displayed an increase in relative peak area and could potentially be used as chemical markers for degradation. The compound hexenedinitrile is responsible for two peaks (4) and (5), one of which decreases and one which

increases. It is possible that the two hexenedinitrile peaks are stable and tend to fluctuate with their given retention times and thus, would not be a good candidate for a chemical degradation marker.

Wool

The most prominent effect that the humidified aging had on wool was the strong odour that was released once the wool was taken out of the humidified sample chamber. Lisovac et al found that a variety of volatile compounds, including sulphur-containing compounds, were emitted with their concentration increasing with temperature and humidity in most cases⁶⁴. Sulphur containing compounds like H₂S have been known to give off a strong odour. Wool displayed the most distinguishable color change of all the textiles used for aging by turning dark brown and becoming brittle upon touch.

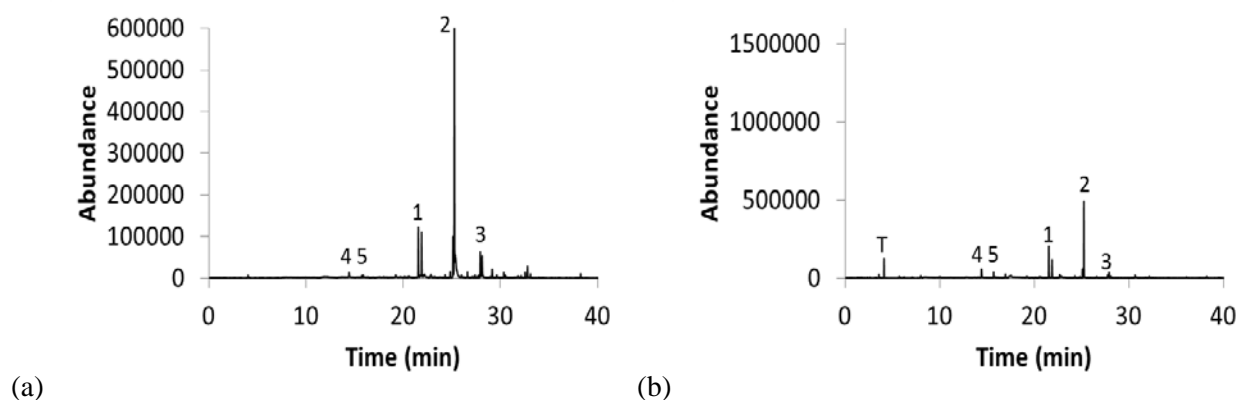


Figure 48. Humidity accelerated aging of 100% wool (a) Un-aged wool (b) Humidity aged wool (62 days at 80°C)



Figure 49. Accelerated humidity aged wool over a period of 62 days at 80°C, 80% relative humidity.

Wool had one compound that appeared in the accelerated humidity aged chromatogram that did not appear in any other chromatogram that wool was used in. Toluene (T) appeared at 4.121 min with the largest relative peak area of the new compounds of 6.70%. Toluene has been observed in other research as a pyrolysis product degrading from phenylalanine in wool⁴².

The compound 2-nitrophenol (1) was the only compound that had displayed an increase in relative peak is from 10.05% to 14.73% from un-aged to accelerated humidity aged. Compounds 4-methyl-2-nitrophenol (2) and 3-nitro-benzoic acid (3) both decreased in relative peak area from un-aged to accelerated humidity aging from 57.88% to 32.01% and 5.10% to 0.97% respectively. These two compounds shared the same decreasing relative peak area as the heat accelerated aging which suggests they could be used as chemical degradation markers.

Cotton

Accelerated humidity ageing had mixed results for the compounds observed. Although the counts for every compound increased, the relative peak area decreased for most.

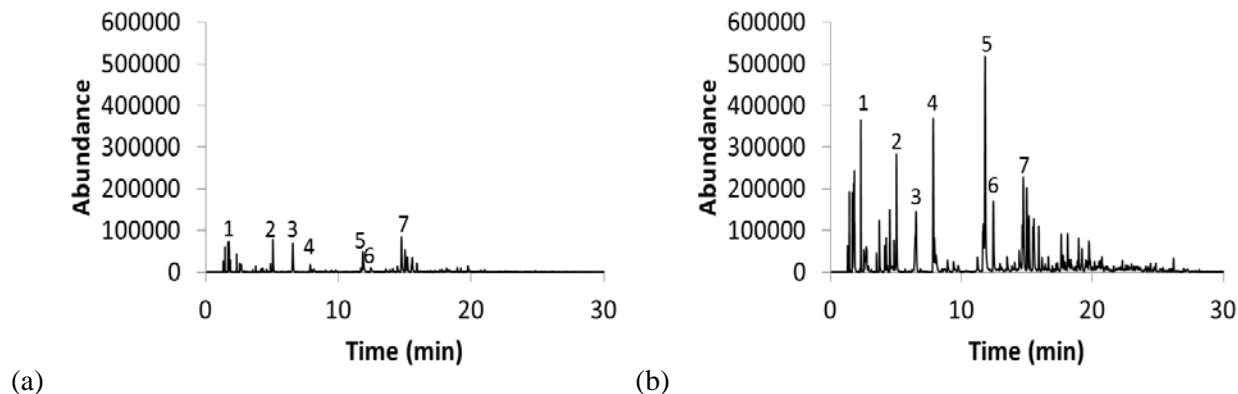


Figure 50. Humidity accelerated aging of 100% cotton (a) Un-aged cotton (b) Humidity aged cotton (62 days at 80°C)

The degradation compounds that have been previously discussed, acetic acid (1), furfural (3), and 5-methyl-2-furfural(7) decreased from the un-aged to the accelerated humidity aged chromatograms with relative peak areas of 6.11% to 2.83%, 9.45% to 5.71%, and 11.75% to 4.89% respectively. Acceleration of oxidation at humid conditions has been observed during cellulose oxidation in the presence of water vapor¹⁹. However, it was not observed for this experiment for the known degradation compounds acetic acid and furfural to display increased relative peak area. Lastly, the labelled compound that had also decreased in relative peak counts from un-aged to accelerated humidity aged chromatogram was (2H) furan-3-one (2) (not previously regarded as a degradation compound). The compounds that had increased in relative peak area are 2-furanmethanol (4), 2(5H)-furanone (5), and 5-methyl-2(5H)-furanone (6) with values of 2.54% to 8.01%, 8.27% to 13.33%, and 1.39% to 4.29% respectively.

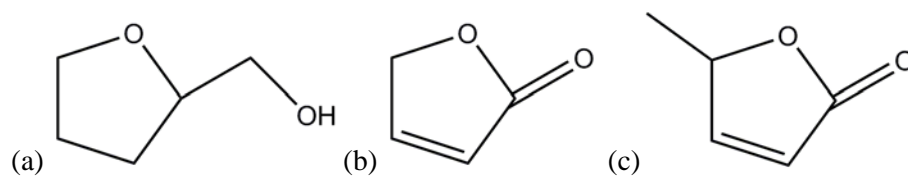


Figure 51. Derivatives of Furfural (a) Furanmethanol (b) 2(5h)-furanone (c) 5-methyl-2(5h)-furanone

Although the expected degradation compounds did not show an increased relative peak area from the un-aged to aged chromatograms, the derivatives of furfural did display increases in relative peak area which could have been directly related to the accelerated aging of the cotton.

4.4 Ultra-Violet (UV) light Accelerated Aging of Textiles

Fibrous proteins are known to discolour from the UV portion of sunlight and this effect is often enhanced by the addition of whitening agents that are applied to textiles⁹⁰. Ultraviolet A (UVA) accounts for roughly 95% (315nm-400nm) of the UV light and UVB is 5% (280 nm-315nm). Textile fibres can absorb these UV rays, which (depending on the structure of the textile fibre) can cause reactions to occur resulting in structure modification and possibly chromophores. Wool and silk are classified as proteinaceous fibres and are expected to display greater photoyellowing effects as they have been previously found to exhibit when exposed to UV for a period of time^{84-86,91}. However, this does not discount the non proteinaceous fibres, as they may degrade by UV light but not adequately display any photoyellowing effects.

Silk

The effects of UV accelerated aging (365 nm) were very similar to the accelerated humidity aging in regards to the chromatographic component of the silk.

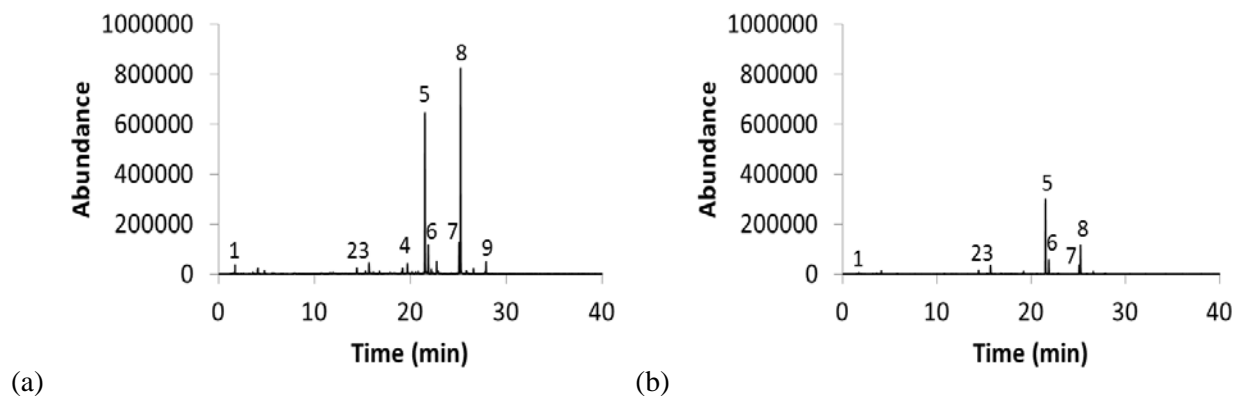


Figure 52. Ultraviolet accelerated aging of 100% silk (a) Un-aged silk (b) UV aged silk (96 hours)

Upon visual appearance, silk displayed minute photoyellowing within the UV accelerated aged silk whereas the humidified sample had a bold yellowing appearance. Post pyrolysis of the UV aged sample led to the following compounds increasing in relative peak area benzaldehyde (2), cyanobenzene (3), and benzylnitrile (6). (+)-Myrtine (9) was found to not be adequately detectable by the chemstation software in the aged chromatogram.

Acrylic

Acrylic displayed similar attributes between the humidity accelerated aging and the UV accelerated aging. Acetic acid (A) increased in relative peak area from 1.03% to 24.65% from the un-aged to the UV accelerated aged chromatogram. This suggests that acetic acid may be a suitable degradation chemical marker for acrylic.

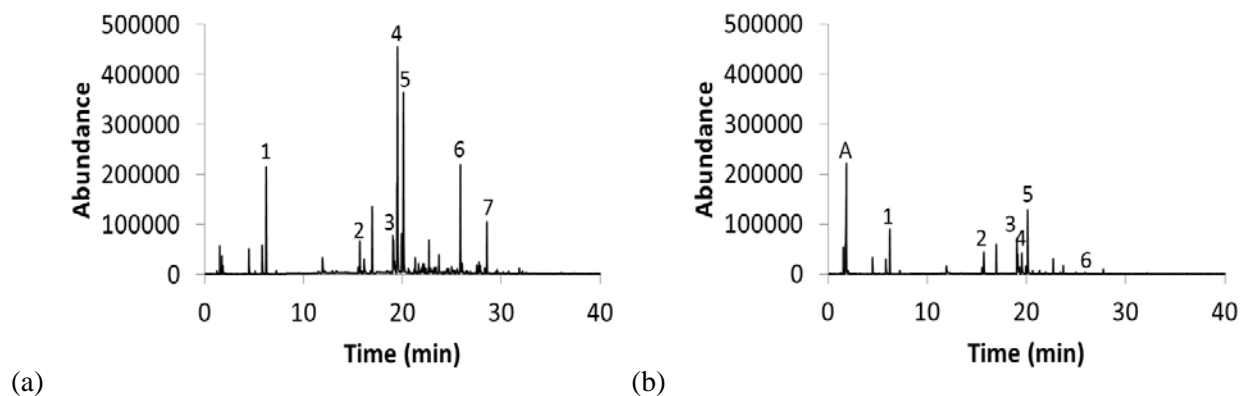


Figure 53. Ultraviolet accelerated aging of 100% acrylic (a) Un-aged acrylic (b) UV aged acrylic (96 hours)

The compounds that showed minimal change in relative peak area from un-aged to UV accelerated aged chromatograms are: hexamethyl-cyclotrisiloxane (1) and succinonitrile (3). Benzonitrile (2), aside from acetic acid was the only compound to display and increase in relative peak area from un-aged to UV accelerated aged chromatograms from 2.88% to 5.20%. Hexenedinitrile (4)(5) and 1,2-benzenedicarbonitrile (6) both displayed decreases in relative peak area in the un-aged to UV accelerated aged chromatograms from 18.42% to 5.75%, 16.69% to 13.03% and 8.44% to 0.35% respectively. 5-methylisophthalonitrile (7) was found to be undetectable using the in the UV accelerated aged chromatogram using the chemstation software.

Wool

Wool keratin has a relatively high UV absorbance within the UV-B region. Compared to other fibrous proteins such as silk fibroin and leather collagen, wool contains more photoactive protein residues including cystine, tryptophan, tyrosine, and phenylalanine which absorb UV/visible radiation and produce chromophores⁹¹.

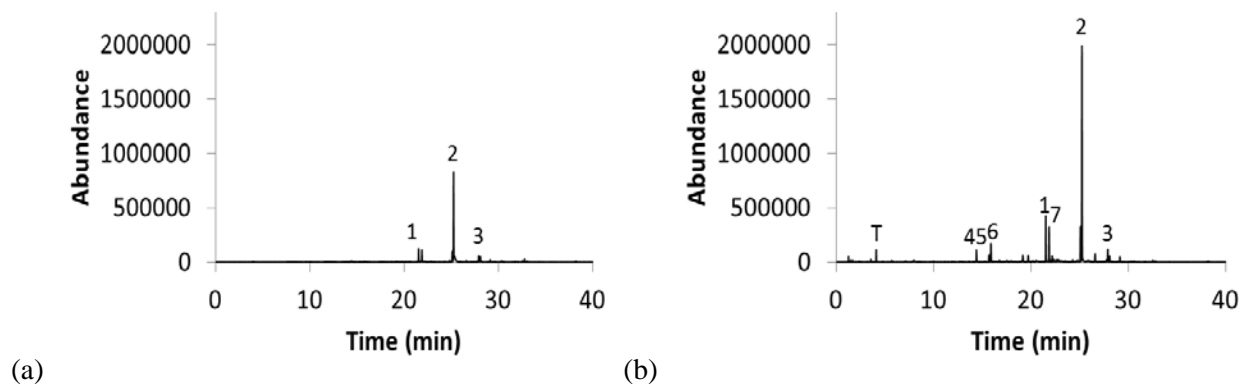


Figure 54. Ultraviolet accelerated aging of 100% wool (a) Un-aged wool (b) UV aged wool (96 hours)

Toluene (T) was a new compound that appeared with a relative peak area of 2.36% which was not quite as high as it was in the humidified chromatogram. Two new compounds not displayed in any of the other chromatograms but the UV aged ones were 1-isocyano-2-methyl-benzene and 2-methyl-5-nitro-benzamine (relative peak areas of 8.30% and 3.15% respectively). The compounds 4-methyl-2-nitro-phenol (2) and benzoic acid (3) both decreased in relative peak counts slightly with 2-nitrophenol displaying relatively no change. Wool did not show the same physical photoyellowing as was expected based on the other accelerated aging processes. A slight yellowing was found on the wool sample after the 96 hour period of UV exposure.

Cotton

Cotton displayed no sign of photoyellowing after 96 hours of UV accelerated aging. However, cotton did display the greatest change in the chromatograph among the textiles that had been UV aged.

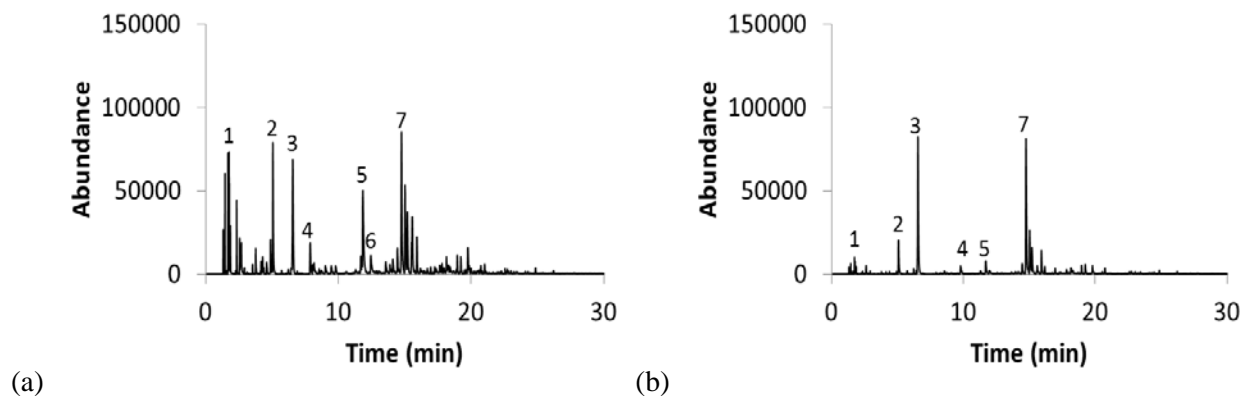


Figure 55. Ultraviolet accelerated aging of 100% cotton (a) Un-aged cotton (b) UV aged cotton (96 hours)

The known cellulose degradation components furfural (3) and 5-methyl-2-furfural (7) displayed a large increase in relative peak area from the un-aged to the UV accelerated aged chromatogram from 9.45% to 30.49% and 11.75% to 28.41% respectively. Acetic acid was the one known cellulose degradation compound that experienced a decrease when the un-aged and UV accelerated aged were compared, with the relative peak area reducing from 6.11% to 1.22%. Acetic acid is a volatile compound and it is possible that the heat produced from the UV lamp caused it to volatilize. 2-furanmethanol (4) and 2(5H)-furanone displayed decreased relative peak areas, while (2H)-furan-3-one displayed no relative change and 5-methyl-2(5H)-furanone (6) was undetectable in the UV accelerated aged chromatogram.

4.4.1 Accelerated Aging Conclusions

The three accelerated aging techniques applied to the textiles, heat, humidity, and UV each affected the textile samples chemically and physically in different ways. Physically, humidity had the greatest effect on the textile samples by distinctively causing a yellowing of each sample as well as a pungent odour from the wool sample. Heat also caused yellowing with wool, cotton, and acrylic. However, it did not compare to the yellowing extent of the humidified samples. UV had little to no effect on the photoyellowing of any of the textiles which could

possibly be due to the lack of whitening agents used within the treatment process of textile samples.

Olefin was the only textile sample that did not display drastic changes both physically or chemically with the aging process. Due to the lack of effect the aging process had on the textile, it this approach for identifying chemical age markers of olefin was considered inapplicable.

Polyester displayed large relative peak area decreases with phenol and benzoic acid and a large increase in relative peak area of biphenyl. It is uncertain whether the combination of heat and air causes the phenol and benzoic acid to form biphenyl creating the drastic change between the three compounds. However, regardless of the formation, biphenyl can be used as a degradation chemical marker as it consistently produced an increase with heat accelerated aging.

Wool produced new compounds throughout the three aging processes. Toluene was a new compound discovered within the UV and humidity aged chromatograms and phenol was found within the UV and heat aged chromatograms. Toluene has been found previously as a degradation compound when using the alkali-catalyzed PyGC method⁴². This could potentially be used as an age degradation marker as well as 1-isocyano-2-methyl-benzene and 2-methyl-5-nitro-benzamine which appeared exclusively in the UV aged chromatograms.

Silk also provided similar results between the humidity and UV aged chromatograms. The common compounds that displayed relative peak area increases were benzaldehyde, cyanobenzene, and benzylnitrile. Each of these compounds could be further investigated for possible degradation chemical markers by determining the concentration of each.

The results for acrylic were successful, as was expected that the synthetic textiles would display the least amount of change once they underwent the accelerated aging process. This was

not the case with acrylic as the compound acetic acid displayed large increases within the humidity and UV aged chromatograms. Benzonitrile also displayed slight increases within all three aging chromatograms. Both acetic acid and benzonitrile are potential degradation chemical markers.

Cotton shared the mixed results as is applied to each of the three accelerated aging techniques. When exposed to heat accelerated aging, cotton did not display any increase for its known degradation compounds. Only when UV accelerated aging was applied, furfural and 5-methyl-2-furfural display large increases in relative peak counts. 2(5H)-furanone experienced increases within the heat and humidity aged chromatograms and 2, 5-furandicarboxaldehyde exclusively displayed a large increase in the heat aged chromatograms.

It appears that each accelerated aging method has different effects on the volatile compounds produced. This could be directly related to the degradation pathway that each affected compound undergoes (e.g. H₂O evaporation, hydrolysis, and UV absorption).

Conclusions

The objective of this work was to assess the application of HS-SPME GC-MS as an analytical method for the analysis of textile objects. The research began by assessing the experimental parameters in which the method would be performed. The effects of temperature on the chromatographic patterns did not show any sign of volatile compounds competing for adsorption sites on the SPME coating. It was found that at higher temperatures (>500°C), the number of volatile compounds increased as well as the signal counts representing each one. It was also determined when performing the temperature optimization that the SPME collection time would need to be determined. The SPME optimal collection time using the PDMS fibre was found to be 5 minutes. This parameter was also determined to be optimal when the S/N was largest. A comparison between the mass of the textile and its effects on the compounds produced was investigated. It was found that when less mass was used, the number of compounds that evolved decreased. However, at a mass of 0.02 mg there were compounds that could be identified and potentially used for identification of the given textile.

When determining the feasibility for identifying chemical markers, a comparison between multiple sources of the same textile was investigated to determine consistency within the chromatograms. By comparing 5 sources of cotton, it was found that the compounds found within the chromatograms are identical. However, it was found that the peak counts for each compound had varied for each source of textile. In order to establish designated compound markers for each textile, a full pyrolysis SPME trial was performed in triplicate for each textile fibre and a minimum of 7 reproducible compounds were chosen for each.

It was found that when combining textiles, the chemical markers could still be identified within the chromatogram. Due to the large number of compounds evolving, it was more difficult to assess textiles blended with olefin. This made it challenging to identify other chemical markers from other textile fibres within the blended mixture. In the case of olefin, a statistical approach is recommended for data analysis (e.g. principle component analysis). In a study previously reported on polymer resins, it was found that the simple compounds gave very busy mass spectra⁸⁴. This was the case with olefin and it is possible that the simplicity of the structure can contribute to noise levels of the chromatogram. Peak overlap can possibly be an issue with an abundant mixture of textiles with varying compositions in the chromatographic pattern. In order to process these compounds for identification, chemometric techniques can be applied to spectroscopic data. Principle component analysis (PCA) is one example of a statistical application that is used for large data matrices such as chromatographic spectra. Cleve *et al.* applied the chemometric PLS2 method to blended textiles for identification with near infrared (NIR) spectrophotometry⁹². It can be used for identifying patterns calculated from variances within large data sets that may be hard to identify using other techniques. Principal components have been calculated for determining the identification of counterfeit and non-counterfeit drugs in combination with HS-SPME GC-MS⁹³. The food industry has also taken advantage of statistical analysis with HS-SPME GC-MS by determining the state of seafood freshness using PCA on the volatile compound profiles⁹⁴. Further research with PCA and larger mixtures of textiles may lead to the identification of multiple textiles in an unknown sample.

Heat, humidity, and UV were the techniques used for accelerated aging. Olefin was found to have no affect from accelerated aging. Wool had the most unique find with the appearance of toluene, which was found exclusively when wool was aged using UV. Cotton,

acrylic, silk and polyester each were found to have increasing relative peak areas with increased accelerated aging for certain compounds. This varied with each accelerated aging method used. For example, silk provided consistent data between the humidity and UV aged chromatograms while cotton was found to only produce noticeable differences in its known degradation compounds using UV accelerated aging. The data comparison between accelerated aging techniques was different for each textile. Noticeable differences could be found exclusively in one technique or among multiple techniques; however, it depended on the textile.

Furthermore, the use of catalysts could be useful for aiding in the pyrolyzation process of textiles. As previously mentioned, catalysts have been used with py-GC-MS⁴⁷. In the case with olefin, this may be a solution for removing unnecessary compounds and peaks from the chromatogram. It may be useful for textile blends containing a large number of individual textiles. The opposite effect may occur as well. Sodium hydroxide, Na₂CO₃, and NaHCO₃ have been found to improve the detection of multiple compounds when it has been applied to wool prior to pyrolyzation⁴². However, difficulty may arise as catalysts have been added within an enclosed compartment for py-GC-MS. With the current HS-SPME GC-MS method, modification of the sample chamber may be needed to accommodate the curing process the textiles would have to initially perform prior to pyrolyzation.

The SPME apparatus provides multiple options for coatings of the graphite sampling syringe as listed in Table 1. It may be beneficial to study the feasibility of other coatings and/or columns for textiles. Polydimethylsiloxane (PDMS) was chosen for this experiment as it is the most commonly used coating for volatile compounds. However, it was unknown what types of volatile compounds would evolve. A polydimethylsiloxane/divinylbenzene (PDMS/DVB) or polydimethylsiloxane/carboxen (PDMS/Carboxen) coating could be evaluated for this method as

both of these are optimal for extracting polar compounds (especially phenols and carboxylic acids)⁵⁸ which were found within wool, silk, polyester and cotton chromatograms.

References

- [1] Cook J. Gordon, *Handbook of Textile Fibres*, Reprint; Merrow Publishing Co. LTD: England, 1993
- [2] Wilding, Houck, Greaves. *Identification of Textile Fibres*, Wood Head Publishing Ltd: England, 2009
- [3] Le Couteur, P.; Burreson, J., *Napoleon's Buttons, How 17 Molecules Changed History*, Tarcher/Putnam Inc.: New York, 2003; pp105-122
- [4] Woodings C., *Regenerated Cellulose Fibres*, Woodhead Publishing LTD: England, 2001
- [5] Bertini, F., Canetti, M., Patrucco, A., & Zoccola, M. (2013). Wool keratin-polypropylene composites: Properties and thermal degradation. *Polymer Degradation and Stability*, 98(5), 980-987
- [6] Plowman, J. E., Deb-Choudhury, S., Clerens, S., Thomas, A., Cornellison, C. D., & Dyer, J. M. (2012). Unravelling the proteome of wool: Towards markers of wool quality traits. *Journal of Proteomics*, 75(14), 4315-4324.
- [7] C. Viney (2000) From Natural Silks to New Polymer Fibres, *The Journal of The Textile Institute*, 91:3, 2-23
- [8] Akyuz, S., Akyuz, T., Cakan, B., & Basaran, S. (2014). Investigations of the historic textiles excavated from ancient ainos (enez – turkey) by multiple analytical techniques. *Journal of Molecular Structure*, 1073, 37-43
- [9] Kundu SC, Kundu B, Talukdar S, Bano S, Nayak S, Kundu J, *et al.* Invited review nonmulberry silk biopolymers. *Biopolymers* 2012; 97(6):455-67.
- [10] R.C. Janaway, *The decomposition of materials associated with buried cadavers*, in: M. Tibbett, D.O. Carter (Eds.), *Soil Analysis in Forensic Taphonomy: Chemical and Biological Effects of Buried Human Remains*, CRC Press, Boca Raton, FL, 2008, pp.153–201
- [11] Yan, L., Chouw, N., & Jayaraman, K. (2014). Flax fibre and its composites – A review. *Composites Part B: Engineering*, 56, 296-317.
- [12] Annis, Patricia A.; Quigley Jr, Thomas W.; Kyllö, Karen E. Useful Techniques in Textile Microscopy, *Textile Chemist & Colorist*. 1992, Vol. 24 Issue 8, p19-22
- [13] Pelton W.; Distinguishing the Cause of Textile Fibre Damage Using the Scanning Electron Microscope (SEM), *Journal of Forensic Sciences*, 1995, Vol. 40, No. 5, pp. 874-882

- [14] Wilson H., Carr C., Hacke M.; Production and validation of model iron-tannate dyed textiles for use as historic textile substitutes in stabilisation treatment studies, *Chemistry Central Journal*. 2012, 6:44
- [15] Liu, J., Guo, D., Zhou, Y., Wu, Z., Li, W., Zhao, F., *et al.* (2011). Identification of ancient textiles from yingpan, xinjiang, by multiple analytical techniques. *Journal of Archaeological Science*, 38(7), 1763-1770
- [16] Bailing Sun, Anmin Huang, Yueping Wang & Junliang Liu (2015) Natural Bamboo (*Neosinocalamus affinis* Keng) Fibre Identification Using FT-IR and 2D-IR Correlation Spectroscopy, *Journal of Natural Fibres*, 12:1, 1-11
- [17] Gray, F. M., Smith, M. J., & Silva, M. B. (2011). Identification and characterization of textile fibres by thermal analysis. *Journal of Chemical Education*, 88(4), 476-479
- [18] Lowe, A. C., Beresford, D. V., Carter, D. O., Gaspari, F., O'Brien, R. C., Stuart, B. H., *et al.* (2013). The effect of soil texture on the degradation of textiles associated with buried bodies. *Forensic Science International*, 231(1–3), 331-339
- [19] Koperska, M. A., Pawcenis, D., Bagniuk, J., Zaitz, M. M., Missori, M., Łojewski, T., *et al.* (2014). Degradation markers of fibroin in silk through infrared spectroscopy. *Polymer Degradation and Stability*, 105, 185-196
- [20] Zhang, X., Berghe, I. V., & Wyeth, P. (2011). Heat and moisture promoted deterioration of raw silk estimated by amino acid analysis. *Journal of Cultural Heritage*, 12(4), 408-411
- [21] Ahmed H., Darwish S. Effect of Museum Conditions on Historical Dyed Silk Fabric with Madder Dye. *J Polym Environ*, (2012) 20:596–606
- [22] Yang C. Infrared spectroscopic analysis of textile materials degradation using photoacoustic detection, *Ind. Eng. Chem. Res.* 1992,31, 617-621
- [23] Wojciechowska, E., Włochowicz, A., Wysocki, M., Pielesz, A., & Weselucha-Birczyńska, A. (2002). The application of fourier-transform infrared (FTIR) and raman spectroscopy (FTR) to the evaluation of structural changes in wool fibre keratin after deuterium exchange and modification by the orthosilicic acid. *Journal of Molecular Structure*, 614(1–3), 355-363
- [24] Chung, C., Lee, M., & Choe, E. K. (2004). Characterization of cotton fabric scouring by FT-IR ATR spectroscopy. *Carbohydrate Polymers*, 58(4), 417-420
- [25] Kavkler, K., & Demšar, A. (2011). Examination of cellulose textile fibres in historical objects by micro-raman spectroscopy. *Spectrochimica Acta Part A: Molecular and Biomolecular Spectroscopy*, 78(2), 740-746

- [26] G. N. Andreev, B. Schrader, H. Schulz, R. Fuchs, S. Popov, N. Handjieva. Non-destructive NIR-FT-Raman analyses in practice. Part 1. Analyses of plants and historic textiles. *Fresenius J Anal Chem* (2001) 371 :1009–1017
- [27] Bruni S., De Luca E, Guglielmi V, Pozzi F. Identification of natural dyes on laboratory-dyed wool and ancient wool, silk, and cotton fibres using attenuated total reflection (ATR) Fourier transform infrared (FT-IR) spectroscopy and Fourier transform Raman spectroscopy. *Appl Spectrosc.* (2011) Sep;65(9):1017-23
- [28] Rosenberg E., Characterisation of historical organic dyestuffs by liquid chromatography–mass spectrometry, *Anal Bioanal Chem* (2008) 391:33–57
- [29] CASADIO F., LEONA M., LOMBARDI J., VAN DUYN R., Identification of Organic Colorants in Fibres, Paints, and Glazes by Surface Enhanced Raman Spectroscopy, *ACCOUNTS OF CHEMICAL RESEARCH*, (2010) 782-791 Vol. 43, No. 6
- [30] Nie S., Emory S., Probing Single Molecules and Single Nanoparticles by Surface-Enhanced Raman Scattering, *Science* (1997): Vol. 275, Issue 5303, pp. 1102-1106
- [31] Ali, E. M. A., Edwards, H. G. M., & Scowen, I. J. (2009). Raman spectroscopy and security applications: The detection of explosives and precursors on clothing. *Journal of Raman Spectroscopy*, 40(12), 2009-2014
- [32] Ali, E. M. A., Edwards, H. G. M., Hargreaves, M. D., & Scowen, I. J. (2010). In situ detection of cocaine hydrochloride in clothing impregnated with the drug using benchtop and portable raman spectroscopy. *Journal of Raman Spectroscopy*, 41(9), 938-943
- [33] Rygula, A., Jekiel, K., Szostak-Kot, J., Wrobel, T. P., & Baranska, M. (2011). Application of FT-Raman spectroscopy for in situ detection of microorganisms on the surface of textiles. *Journal of Environmental Monitoring*, 13(11), 2983-2987
- [34] Rezić, I., Ćurković, L., & Ujević, M. (2010). Simple methods for characterization of metals in historical textile threads. *Talanta*, 82(1), 237-244
- [35] Pranaitytė B., Padarauskas A., Naujalis E., Determination of metals in textiles by ICP-MS following extraction with synthetic gastric juice, *Chemija*. (2008) vol. 19. Nos. 3–4. P. 43–47
- [36] Ide-Ektessabi A., Toque J, Murayama Y., Analysis of Cultural Heritage by Accelerator Techniques and Analytical Imaging. *Application of Nuclear Techniques* (2011) 1412 5-16
- [37] Wilson H., Carr C., Hacke M., Production and validation of model iron-tannate dyed textiles for use as historic textile substitutes in stabilisation treatment studies. *Chemistry Central Journal* (2012) 6:44

- [38] Sobeih, K. L., Baron, M., & Gonzalez-Rodriguez, J. (2008). Recent trends and developments in pyrolysis–gas chromatography. *Journal of Chromatography A*, 1186(1–2), 51-66
- [39] Lewicki, J. P., Albo, R. L. F., Alviso, C. T., & Maxwell, R. S. (2013). Pyrolysis-gas chromatography/mass spectrometry for the forensic fingerprinting of silicone engineering elastomers. *Journal of Analytical and Applied Pyrolysis*, 99, 85-91
- [40] Rendle D., Advances in chemistry applied to forensic science. *Chem. Soc. Rev.* (2005) 34, 1021–1030 | 1021
- [41] Zhu, P., Sui, S., Wang, B., Sun, K., & Sun, G. (2004). A study of pyrolysis and pyrolysis products of flame-retardant cotton fabrics by DSC, TGA, and PY–GC–MS. *Journal of Analytical and Applied Pyrolysis*, 71(2), 645-655
- [42] Takekoshi, Y., Sato, K., Kanno, S., Kawase, S., Kiho, T., & Ukai, S. (1997). Analysis of wool fibre by alkali-catalyzed pyrolysis gas chromatography. *Forensic Science International*, 87(2), 85-97
- [43] Causin, V., Marega, C., Schiavone, S., Guardia, V. D., & Marigo, A. (2006). Forensic analysis of acrylic fibres by pyrolysis–gas chromatography/mass spectrometry. *Journal of Analytical and Applied Pyrolysis*, 75(1), 43-48
- [44] J. C. Hughes, B. B. Wheals and M. J. Mrwhitehouse, Pyrolysis - Mass Spectrometry of Textile Fibres. *Analyst* (1978) Vol. 103, pp. 482-491
- [45] S.J. Clarson, Synthesis and properties of silicones and silicone modified materials, in: S.J. Clarson, J.J. Fitzgerald, M.J. Owen, S.D. Smith, M.E. Van Dyke (Eds.), *ACS Symposium Series*, vol. 838, (2003) pp. 1–10.
- [46] Casanovas, A. M., & Rovira, X. (1987). Determination of reactive comonomers and/or amino resins in acrylic copolymers used in textile industry, by pyrolysis-gas chromatography-mass spectrometry. *Journal of Analytical and Applied Pyrolysis*, 11, 227-232
- [47] Yamada, T., Okumoto, T., Ohtani, H., & Tsuge, S. (1995). Characterization of epoxy resins cured with dicyandiamide in the presence of imidazole catalysts by high-resolution pyrolysis—gas chromatography. *Journal of Analytical and Applied Pyrolysis*, 33, 157-166
- [48] A. Plum, W. Engewald, A. Rehorek, Rapid Qualitative Pyrolysis GC-MS Analysis of Carcinogenic Aromatic Amines from Dyed Textiles. *Chromatographia* (2003), Volume 57, Supplement 1, pp S243-S248
- [49] Ana Serrano, Micaela M. Sousa, Jessica Hallett, João A. Lopes, M. Conceição Oliveira, Analysis of natural red dyes (cochineal) in textiles of historical importance using HPLC and multivariate data analysis. *Anal Bioanal Chem* (2011) 401:735–743

- [50] Recep Karadag , Emine Torgan , Turan Taskopru & Yusuf Yildiz (2015) Characterization of Dyestuffs and Metals from Selected 16–17th-Century Ottoman Silk Brocades by RP-HPLC-DAD and FESEM-EDX, *Journal of Liquid Chromatography & Related Technologies*, 38:5, 591-599
- [51] Surowiec, I., Quye, A., & Trojanowicz, M. (2006). Liquid chromatography determination of natural dyes in extracts from historical scottish textiles excavated from peat bogs. *Journal of Chromatography A*, 1112(1–2), 209-217
- [52] Zhang Z., Pawliszyn, Headspace solid-phase microextraction. *J. Analytical Chemistry* (1993), **65**, 1843-52
- [53] Pawliszyn, J., Solid Phase Micro-extraction: Theory and Practice. Wiley-VCH, 1997
- [54] Wang, S., Oakes, K. D., Bragg, L. M., Pawliszyn, J., Dixon, G., & Servos, M. R. (2011). Validation and use of in vivo solid phase micro-extraction (SPME) for the detection of emerging contaminants in fish. *Chemosphere*, 85(9), 1472-1480
- [55] J. Pawliszyn, New Sampling/Sample Preparation Strategies for Rapid Screening. *Field Screening Europe*, (2001) pp 3-7
- [56] Yun, Z., & Minyan, L. (2014). The method study on emergency detection of aromatic compounds and chlorides based on portable GC-MS. *Procedia Engineering*, 84, 731-735
- [57] Solid Phase Microextraction: Theory and Optimization of Conditions, <https://www.sigmaaldrich.com/Graphics/Supelco/objects/4600/4547.pdf> (accessed Jan 2012)
- [58] Zhang Z., Yang M., Pawliszyn J., Solid-Phase Microextraction. *Analytical Chemistry*,(1994) Vol. 66, No. 17
- [59] Łojewski *et al.* Furfural as a marker of cellulose degradation. A quantitative approach. *Appl Phys A* (2010) 100: 873–884
- [60] Clark *et al.* Degradation product emission from historic and modern books by headspace SPME/GC–MS: evaluation of lipid oxidation and cellulose hydrolysis. *Anal Bioanal Chem* (2011) 399:3589–3600
- [61] Pedersoli *et al.* Non-Destructive Determination of Acetic Acid and Furfural in Books by Solid-Phase Micro-extraction (SPME) and Gas Chromatography-Mass Spectrometry (GC/MS). *Restaurator*, Vol. 32, p. 110–134
- [62] Lattuati-Derieux *et al.* Characterisation of compounds emitted during natural and artificial ageing of a book. Use of headspace-solid-phase microextraction/gas chromatography/mass spectrometry. *Journal of Cultural Heritage* 7 (2006) 123–133

- [63] Zhu, H., Lu, Z., Cai, J., Li, J., & Gao, L. Development of a headspace–SPME–GC/MS method to determine volatile organic compounds released from textiles. *Polymer Testing* 28 (2009) 521–527
- [64] A.M. Lisovac, D. Shooter, Volatiles from sheep wool and the modification of wool odour. *Small Ruminant Research* 2003,49, 115–124
- [65] Hu *et al.* Determination of organophosphorus pesticides in ecological textiles by solid-phase microextraction with a siloxane-modified polyurethane acrylic resin fibre. *Analytica Chimica Acta* 736 (2012) 62– 68
- [66] Douglas A. Skoog, F. James Holler, Stanley R. Crouch, *Principles of Instrumental Analysis*. 6th ed. Thomson Brooks/Cole, 2007
- [67] Bianchin *et al.* Screening of volatile compounds in honey using a new sampling strategy combining multiple extraction temperatures in a single assay by HS-SPME-GC-MS. *Food Chemistry* (2014) 145C:1061-1065
- [68] Sax, N.I. *Dangerous Properties of Industrial Materials*. 4th ed. New York: Van Nostrand Reinhold, 1975., p. 1203
- [69] Michael Ash, Irene Ash, *Handbook of Preservatives*. 1st ed. New York: Synapse Information Resources, 2004, p. 434
- [70] Liu Y., Thibodeaux D., Gamble G. Development of Fourier transform infrared spectroscopy in direct, non-destructive, and rapid determination of cotton fibre maturity. *Textile Research Journal* (2011) 81(15) 1559–1567
- [71] Causin, V., Marega, C., Schiavone, S., & Marigo, A. (2005). A quantitative differentiation method for acrylic fibres by infrared spectroscopy. *Forensic Science International*, 151(2–3), 125-131
- [72] Pielesz, A., Freeman, H. S., Weselucha-Birczyńska, A., Wysocki, M., & Włochowicz, A. (2003). Assessing secondary structure of a dyed wool fibre by means of FTIR and FTR spectroscopies. *Journal of Molecular Structure*, 651–653, 405-418.
- [73] Hubert Lobo, Jose V. Bonilla, *Handbook of Plastics Analysis*. Print ed. New York: Marcel Dekker Inc. 2003
- [74] J. Karger-Kocsis, *Polypropylene Structure, blends and composites*. Hardcover, Netherlands: Springer 1994 Vol. 1
- [75] Voet D., Voet J., Pratt C., *Fundamentals of Biochemistry*. 4th ed. New York : John Wiley & Sons, Inc. 2013, 136-137

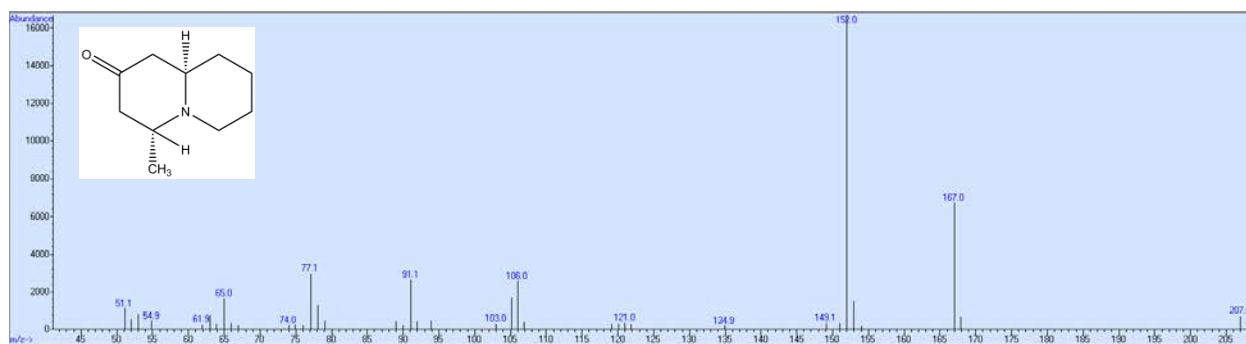
- [76] Dilillo, M., Restivo, A., Degano, I., Ribechini, E., & Colombini, M. P. (2015). GC/MS investigations of the total lipid fraction of wool: A new approach for modelling the ageing processes induced by iron-gallic dyestuffs on historical and archaeological textiles. *Microchemical Journal*, 118, 131-140
- [77] Gaspar *et al.* Volatile organic compounds in paper—an approach for identification of markers in aged books. *Anal Bioanal Chem* (2010) 397:369–380
- [78] Łojewski *et al.* Furfural as a marker of cellulose degradation. A quantitative Approach. *Appl Phys A* (2010) 100: 873–884
- [79] Rackemann, D. W., Bartley, J. P., & Doherty, W. O. S. (2014). Methanesulfonic acid-catalyzed conversion of glucose and xylose mixtures to levulinic acid and furfural. *Industrial Crops and Products*, 52, 46-57
- [80] Marcotullio, G., & de Jong, W. (2011). Furfural formation from d-xylose: The use of different halides in dilute aqueous acidic solutions allows for exceptionally high yields. *Carbohydrate Research*, 346(11), 1291-1293
- [81] Zhang J., *Degradations and Rearrangement Reactions*. Springer-Verlag Berlin Heidelberg (2008)
- [82] Tétreault, J., Dupont, A. -, Bégin, P., & Paris, S. (2013). The impact of volatile compounds released by paper on cellulose degradation in ambient hygrothermal conditions. *Polymer Degradation and Stability*, 98(9), 1827-1837
- [83] B. Girisuta, L. P. B. M. Janssen, and H. J. Heeres, Kinetic Study on the Acid-Catalyzed Hydrolysis of Cellulose to Levulinic Acid. *Ind. Eng. Chem. Res.* 2007, 46, 1696-1708
- [84] Degano, I., Biesaga, M., Colombini, M. P., & Trojanowicz, M. (2011). Historical and archaeological textiles: An insight on degradation products of wool and silk yarns. *Journal of Chromatography A*, 1218(34), 5837-5847
- [85] Dyer *et al.*, Determination of Photo-oxidation Products Within Photoyellowed Bleached Wool Proteins. *Photochemistry and Photobiology* (2006) 82: 551-557
- [86] Dyer, J. M., - Bringans, S. D., & - Bryson, W. G., Characterisation of photo-oxidation products within photoyellowed wool proteins: Tryptophan and tyrosine derived chromophores. *Photochem. Photobiol. Sci.* (2006) 5, 698–706
- [87] Lattuati-Derieux, A., Thao-Heu, S., & Lavédrine, B. (2011). Assessment of the degradation of polyurethane foams after artificial and natural ageing by using pyrolysis-gas chromatography/mass spectrometry and headspace-solid phase microextraction-gas chromatography/mass spectrometry. *Journal of Chromatography A*, 1218(28), 4498-4508

- [88] Migani, V., Weiss, H., Massafra, M. R., Merlo, A., Colleoni, C., & Rosace, G. (2011). Polydimethylsiloxane derivatives side chains effect on syntan functionalized polyamide fabric. *Applied Surface Science*, 257(9), 3904-3912
- [89] Tutaş, M., Sağlam, M., & Yüksel, M. (1991). Investigation of pyrolysis products of polyacrylamide by pyrolysis—gas chromatography. *Journal of Analytical and Applied Pyrolysis*, 22(1), 129-137
- [90] Dyer *et al.* Photoproducts Formed in the Photoyellowing of Collagen in the Presence of a Fluorescent Whitening Agent. *Photochemistry and Photobiology* (2009) 85: 1314–1321
- [91] Nicholls, C. H., and Pailthore, M. T., 50-primary Reactions in the Photoyellowing of Wool Keratin. *J. Textile Inst.* (1976) 67(11), 397–403
- [92] Cleve, E., Bach, E., & Schollmeyer, E. (2000). Using chemometric methods and NIR spectrophotometry in the textile industry. *Analytica Chimica Acta* 420(2), 163-167
- [93] Custers, D., Canfyn, M., Courselle, P., De Beer, J. O., Apers, S., & Deconinck, E. (2014). Headspace–gas chromatographic fingerprints to discriminate and classify counterfeit medicines. *Talanta*, 123, 78-88
- [94] Zhang, Z., Li, G., Luo, L., & Chen, G. (2010). Study on seafood volatile profile characteristics during storage and its potential use for freshness evaluation by headspace solid phase microextraction coupled with gas chromatography–mass spectrometry. *Analytica Chimica Acta*, 659(1–2), 151-158
- [95] Fabbri D., Adamiano A., Torri C. GC-MS determination of polycyclic aromatic hydrocarbons evolved from pyrolysis of biomass. *Anal Bioanal Chem* (2010) 397:309–317
- [96] National Criminal Justice Reference Service, Raman Spectroscopy with Multi-component Searching for Complex Clandestine Laboratory Sample Analysis (I), Raman Spectroscopy as a Rapid, Non-destructive Screening Test for Methamphetamine in Clandestine Laboratory Liquids (II), and Raman Spectroscopy for Enhanced Synthetic Cathinone Analysis (III). <https://www.ncjrs.gov/pdffiles1/nij/grants/248557.pdf> (accessed March 30, 2016)

Appendix

The following mass spectra are associated with the compounds found in Table 4 which were used to identify the textile fibres in this research. A confirmation of the compounds identified by the NIST 2008 9th edition (Wiley Registry®) database is presented.

(+/-)-myrtine (167 g/mol)

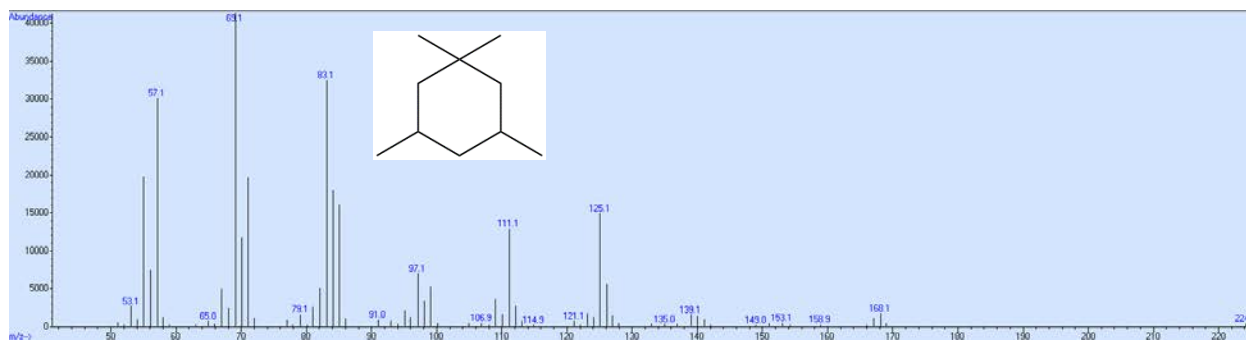


(C₆H₅⁺) m/z = 77 g/mol

(C₇H₇⁺) m/z = 91 g/mol

(C₉H₁₄NO⁺) m/z = 152 g/mol (-CH₃)

1, 1, 3, 5-tetramethyl-cyclohexane (140 g/mol)



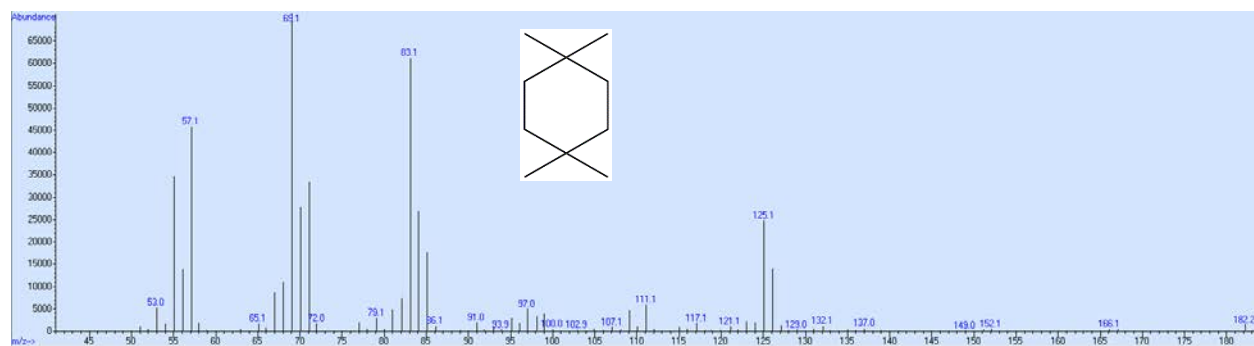
(C₅H₉⁺) m/z = 69 g/mol

(C₆H₁₁⁺) m/z = 83 g/mol

(C₈H₁₅⁺) m/z = 111 g/mol

(C₉H₁₇⁺) m/z = 125 g/mol (-CH₃)

1, 1, 4, 4-tetramethyl-cyclohexane



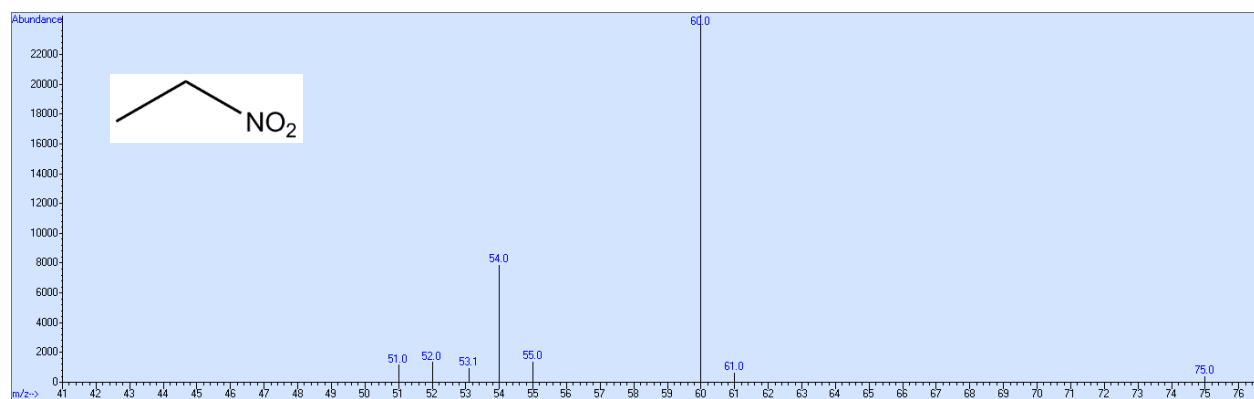
$(C_4H_9^+)$ m/z = 57 g/mol

$(C_5H_9^+)$ m/z = 69 g/mol

$(C_6H_{11}^+)$ m/z = 83 g/mol

$(C_9H_{17}^+)$ m/z = 125 g/mol (-CH₃)

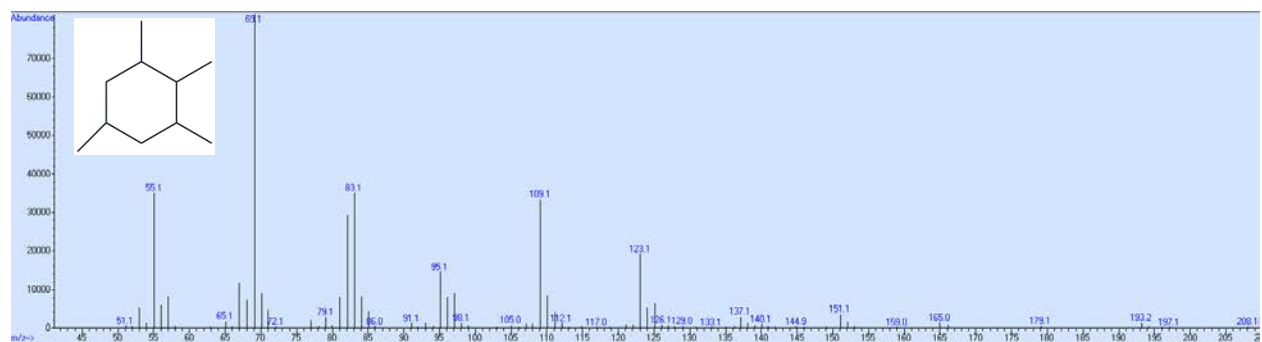
Nitroethane (75 g/mol)



$(CH_2NO_2^+)$ m/z = 60 g/mol

$(C_2H_5NO_2^+)$ m/z = 75 g/mol

1, 2, 3, 5-tetramethyl-cyclohexane



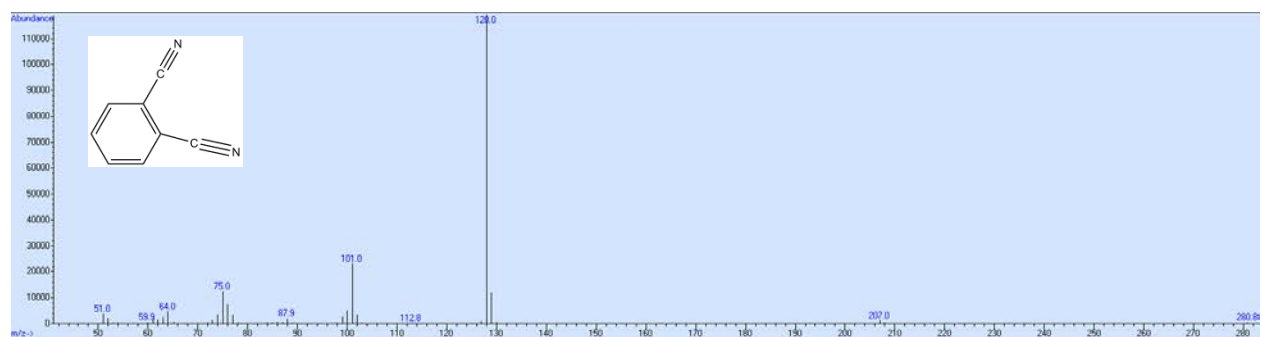
$(C_5H_9^+)$ m/z = 69 g/mol

$(C_6H_{11}^+)$ m/z = 83 g/mol

$(C_8H_{13}^+)$ m/z = 109 g/mol

$(C_9H_{15}^+)$ m/z = 123 g/mol

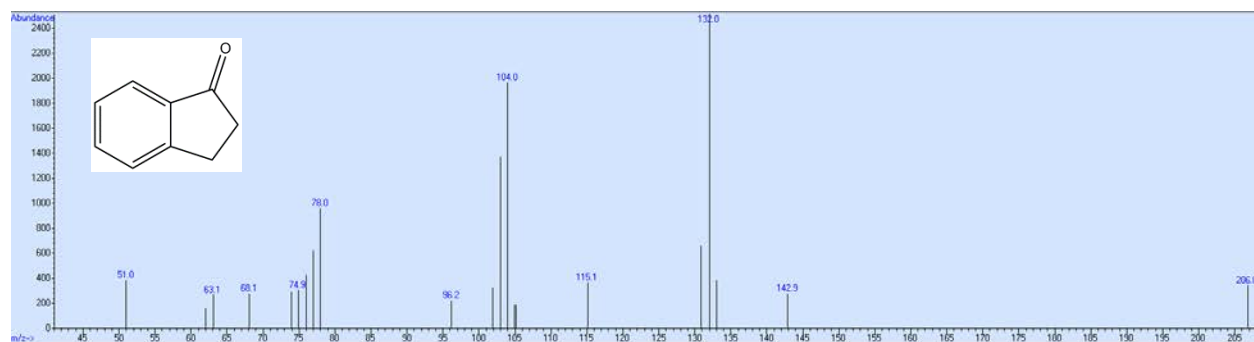
1,2-benzenedicarbonitrile (128 g/mol)



$(C_6H_5^+)$ m/z = 75 g/mol

$(C_7H_4N^+)$ m/z = 101 g/mol

1-indanone (132 g/mol)



(C₆H₆) m/z = 78 g/mol

(C₈H₈⁺) m/z = 104 g/mol

(C₉H₇⁺) m/z = 115 g/mol (-OH)

(C₉H₈O⁺) m/z = 132 g/mol

1-phenylethanone (120 g/mol)

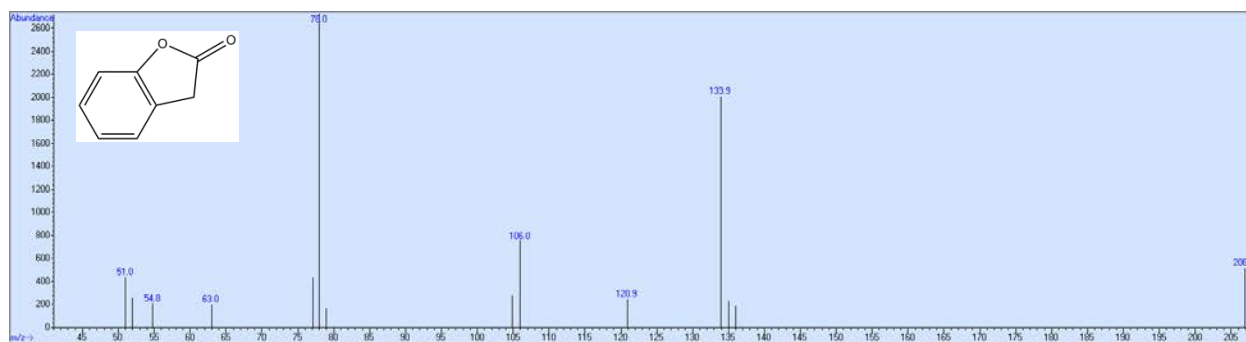


(C₆H₅⁺) m/z = 77 g/mol

(C₆H₆CO⁺) m/z = 106 g/mol

(C₈H₈O⁺) m/z = 120 g/mol

2 (3H) – benzofuranone (134 g/mol)

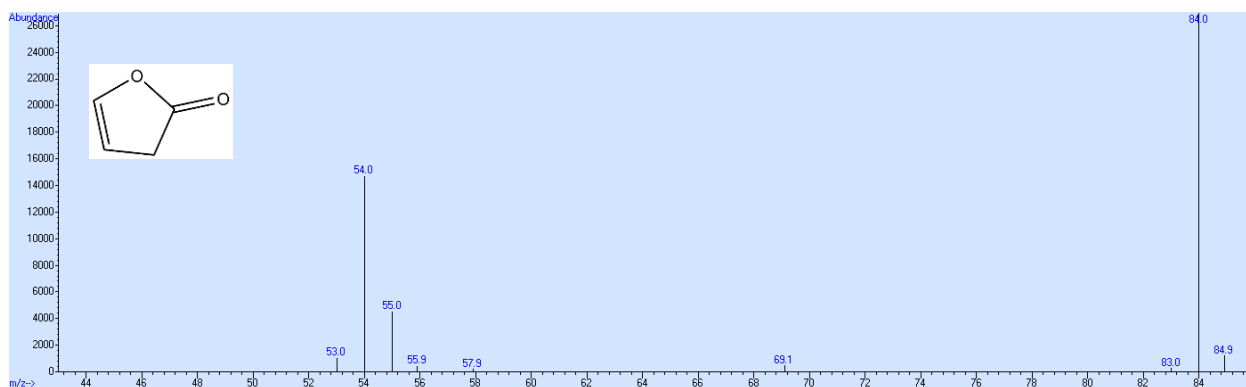


(C₆H₆) m/z = 78 g/mol

(C₆H₆CO⁺) m/z = 106 g/mol

(C₇H₈CO⁺) m/z = 120 g/mol

2(H)-furan-3-one (84 g/mol)

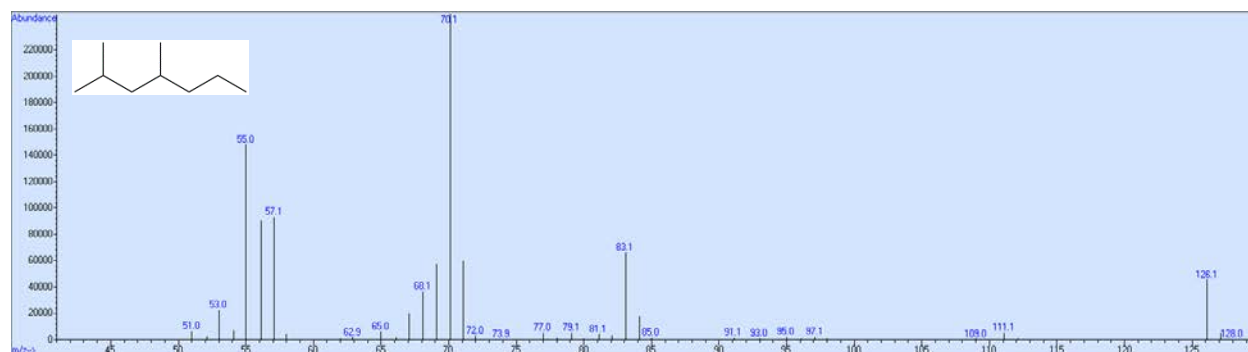


(C₃H₂O⁺) m/z = 54 g/mol

(C₃H₃O⁺) m/z = 55 g/mol

(C₄H₄O₂⁺) m/z = 84 g/mol

2,4-Dimethylheptane (128 g/mol)

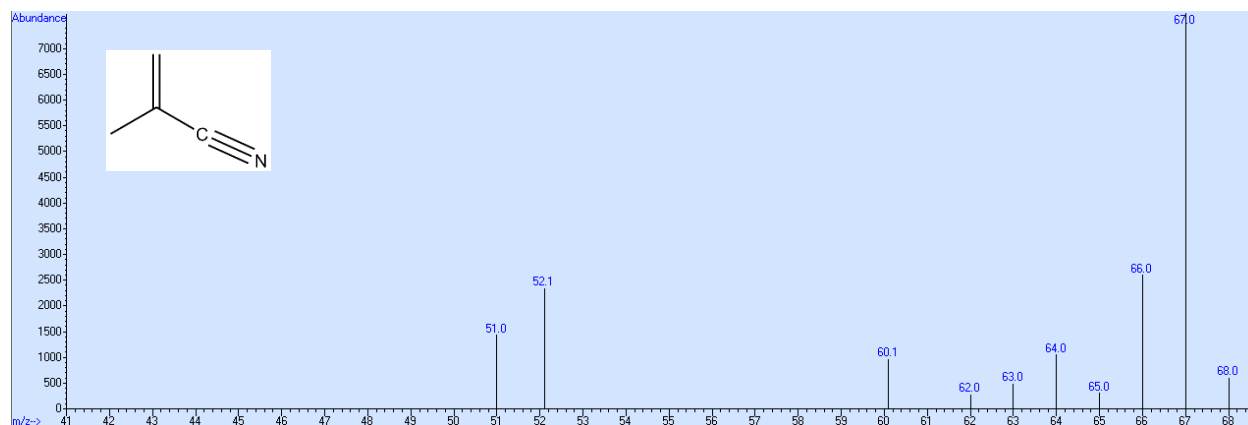


$(C_4H_7^+)$ m/z = 55 g/mol

$(C_5H_{10}^+)$ m/z = 70 g/mol

$(C_6H_{11}^+)$ m/z = 83 g/mol

2-methyl-2-propenenitrile (67 g/mol)

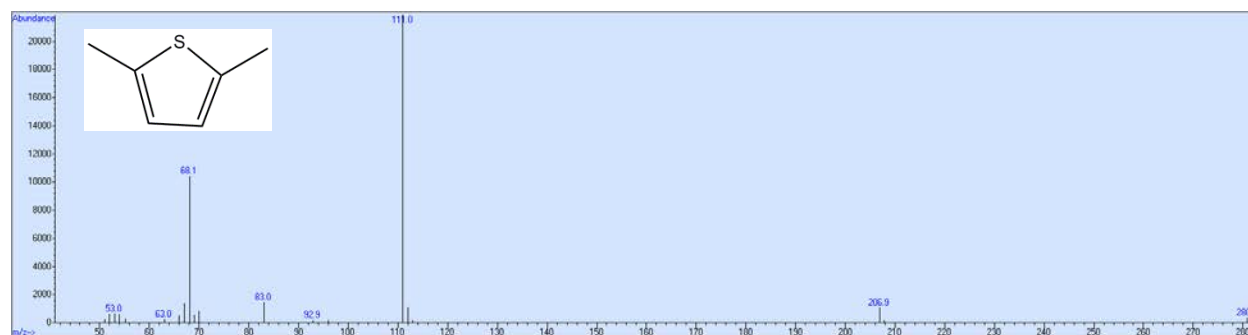


$(C_3H_2N^+)$ m/z = 52 g/mol

$(C_4H_4N^+)$ m/z = 66 g/mol (-H)

$(C_4H_5N^+)$ m/z = 67 g/mol

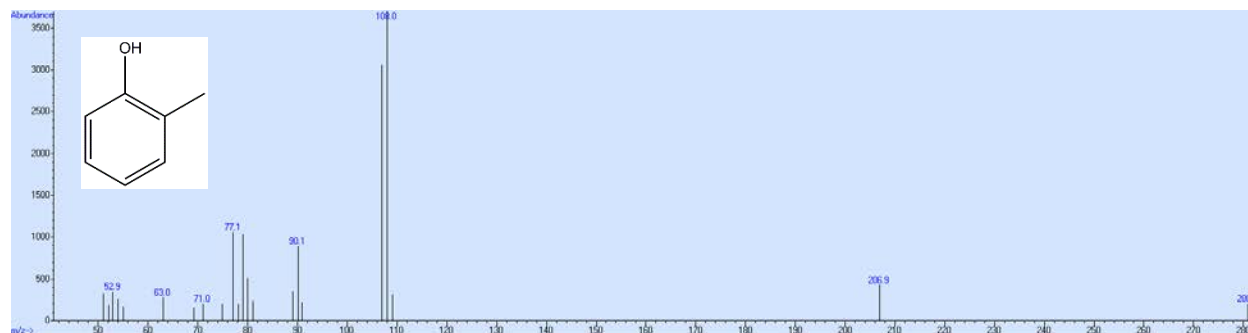
2-methyl-5-methylthiophene (112 g/mol)



$(C_5H_8^+)$ m/z = 68 g/mol

$(C_6H_7S^+)$ m/z = 111 g/mol

2-methyl-phenol (108 g/mol)

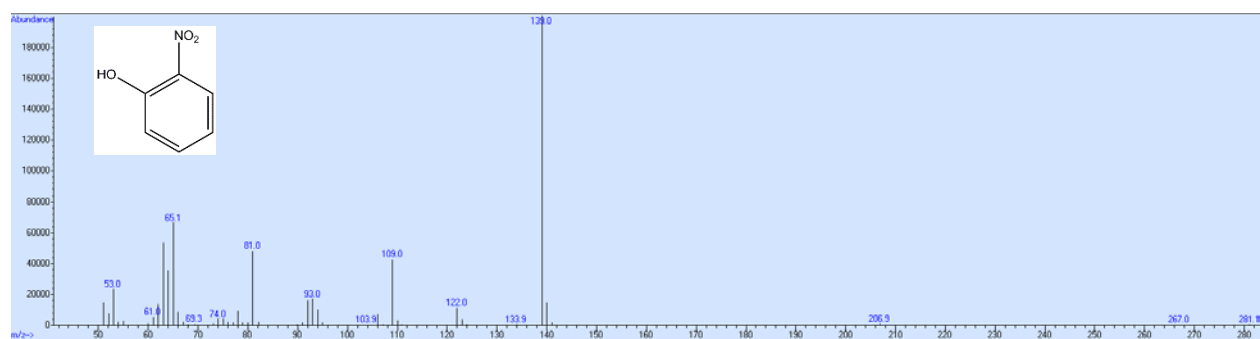


$(C_6H_5^+)$ m/z = 77 g/mol

$(C_7H_6^+)$ m/z = 90 g/mol

$(C_7H_8O^+)$ m/z = 108 g/mol

2-nitro-phenol (139 g/mol)

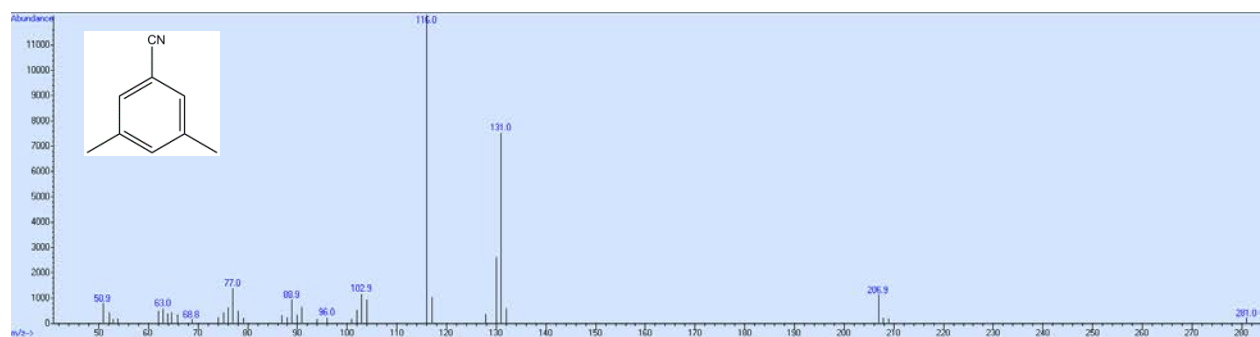


$(C_5H_5^+)$ m/z = 65 g/mol

$(C_6H_5O_2^+)$ m/z = 109 g/mol

$(C_6H_5NO_3^+)$ m/z = 139 g/mol

3,5-dimethyl-benzonitrile (131 g/mol)

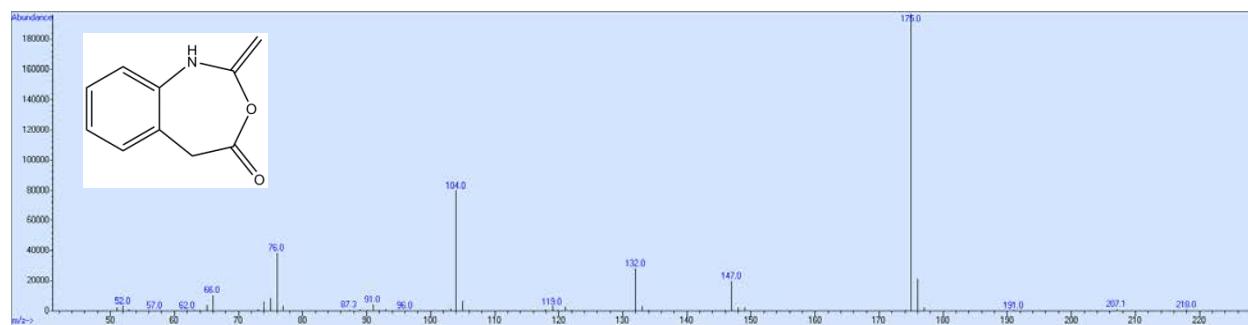


$(C_6H_5^+)$ m/z = 77 g/mol

$(C_6H_5CN^+)$ m/z = 103 g/mol

$(C_7H_6CN^+)$ m/z = 116 g/mol

3-methyliden-2,3,4,5-tetrahydro-1-benzoxazepin-one (175 g/mol)

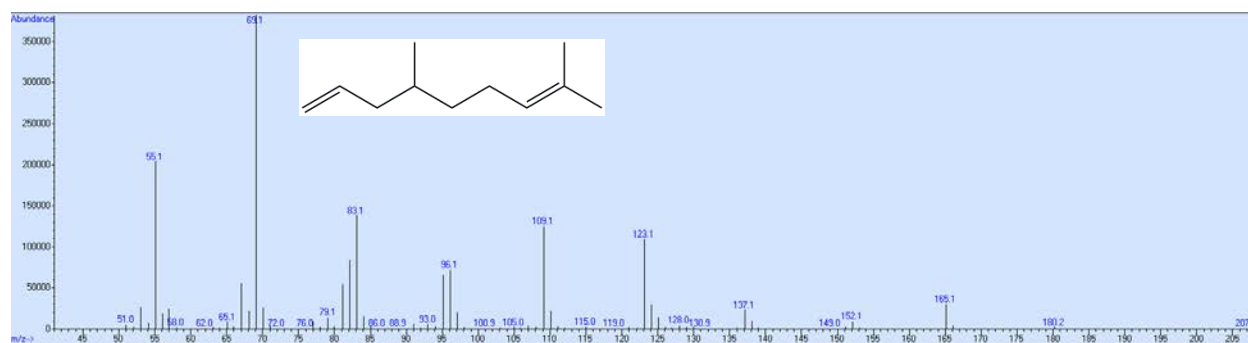


$(C_6H_4CO^+)$ m/z = 104 g/mol

$(C_9H_8O^+)$ m/z = 132 g/mol

$(C_9H_9NO^+)$ m/z = 147 g/mol

4,8-dimethyl-1,7-nonadiene (152 g/mol)

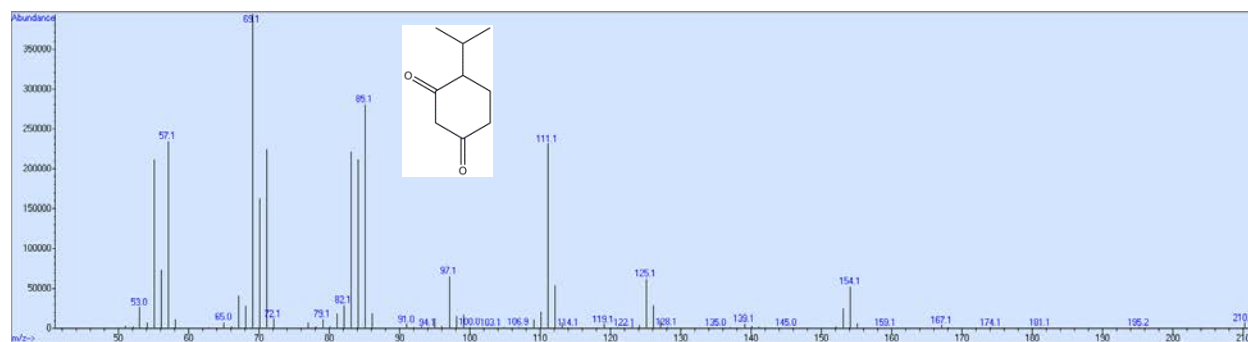


$(C_5H_9^+)$ m/z = 69 g/mol

$(C_6H_{11}^+)$ m/z = 83 g/mol

$(C_{10}H_{17}^+)$ = 137 g/mol

4-isopropyl-1,3-cyclo-hexanedione (154 g/mol)

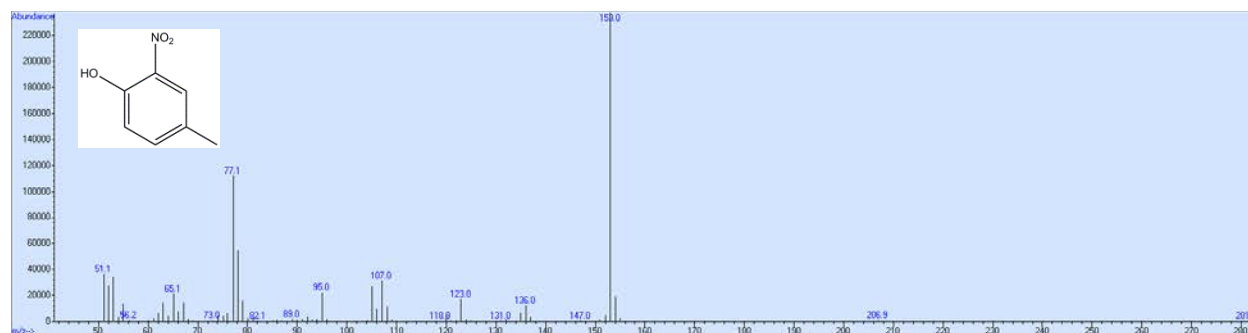


$(C_5H_9^+)$ m/z = 69 g/mol

$(C_5H_5O_2^+)$ m/z = 97 g/mol

$(C_6H_7O_2^+)$ m/z = 111 g/mol

4-methyl-2-nitro-phenol (153 g/mol)

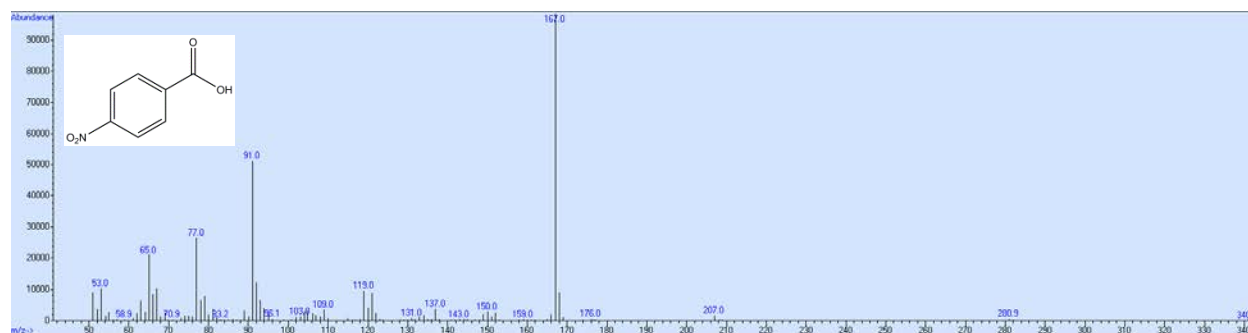


$(C_6H_5^+)$ m/z = 77 g/mol

$(C_7H_7O^+)$ m/z = 107 g/mol

$(C_7H_7NO_3^+)$ m/z = 153 g/mol

4-nitro-benzoic acid (167 g/mol)

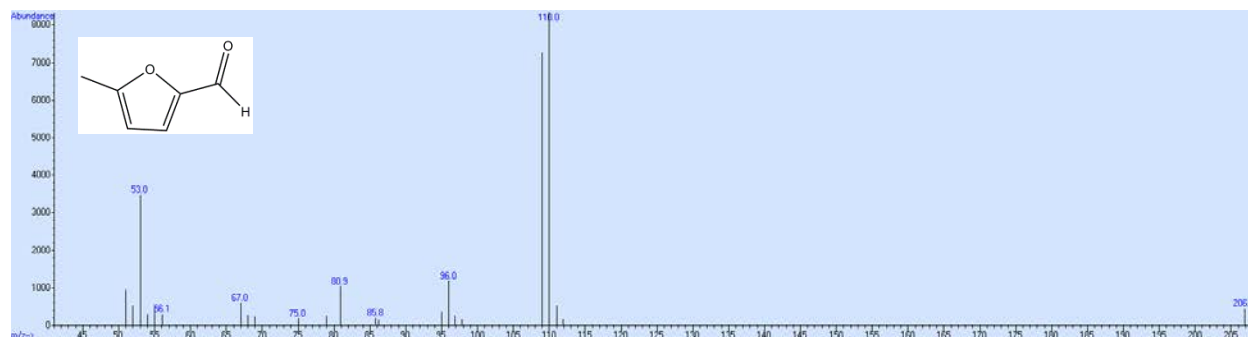


(C₅H₅⁺) m/z = 65 g/mol

(C₆H₅⁺) m/z = 77 g/mol

(C₇H₇⁺) m/z = 91 g/mol

5-methyl furfural (110 g/mol)

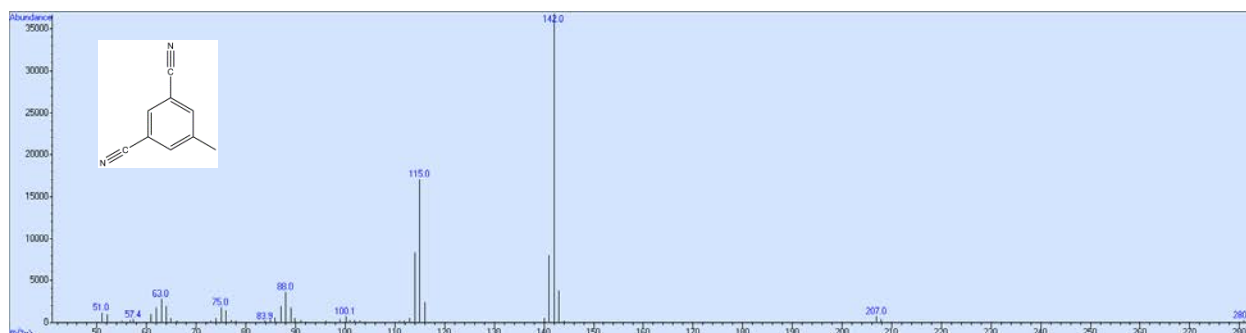


(C₄H₃O⁺) m/z = 67 g/mol

(C₅H₄O⁺) m/z = 80 g/mol

(C₅H₄O₂⁺) m/z = 96 g/mol

5-methyl isophthalonitrile (142 g/mol)

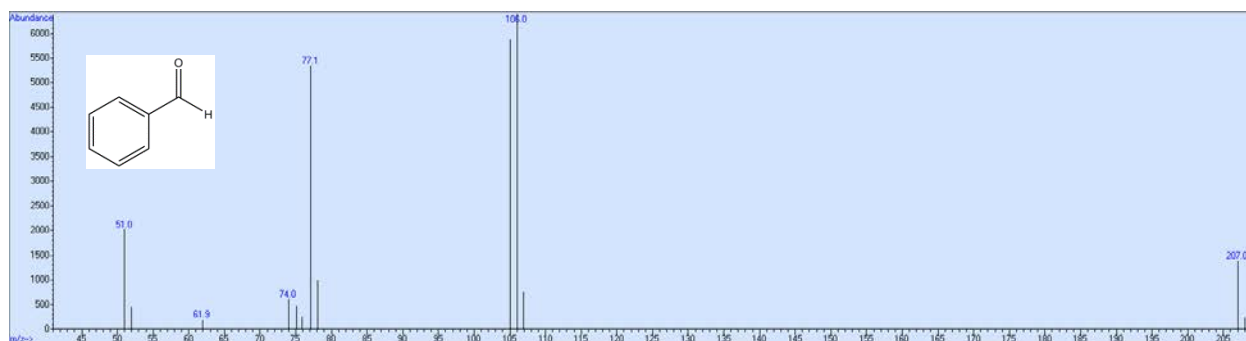


$(C_7H_4^+)$ m/z = 88 g/mol

$(C_8H_5N^+)$ m/z = 115 g/mol

$(C_9H_6N_2^+)$ m/z = 142 g/mol

Benzaldehyde (106 g/mol)

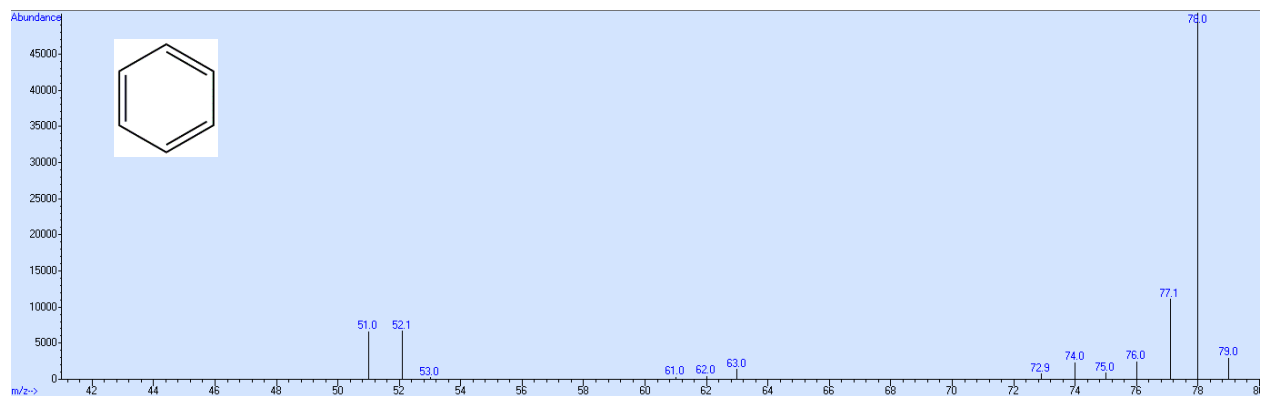


$(C_4H_3^+)$ m/z = 51 g/mol

$(C_6H_5^+)$ m/z = 77 g/mol

$(C_6H_6O^+)$ m/z = 106 g/mol

Benzene (78 g/mol)

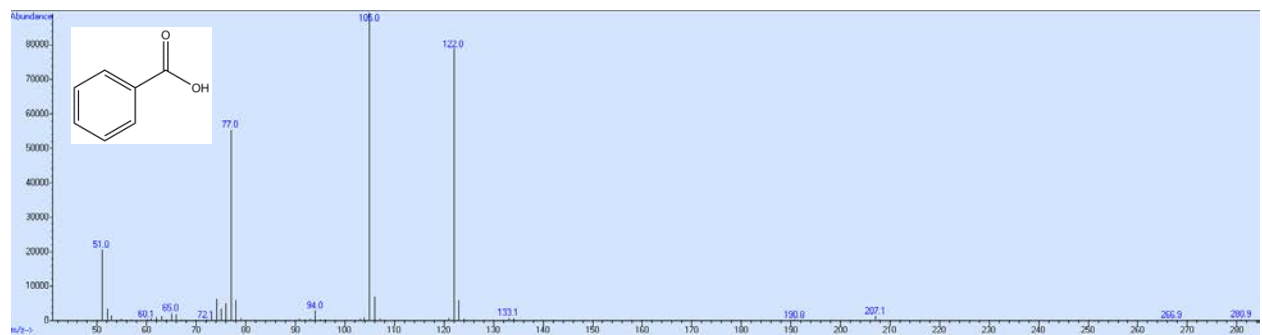


$(C_4H_3^+)$ m/z = 51 g/mol

$(C_6H_5^+)$ m/z = 77 g/mol

$(C_6H_6^+)$ m/z = 78 g/mol

Benzoic acid (122 g/mol)

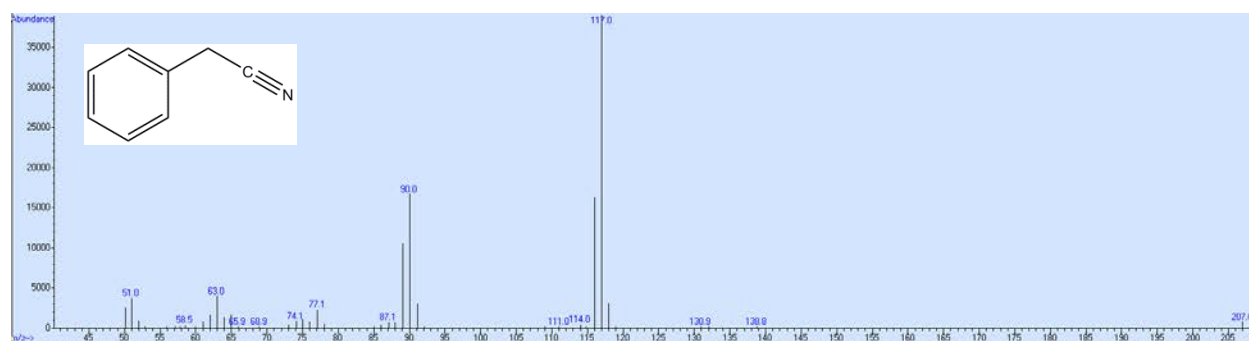


$(C_4H_3^+)$ m/z = 51 g/mol

$(C_6H_5^+)$ m/z = 77 g/mol

$(C_7H_5O^+)$ m/z = 106 g/mol

Benzyl nitrile (117 g/mol)

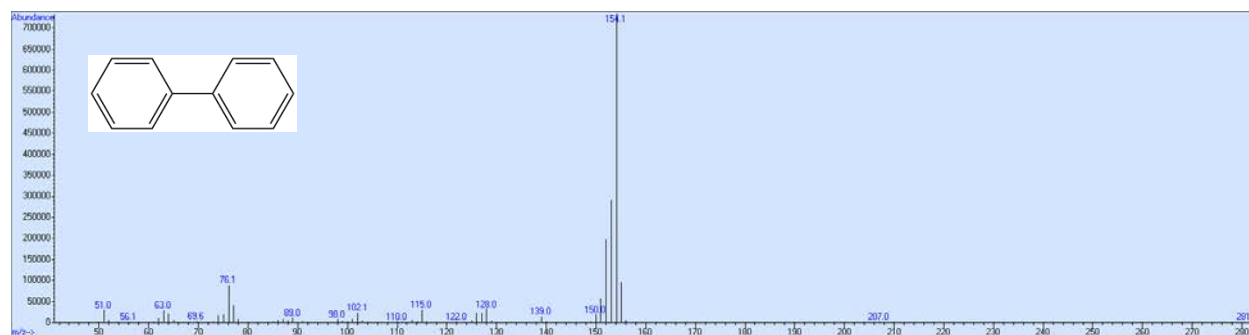


$(C_4H_3^+)$ m/z = 51 g/mol

$(C_6H_5^+)$ m/z = 77 g/mol

$(C_7H_6^+)$ m/z = 90 g/mol

Biphenyl (154 g/mol)

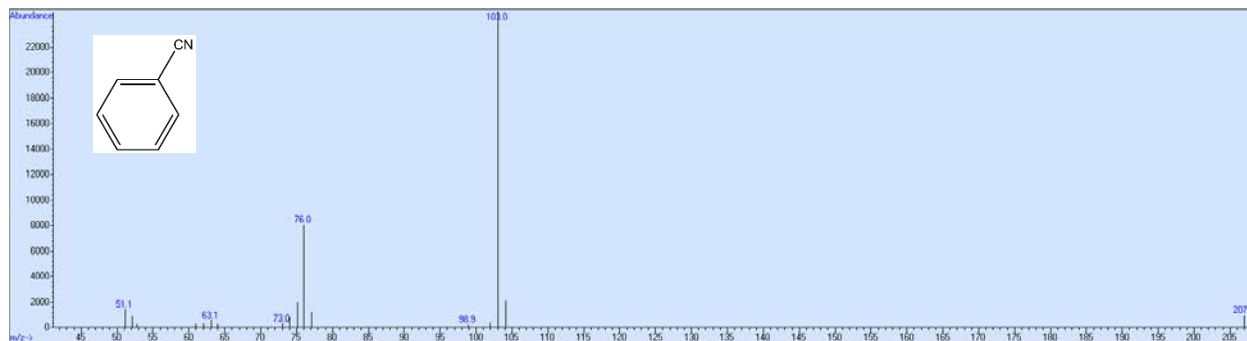


$(C_4H_3^+)$ m/z = 51 g/mol

$(C_6H_4^+)$ m/z = 76 g/mol

$(C_{12}H_{10}^+)$ m/z = 154 g/mol

Cyanobenzene (103 g/mol)

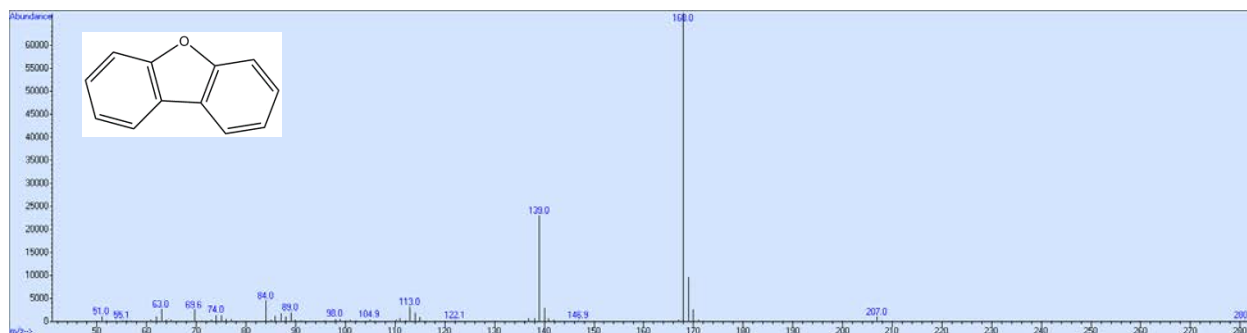


$(C_4H_3^+)$ m/z = 51 g/mol

$(C_6H_4^+)$ m/z = 76 g/mol

$(C_7H_5N^+)$ m/z = 103 g/mol

Dibenzofuran (168 g/mol)

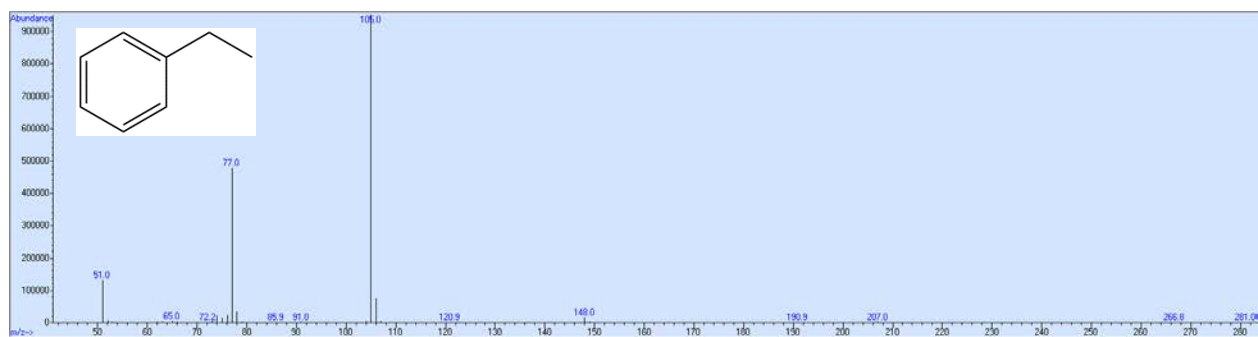


$(C_4H_3^+)$ m/z = 51 g/mol

$(C_{11}H_7^+)$ m/z = 139 g/mol (-COH)

$(C_{12}H_8O^+)$ m/z = 168 g/mol

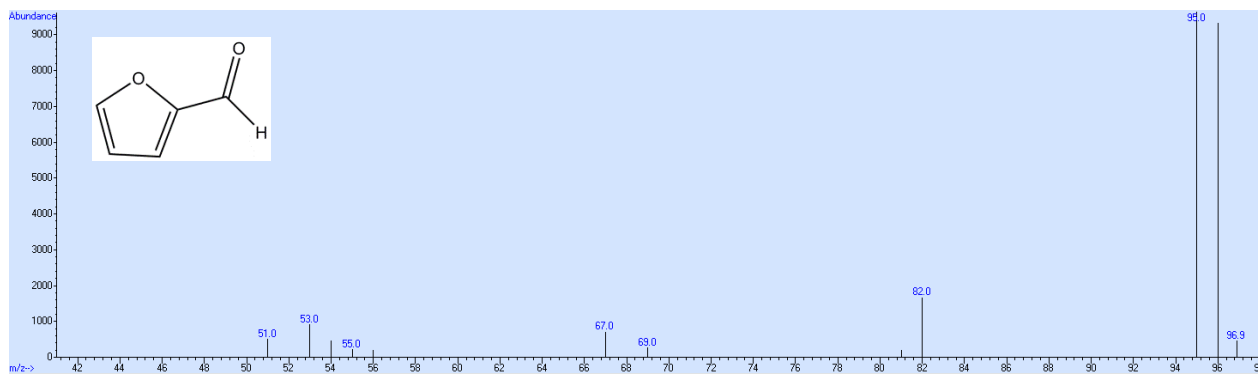
Ethylbenzene (106 g/mol)



(C₄H₃⁺) m/z = 51 g/mol

(C₆H₅⁺) m/z = 77 g/mol

Furfural (96 g/mol)

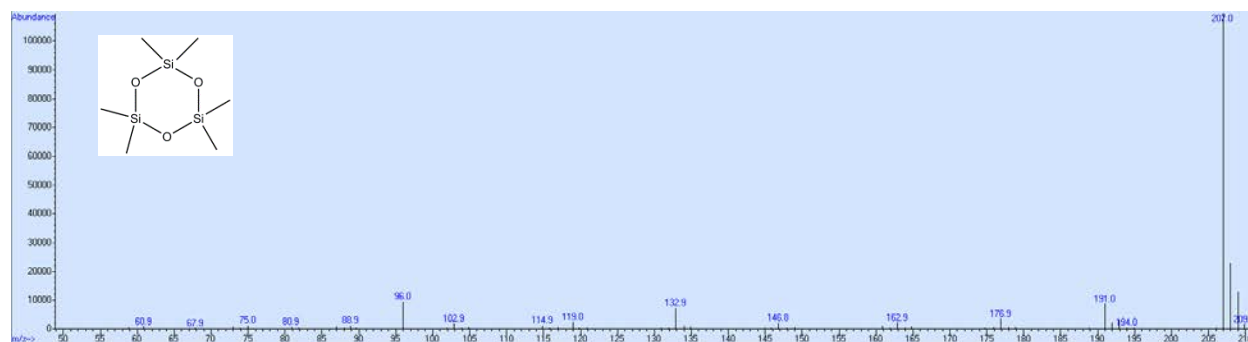


(C₄H₃⁺) m/z = 51 g/mol

(C₄H₃O⁺) m/z = 67 g/mol

(C₃H₂O⁺) m/z = 82 g/mol

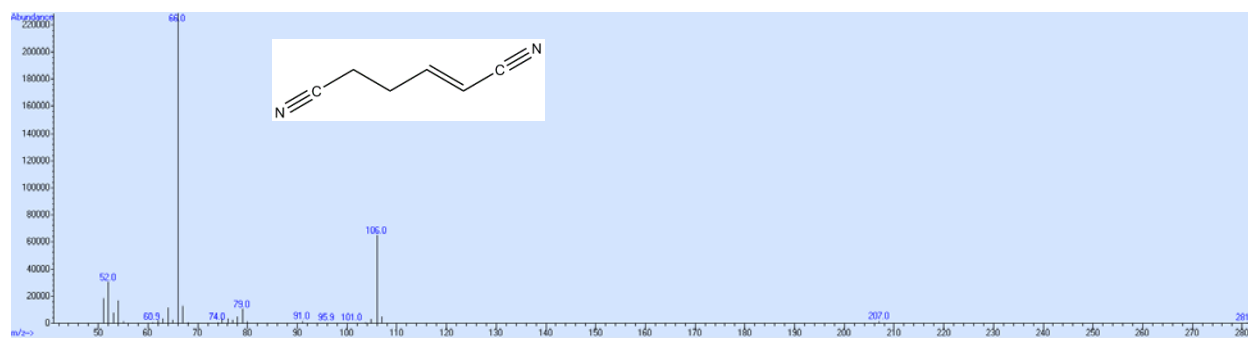
Hexamethyl-cyclotrisiloxane (222 g/mol)



$(C_5H_{15}O_3Si_3^+)$ m/z = 207 g/mol

$(C_6H_{18}O_3Si_3^+)$ m/z = 222 g/mol

2-hexenedinitrile (106 g/mol)

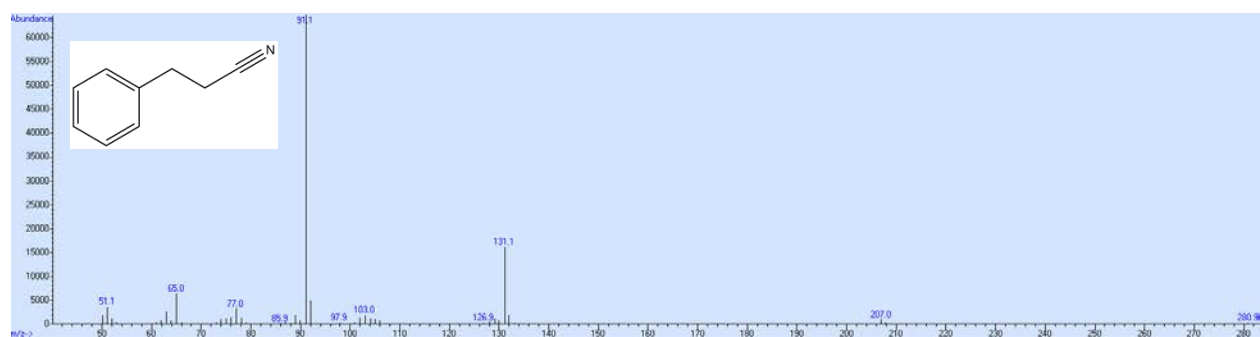


$(C_4H_4^+)$ m/z = 52 g/mol

$(C_4H_4N^+)$ m/z = 66 g/mol

$(C_6H_6N_2^+)$ m/z = 106 g/mol

Hydrocinnamionitrile (131 g/mol)

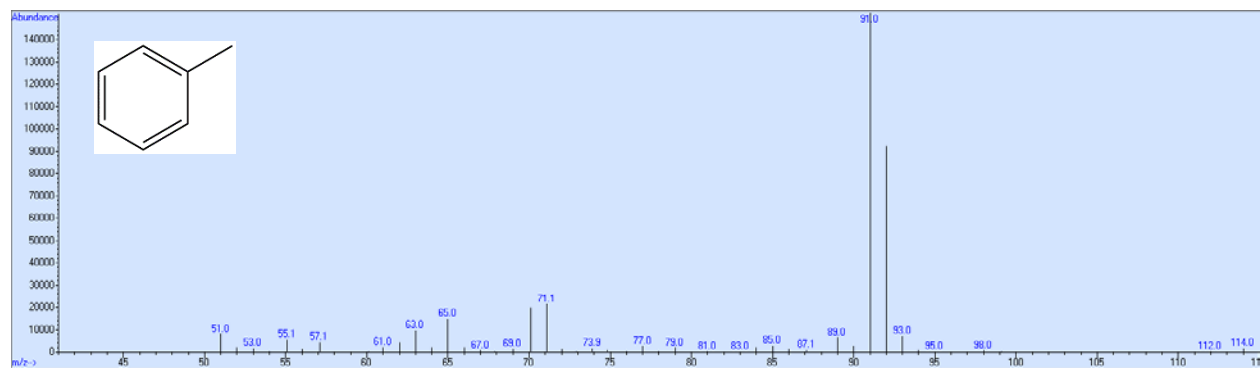


(C₄H₃⁺) m/z = 51 g/mol

(C₆H₅⁺) m/z = 77 g/mol

(C₇H₇⁺) m/z = 91 g/mol

Methylbenzene (92 g/mol)

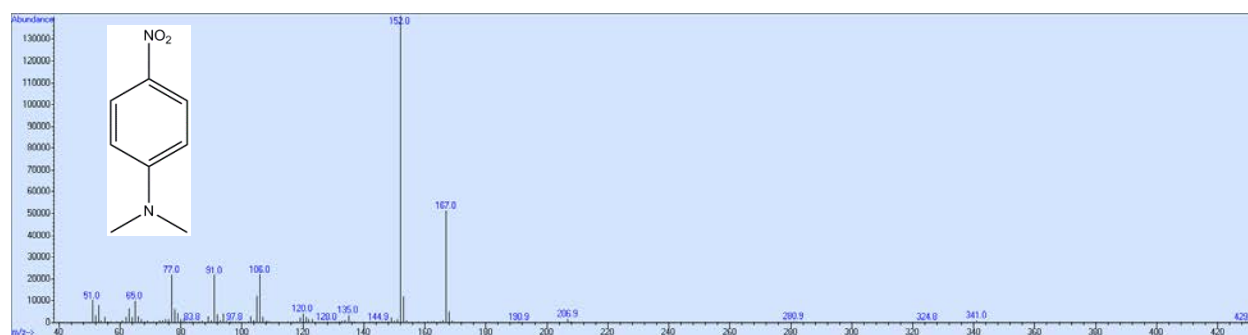


(C₄H₃⁺) m/z = 51 g/mol

(C₆H₅⁺) m/z = 77 g/mol

(C₇H₇⁺) m/z = 91 g/mol

N, N-Dimethyl-4-nitroaniline (166 g/mol)



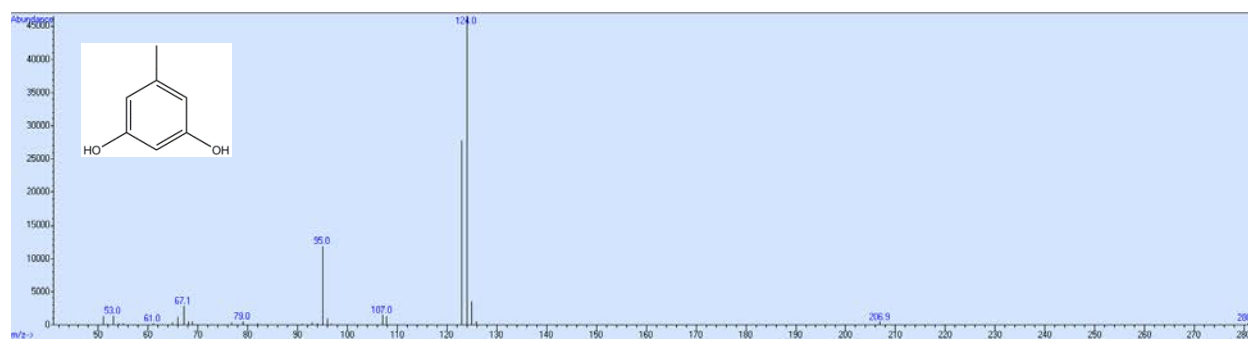
$(C_6H_5^+)$ m/z = 77 g/mol

$(C_6H_5N^+)$ m/z = 91 g/mol

$(C_7H_8N^+)$ m/z = 106 g/mol

$(C_7H_8N_2O_2^+)$ m/z = 152 g/mol

Orcinol (124 g/mol)

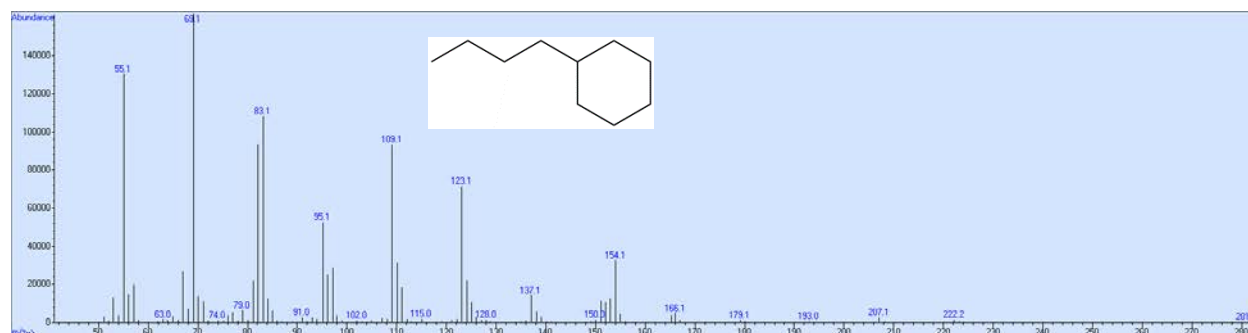


$(C_6H_7O^+)$ m/z = 95 g/mol

$(C_7H_7O^+)$ m/z = 107 g/mol

$(C_7H_8O_2^+)$ m/z = 124 g/mol

Pentylcyclohexane (154 g/mol)



$(C_4H_7^+)$ m/z = 55 g/mol

$(C_5H_9^+)$ m/z = 69 g/mol

$(C_6H_{11}^+)$ m/z = 83 g/mol

Phenol (94 g/mol)

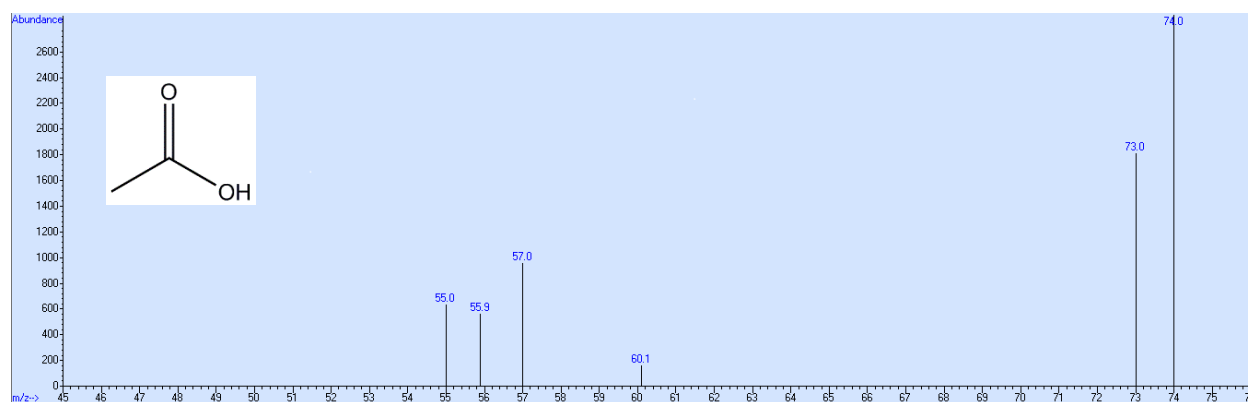


$(C_4H_3^+)$ m/z = 51 g/mol

$(C_5H_6^+)$ m/z = 66 g/mol

$(C_6H_6O^+)$ m/z = 94 g/mol

Propanoic acid (74 g/mol)

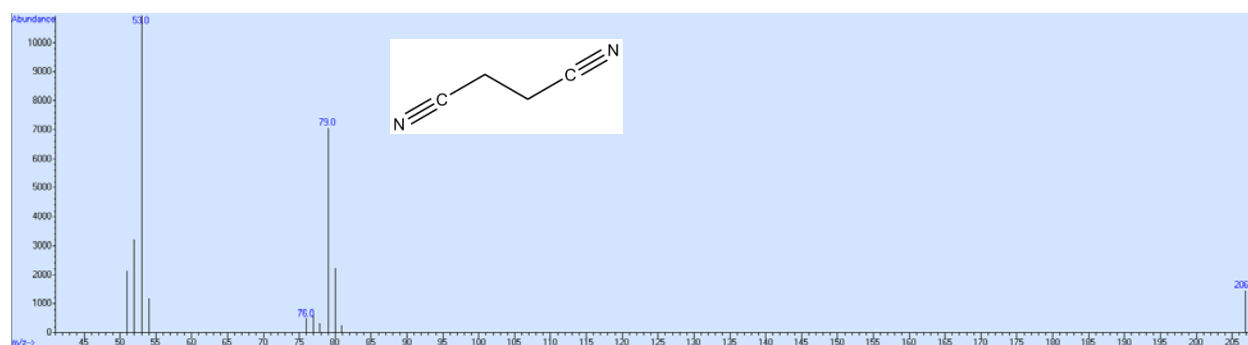


$(C_3H_5O^+)$ m/z = 57 g/mol

$(C_3H_5O_2^+)$ m/z = 73 g/mol (-H)

$(C_3H_6O_2^+)$ m/z = 74 g/mol

Succinonitrile (80 g/mol)



$(C_3H_3N^+)$ m/z = 53 g/mol

$(C_4H_3N_2^+)$ m/z = 79 g/mol (-H)

$(C_4H_4N_2^+)$ m/z = 80 g/mol